Spring 8-2021

Hybrid Cyclic-Linear Cell-Penetrating Peptides Containing Alternative Positive and Hydrophobic Residues as Molecular Transporters

Sorour Khayyatnejad Shoushtari
Chapman University, khayyatnejadshoushta@chapman.edu

Hybrid Cyclic-Linear Cell-Penetrating Peptides Containing Alternative Positive and Hydrophobic Residues as Molecular Transporters

A Thesis by

Sorour Khayyatnejad Shoushtari

Chapman University

Irvine, CA

School of Pharmacy

Submitted in partial fulfillment of the requirements for the degree of

Master of Science in Pharmaceutical Sciences

August 2021

Committee in charge:

Keykavous Parang, Pharm.D., Ph.D.,Chair

Rakesh Tiwari, Ph.D.

Hamidreza Montazeri Aliabadi, Ph.D.

The thesis of Sorour Khayyatnejad Shoushtari is approved.

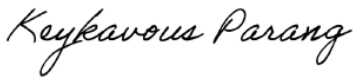

Keykavous Parang, Pharm.D., Ph.D., Chair

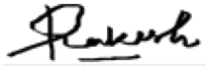

Rakesh Tiwari, Ph.D.

Hamidreza Montazeri Aliabadi, Ph.D.

June 2021

Hybrid Cyclic-Linear Cell-Penetrating Peptides Containing Alternative Positive and Hydrophobic Residues as Molecular Transporters

by Sorour Khayyatnejad Shoushtari

ACKNOWLEDGMENT

First and foremost, I would like to express the deepest appreciation to my supervisor Dr. Keykavous Parang for his invaluable advice, continuous support, and patience during my master's study. Without his timely suggestions, prompt response, kindness, this thesis would not have been possible. Also, I would thank my esteemed committee member, Dr. Tiwari, for his guidance and persistent help. He is a very welcoming person, especially when I had so many questions in my mind, and thanks for all his encouragement to keep me on the path. My sincere thanks also go to Dr. Montazeri for letting me choose him as my committee member and for all his constructive feedback. I thank my fellow lab members for their guidance and patience. Last but not least, I owe a tremendous sense of gratitude to my wonderful husband, Ramtin, for supporting and encouraging me spiritually all through my study.

ABSTRACT

Hybrid Cyclic-Linear Cell-Penetrating Peptides Containing Alternative Positive and Hydrophobic Residues as Molecular Transporters

by Sorour Khayyatnejad Shoushtari

The cell membrane properties create a significant obstacle in intracellular delivery of cell-impermeable and negatively charged molecules. Amphiphilic cyclic peptides containing alternative arginine and tryptophan such as $[WR]_5$ have been shown to enhance the transport of cargo molecules across the cell membrane. Herein, we report the synthesis and biological evaluation of a novel series of hybrid cyclic-linear peptides containing alternative positive and hydrophobic amino acids on the ring and side-chain $[(RW)_5]K(RW)_X$ (X=1-5) to compare their molecular transporter efficiency. The peptides were synthesized through Fmoc solid-phase peptide synthesis. Final compounds were purified by a reversed-phase HPLC (high performance liquid chromatography). The chemical structures of the final products were confirmed by MALDI-TOF (Matrix Assisted Laser Desorption/Ionization).

In vitro cytotoxicity of the peptides was evaluated in human leukemia carcinoma cell line (CCRF-CEM), human ovarian adenocarcinoma cells (SK-OV-3), human epithelial embryonic kidney healthy (HEK-293), and human epithelial mammary gland adenocarcinoma cells (MDA-MB-231) using the MTS assay. The peptides did not exhibit any significant cytotoxicity at the concentration of 10 μM in CCRF-CEM, HEK-293, MDA-MB-231, and SK-OV-3 cells after 3 h incubation.

The cellular uptake of a fluorescence-labeled phosphopeptide (F′-GpYEEI) and anti-HIV drugs (lamivudine (F′-3TC), emtricitabine (F′-FTC), Stavudine (F′-d4T)), where F′ is carboxyfluorescein, were measured in the presence of the peptides in CCRF-CEM and SK-OV-3 cells. Among all peptides, $[(RW)_5K](RW)_5$ (10 μM) was the most efficient transporter and improved the cellular uptake of F′-GpYEEI (2 μM) by 18 and 11-fold in CCRF-CEM and SK-OV-3, respectively, when compared with F′-GpYEEI alone and in the presence of $[WR]_5$.

The cellular uptake of F′-$[(RW)_5K](RW)_5$ was increased in a time- and concentration-dependent manner. The FACS (fluorescence-activated cell sorting) analysis and confocal microscopy results indicate that the cellular uptake of fluorescent-labeled peptide (F'-$[(RW)_5K](RW)_5$) was partially inhibited by chlorpromazine endocytosis inhibitors after 3 h incubation in MDA-MB-231 cells, which suggests the partial uptake through the clathrin-mediated endocytosis pathway. Intracellular localization (mostly in the cytosol) of F'-$[(RW)_5K](RW)_5$ after 3 h incubation in MDA-MB-231 cells was confirmed by confocal microscopy. These data suggest the potential of this series of hybrid cyclic-linear peptides compared to $[WR]_5$ as molecular transporters of large molecules, such as a negatively charged phosphopeptide.

TABLE OF CONTENTS

LIST OF TABLES

LIST OF FIGURES

LIST OF SCHEMES

LIST OF ABBREVIATIONS

ATCC	American Type Culture Collection
ACN	Acetonitrile
Boc	Tert-butyloxycarbonyl group
CCRF-CEM	Human leukemia carcinoma cell line
CPPs	Cell-penetrating Peptides
DCM	Dichloromethane
Dde	1-(4,4-Dimethyl-2,6-dioxocyclohexylidene)ethyl
DTT	Dithiothreitol
DIC	*N*,*N'*-Diisopropylcarbodiimide
DIPEA	*N*,*N*-Diisopropylethylamine
DMF	*N*,*N*-Dimethylformamide
Dox	Doxorubicin
FAM	5(6)-carboxyfluorescein
F´-3TC	Fluorescence-labeled lamivudine
F´-d4T	Fluorescence-labeled stavudine
F´-FTC	Fluorescence-labeled emtricitabine
F´-GpYEEI	Fluorescence-labeled phosphopeptide
FACS	Fluorescence Activated Cell Sorting
FBS	Fetal Bovine Serum
FITC	Fluorescein isothiocyanate isomer I
Fmoc	*N*-Fluorenylmethoxycarbonyl
HBTU	2-(1H-benzotriazol-1-yl)-1,1,3,3tetramethyluroniuhexa fluorophosphate
HEK-293	Human epithelial embryonic kidney healthy
Hela	Human epithelial cervix adenocarcinoma cells
HIV	Human immunodeficiency virus
HOAt	1-Hydroxy-7-azabenzotriazole
HPLC	High Performance Liquid Chromatography
K	Lysine
MALDI	Matrix-Assisted Laser Desorption/Ionization
MDA-MB-231.	Human epithelial mammary gland adenocarcinoma cells
PBS	Phosphate-Buffered Saline
PLGA	Poly lactic-glycolic acid;

R	Arginine
siRNA	Oligonucleotides
SK-OV-3	Human ovarian adenocarcinoma
SPPS.	Solid-phase synthesis
TFA	Trifluoroacetic Acid
W	Tryptophan

CHAPTER 1

Background, Significance, and Aims

Introduction

Statement of Problem

A negatively charged and highly hydrophobic phospholipid bilayer membrane is crucial for the cell's survival and functions. These structures protect living cells from the outside environment, only allowing mainly the entrance of the small molecular size compounds inside the cell [1]. The plasma membrane presents a significant challenge in delivering many biologically active agents, such as macromolecules, negatively charged molecules, and some hydrophilic agents, which cannot appropriately reach the target site efficiently [2]. To overcome this limitation and subverting the membrane barrier, promising cellular delivery systems are needed. Numerous drug delivery systems have been developed to overcome physicochemical problems and biological obstacles with controlled release formulations for clinical applications, such as liposome, polylactic-glycolic acid, and cell-penetrating peptides.

Liposomes have been frequently studied as drug delivery carriers because they have the potential to achieve the goals of delivery when properly produced [3]. Although encapsulating the drugs inside the liposome can decrease the toxicity and increase drug delivery efficiency, drug leakage and aggregation have been seen for very hydrophilic anticancer medicines like doxorubicin (Dox) [4]. Moreover, Liposomes are recognized as foreign objects by the mononuclear phagocytic system (MPS). As a result, they are cleared from the bloodstream [5]. Polyethylene glycol (PEG)-liposomal Dox is a formulation of the anthracycline Dox, in which the drug is encapsulated in PEG-coated liposome, reducing the percentage of uptake by macrophages and improving blood circulation time [6]. However, PEGylation leads to a significant decrease in cellular uptake and endosomal escape [7].

Polylactic-glycolic acid (PLGA) is one of the most popular biodegradable polymers since its hydrolysis leads to metabolite monomers, lactic acid, and glycolic acid. PLGA is approved by the FDA, and also, it has minimal systemic toxicity because its two monomers are endogenous and easily metabolized by the body via the Krebs cycle [8]. However, they are some limitations associate with their applications in drug delivery. The acidic degradation of PLGA decreases the local pH, which leads to suppressing protein degradation during release and preventing protein aggregation and deactivation during the harsh encapsulation process [9]. They are many factors affecting PLGA degradation and drug release, such as the effect of composition, crystallinity, molecular weight, drug type, size and shape of a matrix, pH, enzymes, and drug load. These factors should be considered to adjust the degradation and drug release mechanism for the desired application [10]. It has been reported that PLGA-based nanoparticles have some drawbacks, such as low drug loading described for many drugs, the high cost of production, and the difficulty of the scale-up [11].

Cell-Penetrating Peptides (CPPs)

Using an efficient and safe drug delivery system can modify the efficacy and toxicity of anticancer drugs and cell impermeable compounds like negatively charged phosphopeptides and siRNA (small interfering Ribonucleic Acid). The discovery of cell-penetrating peptides (CPPs) is one of the breakthroughs of the last 20 years [12] as a promising class of peptide carriers that are capable of internalization into cells without interruption of the plasma membrane [13]. CPPs are short, positively charged molecules with 5-30 amino acids abundant in lysine or arginine residues that have the potential to facilitate cellular internalization and load a wide variety of cargos. CPPs are also known as protein transduction domains (PTDs) [14].

Biocompatibility, bioactivity, and the unique structural properties of some of the CPPs allow them to cross the cell membrane without showing cytotoxicity at their experimental concentration.

Previous studies have introduced a homochiral cyclic peptide $[WR]_5$ containing alternative arginine (R) and tryptophan (W) residues as a molecular transporter of bioactive compounds. The data showed that the presence of alternative positively charged and hydrophobic residues significantly improved the cellular permeability of several compounds, such as phosphopeptides and siRNA, without causing cytotoxicity at the experimental concentration [15-16]. This project aims to determine the structure-activity relationship of a new class of hybrid peptides composed of a linear chain attached to the cyclic peptide. Both the linear and cyclic components contain the appropriate alternative positively charged and hydrophobic residues. To the best of our knowledge, this is the first report of hybrid cyclic-linear peptides containing alternative arginine and tryptophan residues.

Hybrid cyclic-linear peptides

Hybrid cyclic-linear peptides are a new generation of peptides that combine the cyclic ring linked through the linker to the linear tail. It is expected that they should have more stability against the protease than the corresponding linear peptides alone because of the presence of cyclic components.

Oh et al. synthesized novel acylated cyclic polyarginine peptides and examined them as CPPs and potential molecular transporters. The peptides consisted of a class of nine different linear and hybrid cyclic-linear polyarginine peptides containing 5 and 6 arginines, namely, R5 and R6, which were attached to the long-chain fatty acids through the lysine linker. Acylated cyclic

polyarginine peptides showed higher potency as molecular transporter of fluorescence-labeled phosphopeptide (F'-GpYEEI) than the corresponding linear counterparts and cyclic polyarginine peptides without fatty acid. The mechanistic studies showed the energy-dependent endocytosis pathways as a major cellular uptake mechanism. Cyclization and acylation reactions on the peptide structure enhanced the intracellular uptake of polyarginine peptides even they carried a short length of sequence [17].

In another effort, Do et al. reported the synthesis number of amphiphilic difatty acyl linear and cyclic R_5K_2 peptide conjugates to increase the siRNA delivery. The flow cytometry demonstrated that among all synthesized peptides, the LP-C16, LP-C18, and CP-C16 with 1,2-dioleoyl-sn-glycero-3-phosphoethanolamine (DOPE) addition, significantly improved internalization of fluorescence-labeled siRNA (FAM-siRNA). The results from the study suggested the potential optimization of difatty acyl peptide/lipid nanoparticles is required for effective siRNA delivery [18]

Hall et al. designed a multicomponent siRNA delivery composed of linear or cyclic fatty acyl peptide conjugates and hybrid cyclic/linear peptides, namely LP-C18, CP-C18, $[R_5K]W_5$, $[R_6K]W_6$, and $[R_5K]W_7$ containing four different PLANA formulations (A−D). The results showed that PLANAs C and D improved the cellular uptake of siRNA with 80-90% siRNA-positive cells for LP-C18, CP-C18, $[R_5K]W_5$, and $[R_6K]W_6$ [19].

Ichimizu et al. studied a series of palmitoyl-poly-arginine peptides (CPPs) containing the cyclic polyarginine and palmitic acid linear tail. They evaluated and reported the cell-penetrating effects after forming a complex with HSA (human serum albumin) for use in intracellular drug delivery. The number of arginine residues, shapes (linear or cyclic), stereochemistry (L- or D-isoform) of the poly-arginine peptide backbone was optimized by examining the structure-activity

relationship. The result from the flow cytometry indicated that the cellular uptake of HSA was enhanced by increasing the number of arginine residues. The cyclic peptide exhibited higher cellular uptake compared to the corresponding linear counterpart, and the ability of cell-penetrating was also improved by D-arginine compared to the L-form of arginine. As a result, among all evaluated CPPs, a cyclic polypeptide made up D-dodecaarginines, palmitoyl-cyclic-$(D\text{-}Arg)_{12}$ was the most efficient and improved the cellular uptake of HSA in HeLa cells. Macropinocytosis was responsible for the majority of the cellular uptake of the palmitoyl-cyclic-$(D\text{-}Arg)_{12}$/HSA complex, with the minor involvement of clathrin-mediated endocytosis. The pharmacological activity results showed that palmitoyl-cyclic-$(D\text{-}Arg)_{12}$/HSA, which was used for loading a number of drugs in three different modes (a) an HSA-paclitaxel non-covalent complex, b) an HSA-doxorubicin covalent conjugate, and c) an HSA-thioredoxin fusion protein), greatly increased cell-penetrating efficiency along with significant enhancement in pharmacological activity [20].

Traboulsi et al. designed a series of macrocyclic arginine-rich cell-penetrating peptides by adjusting the ring size, site of cyclization, and stereochemistry of the arginine residues and studied their structure−uptake relationship using a combination of flow cytometry and confocal microscopy. The FITC labeled of the peptides were synthesized to evaluate their cellular penetration properties through flow cytometry and confocal microscopy in Hela cells. In order to determine the effect of stereochemistry and mode of cyclization, the cellular uptake studies of the various fluorescent-labeled macrocyclic peptides with different numbers of residues on the endo- and exocyclic position were performed. The results showed that the fluorescent-labeled macrocycle contained 4 endocyclic and 3 exocyclic arginine residues displayed a stronger signal compared with the other peptides of this family [21].

Mozaffari et al. showed that hybrid cyclic-linear peptides containing arginine residues on the ring and tryptophan residues on the side chain, $[R_6K]W_6$ and $[R_5K]W_5$, could improve the delivery of siRNA. $[R_6K]W_6$ showed the highest cellular uptake in MDA-MB-231 cells. The presence of positively charged on the ring and hydrophobic residues on the side chain improved the interaction with the negatively charged phosphate and hydrophobic chains in the cellular phospholipid bilayer, respectively, and enhanced cellular delivery of siRNA [22].

Hypothesis and Rationale

Despite some of the CPPs' ability to transport other molecules and their low cytotoxicity, there are some limitations associated with their use. One of the drawbacks of CPPs is endosomal entrapment. To release the CPPs from endosomes, additional auxiliary compounds or charged polymers may be required. Furthermore, there may be some cytotoxicity associated with these auxiliary compounds [23]. Thus, the novel CPPs with specific sequences and optimal balance of positively-charged and hydrophobic residues are needed to bypass endosomal uptake and improve the internalization of cell-impermeable compounds, such as phosphopeptides oligodeoxynucleotides and other drugs. Cyclic peptide $[WR]_5$ containing alternative arginine (R) and tryptophan (W) residues has been previously reported to bypasses the endosomal uptake and to significantly enhance the cellular uptake of cell-impermeable compounds [15-16]. In general, the cyclic nature of the peptide improves the stability against proteases versus linear CPPs [23].

The hypothesis underlying this project is that hybrid cyclic-linear peptides containing alternative positive and hydrophobic amino acids will act as more efficient CPPs and molecular transporters versus the corresponding either cyclic or linear peptides. The cyclic ring's sequence maintenance was inspired by the previously reported cyclic peptide, $[WR]_5$ [15], and the addition

of the linear side-chain with alternative positive and hydrophobic residues led to the generation of new hybrid-cyclic linear peptides. The objective of this research was to determine the optimal sequence of hybrid cyclic-linear peptides containing alternate positive and hydrophobic residues that can enhance the cellular uptake of the drugs and to establish the structure-activity relationship. This project has three specific Aims:

Specific Aim 1. Design and synthesize hybrid cyclic-linear cell-penetrating peptides containing alternative positive and hydrophobic residues.

Five hybrid cyclic-linear peptides containing alternative arginine and tryptophan residues, namely, $[(RW)_5K](RW)$, $[(RW)_5K](RW)_2$, $[(RW)_5K](RW)_3$, $[(RW)_5K](RW)_4$, $[(RW)_5K](RW)_5$ (Figure 1) were synthesized through Fmoc solid-phase chemistry followed by the cyclization in the solution phase. The linear peptides were assembled on the solid phase. The free *N*-terminal of the last amino acid was capped with acetic anhydride to prevent the undesired reaction. After resin cleavage, the cyclization occurred between the free amino group of lysine with the carboxylic acid of the *C*-terminal arginine. The final deprotection of the side chains was afforded the hybrid peptides. The corresponding linear peptides namely, $(RW)_5K(RW)$, $(RW)_5K(RW)_2$, $(RW)_5K(RW)_3$, $(RW)_5K(RW)_4$, and $(RW)_5K(RW)_5$ were synthesized as controls (Figure 2).

The rationale of this design is based on the presence of alternate positively charged residues of arginine and hydrophobic residues of tryptophan, which assist in cellular penetration. The guanidinium group of arginine allows interaction with the cell membrane in three possible directions resulting in better interactions of the peptide with the cell surface through a large number of electrostatic interactions with a negatively charged phosphate group of the cell membrane [24]. Moreover, the peptide internalization can improve by the interaction between hydrophobic

tryptophan residues and the cell membrane lipids, which lead to disruption of the outer phospholipid monolayer [25]. The numbers of the arginine and tryptophan residues on the side chain were modified to determine the optimal number of amino acids for the most efficient cellular uptake. The study allowed us to examine whether conjugating of a linear chain through a lysine linker to the cyclic peptide and increasing the number of alternative arginine and tryptophan residues on the linear tail can improve the cellular uptake of the cell-impermeable compounds versus $[WR]_{5,}$ which has been shown to lead to a significant improvement in cellular uptake. The synthesized peptides had a cyclic component since the cyclic peptides are more stable compared to the linear ones against proteases [23].

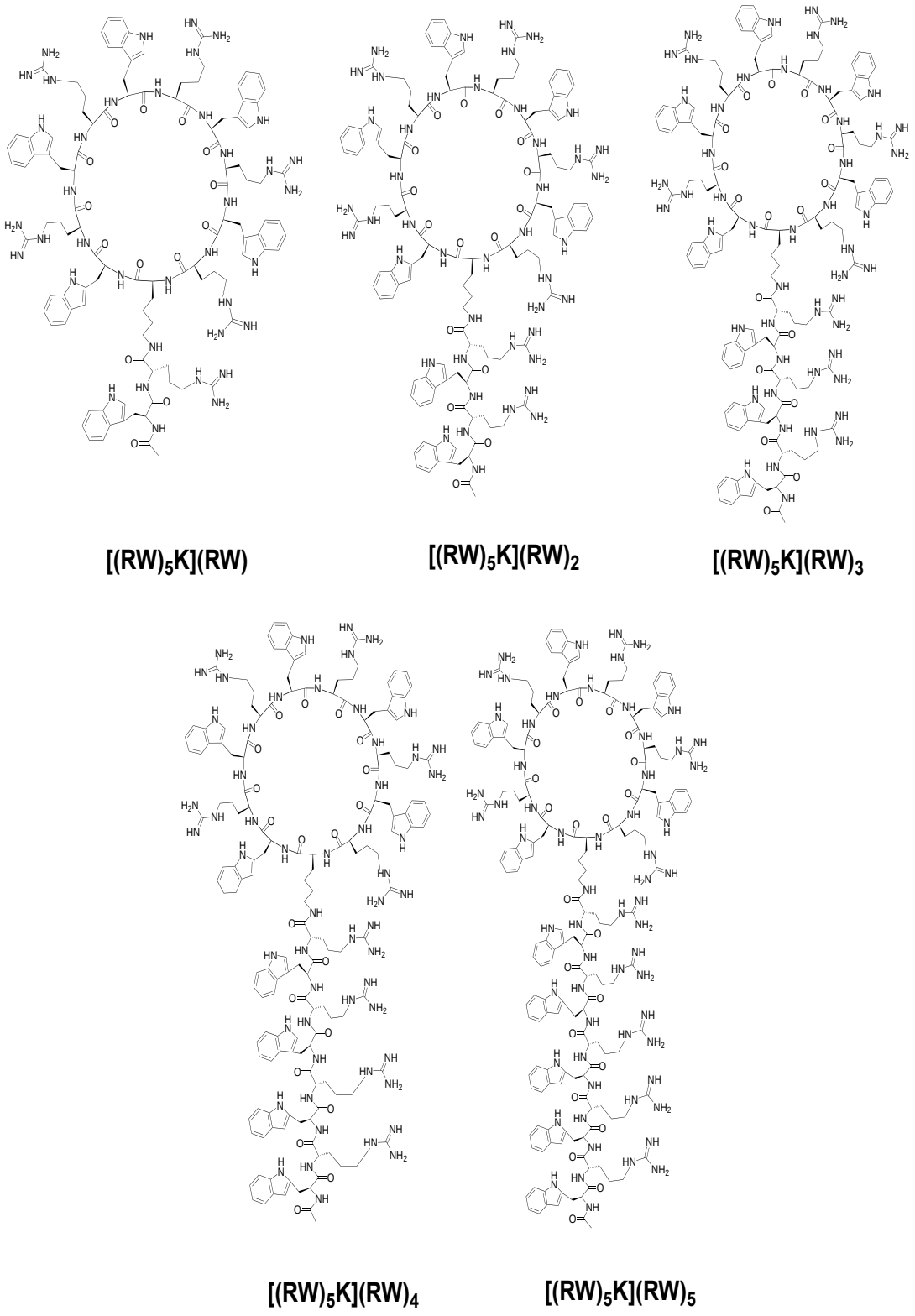

Figure 1. Chemical structures of synthesized cyclic peptides.

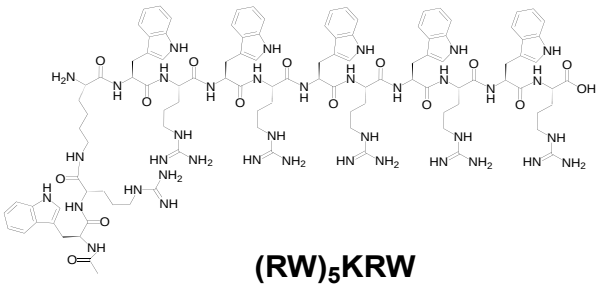

$(RW)_5KRW$

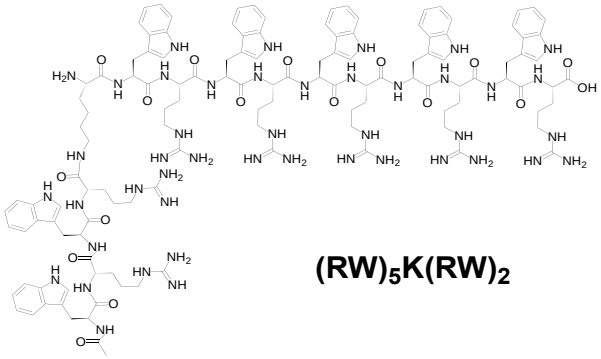

$(RW)_5K(RW)_2$

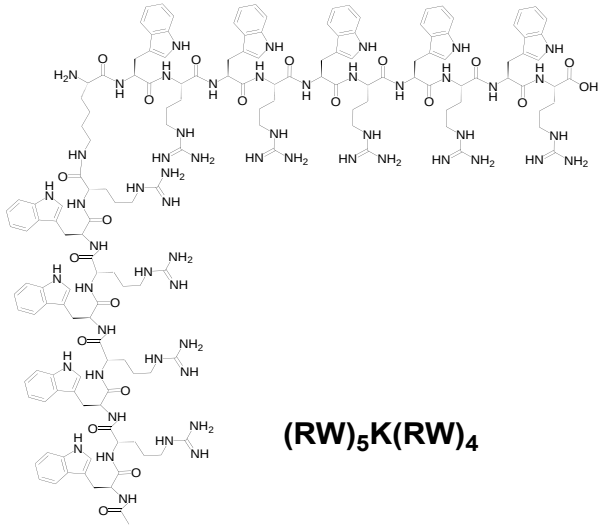

$(RW)_5K(RW)_4$

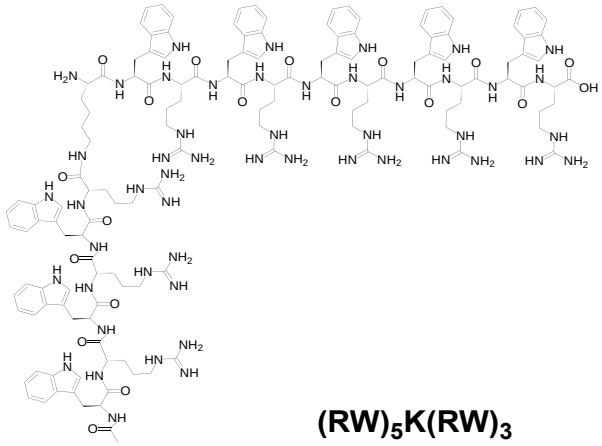

$(RW)_5K(RW)_3$

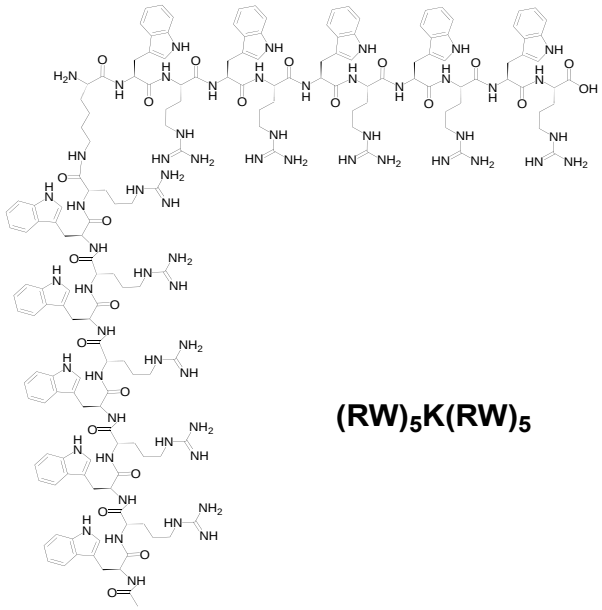

$(RW)_5K(RW)_5$

Figure 2. Chemical structures of synthesized linear peptides.

A**im 2. Evaluate cytotoxicity and molecular transporter properties of the cell-impermeable compounds.**

The cytotoxicity of synthesized hybrid cyclic-linear peptides in different concentrations was determined by the MTS (AQueous one solution cell proliferation) assay. This assay was performed to quantify cell proliferation in CCRF-CEM (ATCC# CCL-119, leukemia cell line), HEK 293 (ATCC# CRL-1573, human embryonic kidney 293 cell line), SK-OV-3 cells (ATCC# HTB-77, ovarian adenocarcinoma), and MDA-MB-231 (ATCC No. HTB-26, human epithelial mammary gland/breast adenocarcinoma cells). After the determination of an appropriate non-toxic concentration for each peptide, the cellular uptake studies were conducted by using the non-toxic concentration of all peptides to determine the cellular uptake of the physical mixture of fluorescence-labeled phosphopeptides (F′-GpYEEI) and anti-HIV drugs (lamivudine (F′-3TC), emtricitabine (F′-FTC)), and stavudine (F′-d4T)), where F′ is carboxyfluorescein, with the synthesized peptides in cancer cells. The studies were also performed in the absence of the synthesized peptide as control and comparing the efficiency of the hybrid peptides as a molecular transporter. A peptide with the best cellular uptake and optimal structure-activity relationship was selected to determine the cellular uptake mechanism.

Aim 3. Determination of cellular uptake mechanism of the peptides.

The two major cellular uptake mechanisms include direct penetration and endocytosis. Pore formation, inverted micelle formation, and carpet-like model are different mechanisms that have been described by direct penetration. The initial stage of all of these mechanisms is the interaction of positively charged CPPs with negatively charged membrane components through an energy-independent pathway [26]. Endocytosis is an energy-dependent pathway in which the

entrapment of some compounds in endosomes prevents them from reaching the target site in the cytoplasm or nucleus and decreases bioavailability [15]. The optimal approach is needed to promote endosome escape or bypassing the endosomal uptake. For this purpose, the fluorescence-labeled analog of the selected hybrid cyclic-linear peptide was synthesized. The cellular uptake of the fluorescence-labeled selected peptide was investigated in the presence and absence of different endocytosis inhibitors. Endosomal inhibitors, such as chloroquine, chlorpromazine, Methyl-β-cyclodextrin, and nystatin, were used to inhibit energy-dependent cellular uptake. Confocal microscopy was used to reveal the localization of the fluorescence-labeled peptide and confirm the results of mechanistic studies from flow cytometry.

Justification and significance of the study

The impermeability of biological membranes is a significant challenge in drug delivery. Many useful therapeutic agents are either cell-impermeable macromolecules or highly hydrophilic compounds that are not able to penetrate the plasma without interruption of the cell membrane [27]. With the arrival of CPPs in the drug delivery field, the limitations of the other drug delivery systems may be overcome. Owing to the biocompatibility, bioactivity, ease of synthesis, and functionalization of CPPs, they are found to be promising candidates for intracellular delivery. Improved stability and efficient cellular penetration of the cyclic CPPs make them suitable alternatives to linear counterparts [25]. By covalent and non-covalent (physical mixture) attachment of CPPs to bioactive cargos, effective delivery of molecules of interest into the cell can be achieved [28]. As a result, the design of alternated clinically effective and non-toxic drug delivery systems are urgently required.

Previous studies have shown that cyclic peptide $[WR]_5$ containing alternative positively charged and hydrophobic residues could efficiently improve the cellular uptake of some cell-impermeable compounds by the interaction between the arginine and negatively charged phospholipids and tryptophan chain with hydrophobic residues of the phospholipid bilayer [15]. The data confirmed that cyclic peptides containing alternating tryptophan and arginine residues, $[WR]_4$ and $[WR]_5$, improved the cellular uptake of compounds, such as anti-HIV drugs, Dox, phosphopeptides, and siRNA or generated peptide nanostructures [29]. Another study showed that hybrid cyclic-linear peptides containing arginine residues on the ring and tryptophan residues on the side chain, $[R_6K]W_6$ and $[R_5K]W_5$, could improve the delivery of siRNA [22] Further studies were required to find the optimal structure of hybrid cyclic-linear peptide by maintaining the $[WR]_5$ scaffold to improve the molecular transporter properties. Our studies were conducted to identify the optimal sequence by adding the linear tail containing the alternate W and R residues, to generate the new hybrid cyclic-linear peptides, and to determine the effect of the increasing number of arginine and tryptophan on the linear tail on the permeability of the cell membrane. Herein, we focused on the structure-cellular uptake relationship of $[(RW)_5K](RW)_x$ analogs to determine the optimal number of arginine and tryptophan residues on the linear tail for efficient molecular transporter properties. The data indicated that $[(RW)_5K](RW)_5$ was the most efficient molecular transporter among all the tested peptides, as shown by the delivery of the fluorescence-labeled phosphopeptide (F'-GpYEEI) and antiviral drugs. The cellular uptake of the fluorescence-labeled of the peptide exhibited time- and concentration-dependent uptake and localization mostly in the cytosol of CPPs. The work here introduces a new generation of CPPs with potential biomedical applications. These studies advance scientific knowledge in the area of developing more efficient and less cytotoxic CPPs.

References

1. Watson, H. (2015). Biological membranes. *Essays in Biochemistry, 59*, 43-69. doi:10.1042/bse0590043
2. Zhang, R., Qin, X., Kong, F., Chen, P., & Pan, G. (2019). Improving cellular uptake of therapeutic entities through interaction with components of cell membrane. *Drug Delivery, 26*(1), 328-342. doi:10.1080/10717544.2019.1582730
3. Olusanya, T., Haj Ahmad, R., Ibegbu, D., Smith, J., & Elkordy, A. (2018). Liposomal drug delivery systems and anticancer drugs. *Molecules, 23*(4), 907. doi:10.3390/molecules23040907
4. Akbarzadeh, A., Rezaei-Sadabady, R., Davaran, S., Joo, S. W., Zarghami, N., Hanifehpour, Y., Nejati-Koshki, K. (2013). Liposome: classification, preparation, and applications. *Nanoscale Research Letters, 8*(1). doi:10.1186/1556-276x-8-102
5. Suk, J. S., Xu, Q., Kim, N., Hanes, J., & Ensign, L. M. (2016). PEGylation as a strategy for improving Nanoparticle-based drug and gene delivery. *Advanced Drug Delivery Reviews, 99*, 28-51. doi:10.1016/j.addr.2015.09.012
6. Romberg, B., Hennink, W. E., & Storm, G. (2007). Sheddable coatings for long-circulating Nanoparticles. *Pharmaceutical Research, 25*(1), 55-71. doi:10.1007/s11095-007-9348-7
7. Nosova, A. S., Koloskova, O. O., Nikonova, A. A., Simonova, V. A., Smirnov, V. V., Kudlay, D., & Khaitov, M. R. (2019). Diversity of PEGylation methods of liposomes and their influence on RNA delivery. *MedChemComm,10*(3), 369-377. doi:10.1039/c8md00515j

8. Danhier, F., Ansorena, E., Silva, J. M., Coco, R., Le Breton, A., & Préat, V. (2012). PLGA-based nanoparticles: An overview of biomedical applications. *Journal of Controlled Release, 161*(2), 505-522. doi:10.1016/j.jconrel.2012.01.043
9. McDonough, J., Dixon, H., & Ladika, M. (2010). Nasal delivery of micro- and nano-encapsulated drugs. *Handbook of Non-Invasive Drug Delivery Systems*, 193-208. doi:10.1016/b978-0-8155-2025-2.10008-3
10. Makadia, H. K., & Siegel, S. J. (2011). Poly lactic-co-glycolic Acid (PLGA) as biodegradable controlled drug delivery carrier. *Polymers, 3*(3), 1377-1397. doi:10.3390/polym3031377
11. Danhier, F., Ansorena, E., Silva, J. M., Coco, R., Le Breton, A., & Préat, V. (2012). PLGA-based nanoparticles: An overview of biomedical applications. *Journal of Controlled Release, 161*(2), 505-522. doi:10.1016/j.jconrel.2012.01.043
12. Jobin, M.-L., Blanchet, M., Henry, S., Chaignepain, S., Manigand, C., Castano, S., Lecomte, S., Burlina, F., Sagan, S., & Alves, I. D. (2015). The role of tryptophans on the cellular uptake and membrane interaction of arginine-rich cell penetrating peptides. *Biochimica Et Biophysica Acta (BBA) - Biomembranes*, *1848*(2), 593–602. https://doi.org/10.1016/j.bbamem.2014.11.013
13. Jafari, S., Maleki Dizaj, S., & Adibkia, K. (2017). Cell-penetrating peptides and their analogues as novel nanocarriers for drug delivery. *BioImpacts, 5*(2), 103-111. doi:10.15171/bi.2015.10
14. Javadzadeh, Y., & Azharshekoufeh Bahari, L. (2017). Therapeutic nanostructures for dermal and Transdermal drug delivery. *Nano- and Microscale Drug Delivery Systems,* 131-146. doi:10.1016/b978-0-323-52727-9.00008-x

15. Mandal, D., Shirazi, A.N., & Parang, K. (2011). Cell-penetrating homochiral cyclic peptides as nuclear-targeting molecular transporters. *Angewandte Chemie, 123*(41), 9807-9811. doi:10.1002/ange.201102572
16. Shirazi, A.N., Tiwari, R. K., Oh, D., Banerjee, A., Yadav, A., & Parang, K. (2013). Efficient delivery of cell impermeable phosphopeptides by a cyclic peptide amphiphile containing tryptophan and arginine. *Molecular Pharmaceutics, 10*(5), 2008-2020. doi:10.1021/mp400046u
17. Oh, D., Shirazi, A.N., Northup, K., Sullivan, B., Tiwari, R. K., Bisoffi, M., & Parang, K. (2014). Enhanced cellular uptake of short polyarginine peptides through fatty acylation and cyclization. *Molecular Pharmaceutics,11*(8), 2845-2854. doi:10.1021/mp500203e
18. Do, H., Sharma, M., El-Sayed, N. S., Mahdipoor, P., Bousoik, E., Parang, K., & Montazeri Aliabadi, H. (2017). Difatty acyl-conjugated linear and cyclic peptides for Sirna delivery. *ACS Omega, 2*(10), 6939-6957. doi:10.1021/acsomega.7b00741
19. Hall, R., Alasmari, A., Mozaffari, S., Mahdipoor, P., Parang, K., & Montazeri Aliabadi, H. (2021). Peptide/Lipid-Associated nucleic Acids (PLANAS) as a multicomponent Sirna delivery system. *Molecular Pharmaceutics,18*(3), 986-1002. doi:10.1021/acs.molpharmaceut.0c00969
20. Ichimizu, S., Watanabe, H., Maeda, H., Hamasaki, K., Nakamura, Y., Chuang, V. T., Kinoshita, R., Nishida, K., Tanaka, R., Enoki, Y., Ishima, Y., Kuniyasu, A., Kobashigawa, Y., Morioka, H., Futaki, S., Otagiri, M., & Maruyama, T. (2018). Design and tuning of a cell-penetrating albumin derivative as a versatile nanovehicle for intracellular drug delivery. *Journal of Controlled Release, 277*, 23–34. https://doi.org/10.1016/j.jconrel.2018.02.037

21. Traboulsi, H., Larkin, H., Bonin, M., Volkov, L., Lavoie, C. L., & Marsault, É. (2015). Macrocyclic cell penetrating Peptides: A study of structure-penetration properties. *Bioconjugate Chemistry, 26*(3), 405-411. doi:10.1021/acs.bioconjchem.5b00023
22. Mozaffari, S., Bousoik, E., Amirrad, F., Lamboy, R., Coyle, M., Hall, R., Alasmari, A., Mahdipoor, P., Parang, K., & Montazeri Aliabadi, H. (2019). Amphiphilic Peptides for Efficient siRNA Delivery. *Polymers*, *11*(4), 703. https://doi.org/10.3390/polym11040703
23. Reissmann, S. (2014). Cell penetration: Scope and limitations by the application of cell-penetrating peptides. *Journal of Peptide Science, 20*(10), 760-784. doi:10.1002/psc.2672
24. Sokalingam, S., Raghunathan, G., Soundrarajan, N., & Lee, S. (2012). A study on the effect of surface lysine to arginine mutagenesis on protein stability and structure using green fluorescent protein. *PLoS ONE, 7*(7). doi:10.1371/journal.pone.0040410
25. Park, S. E., Sajid, M. I., Parang, K., & Tiwari, R. K. (2019). Cyclic cell-penetrating peptides as efficient intracellular drug delivery tools. *Molecular Pharmaceutics, 16*(9), 3727-3743. doi:10.1021/acs.molpharmaceut.9b00633
26. Derakhshankhah, H., & Jafari, S. (2018). Cell penetrating peptides: A concise review with emphasis on biomedical applications. *Biomedicine & Pharmacotherapy, 108,* 1090-1096. doi:10.1016/j.biopha.2018.09.097
27. Derossi, D., Chassaing, G., & Prochiantz, A. (1998). Trojan peptides: The penetratin system for intracellular delivery. *Trends in Cell Biology, 8*(2), 84-87. doi:10.1016/s0962-8924(98)80017-2

28. Koren, E., & Torchilin, V. P. (2012). Cell-penetrating peptides: breaking through to the other side. *Trends in Molecular Medicine, 18*(7), 385-393. doi:10.1016/j.molmed.2012.04.012

29. Hanna, S. E., Mozaffari, S., Tiwari, R. K., & Parang, K. (2018). Comparative molecular transporter efficiency of cyclic Peptides containing tryptophan and arginine residues. *ACS Omega, 3*(11), 16281-16291. doi:10.1021/acsomega.8b02589

CHAPTER 2

Design and Evaluation of Hybrid Cyclic-Linear Cell-Penetrating Peptides Containing Alternative Positive and Hydrophobic Residues As Molecular Transporters of the Cell-Impermeable Compounds

Abstract

Five hybrid cyclic-linear peptides containing alternative arginine and tryptophan residues, namely, [$(RW)_5$K](RW), [$(RW)_5$K]$(RW)_2$, [$(RW)_5$K]$(RW)_3$, [$(RW)_5$K]$(RW)_4$, [$(RW)_5$K]$(RW)_5$, and their corresponding linear peptides were synthesized through Fmoc solid-phase chemistry. The NH_2-Arg(Pbf)-2-chlorotrityl resin was used as the solid support for the linear peptide synthesis. The coupling of the residues was accomplished in the presence of HBTU and DIPEA. After the resin cleavage, the cyclization was performed in the presence of DIC and HOAT in the solution phase to afford hybrid cyclic-linear peptides. Furthermore, [$(RW)_5$K]$(RW)_5$ was conjugated with fluorescein isothiocyanate isomer I (FITC) through β-alanine to afford fluorescently-labeled conjugate F′-[$(RW)_5$K]$(RW)_5$, where F′ is fluorescein, in the solution phase. High-resolution MALDI-TOF and Q-TOF were used to confirm the chemical structure of the final product. All the peptides were purified using reversed-phase High-Performance Liquid Chromatography (HPLC). A cell viability assay (MTS) was employed in three different cancer cell lines to evaluate the cytotoxicity of synthesized linear and hybrid cyclic-linear peptides, including CCRF-CEM, SK-OV-3, MDA-MB-231 cells, and one normal cell (HEK-293). The peptides did not exhibit any significant cytotoxicity at 10 μM and 3 h incubation. Cellular uptake studies were performed by FACS (fluorescence-activated cell sorting) using CCRF-CEM and SK-OV-3 cells to measure the cellular uptake of a fluorescence-labeled phosphopeptide (F´-GpYEEI), and anti-HIV drugs (lamivudine (F´-3TC), emtricitabine (F´-FTC), stavudine (F´-d4T)) in the presence of hybrid cyclic-linear peptides (10 μM) after 3h incubation. The cellular uptake was enhanced by increasing the number of arginine and tryptophan in the sequence. Among all peptides, [$(RW)_5$K]$(RW)_5$ (10 μM) was the most efficient molecular transporter and improved the cellular uptake of F′-GpYEEI (2 μM) by 18 and 11-fold in CCRF-CEM and SK-OV-3,

respectively, when compared with F′-GpYEEI alone. $[(RW)_5K](RW)_5$ showed to be a significantly more efficient transporter than other synthesized peptides here and $[WR]_5$ in the delivery of a larger linear phosphopeptide F′-GpYEEI in comparison to small molecules (i.e. F´-3TC, F´-FTC, and F´-d4T).

1. Background

According to estimates from the World Health Organization (WHO), cancer is the second leading cause of death globally (about 1 death in 6) [1]. One of the major obstacles to finding effective therapeutics against cancer is the inefficiency of drug delivery systems. One reason for this could be the therapeutic agents' inability to cross the plasma membrane of cancer cells, a semi-permeable hydrophobic layer that separates the cell from the outside environment. Diffusion allows small hydrophobic molecules to pass across the cell membrane. Hydrophilic molecules immersed in the blood or bound to plasma proteins, on the other hand, are unable to pass through the membrane without energy consumption [2].

Additionally, macromolecular compounds that can carry hydrophobic drugs must be transferred to the cytoplasm through energy-dependent mechanisms rather than crossing the cell membrane directly [2]. Cell-penetrating peptides (CPPs) are short oligopeptides with 5-30 amino acids usually rich in lysine and arginine. They are able to cross biological membranes via both energy-dependent and energy-independent processes [3]. Various cargos such as low-molecular-weight anticancer and antiviral drugs, and negatively charged molecules (e.g., phosphopeptides and nucleic acids) can be delivered by CPPs [4-7]. Biocompatibility, bioactivity, and the unique structural properties of some of the CPPs allow them to cross the cell membrane without showing cytotoxicity at their experimental concentration.

Previous studies have introduced a homochiral cyclic peptide $[WR]_5$ containing alternative arginine (R) and tryptophan (W) residues as a molecular transporter of bioactive compounds [8]. Furthermore, several novel homochiral cyclic peptides containing tryptophan (W) and arginine (R) residues were designed in our laboratory for enhanced delivery of a phosphopeptide [4], lamivudine [4,8], doxorubicin (Dox) [9], paclitaxel, camptothecin [10], curcumin [11], selenium nanoparticles [12], and gold nanoparticles [13]. In these studies, selected cyclic peptides offered several advantages including, nuclear delivery of an anticancer drug, endocytosis-independent uptake, low cytotoxicity, biocompatibility, hydrophobic drug entrapment through non-covalent interactions, and drug delivery through conjugation with the drug.

Further studies were required to improve the molecular transporter properties by optimizing peptide sequences. We envisaged this goal by maintaining the $[WR]_5$ scaffold and adding a linear tail to generate novel hybrid cyclic-linear peptides. The effect of the increasing number of arginine and tryptophan residues on the linear tail was investigated on the molecular transporter property. Therefore, a number of hybrid cyclic-linear peptides containing alternate arginine and tryptophan residues ($[(RW)_5K](RW)_x$ analogs) were synthesized through Fmoc solid-phase chemistry and solution phase cyclization. Then, their molecular transporter properties were compared with $[WR]_5$ to determine the optimal number of arginine and tryptophan residues on the linear tail for efficient delivery. Herein, I have provided a general description and summary of techniques that were used for the synthesis of the peptides, evaluation of their cytotoxicity, and molecular transporter properties.

1.1. Peptide synthesis

Peptides have gained a lot of attention in drug delivery because of their biocompatibility, bioactivity, ease of synthesis and functionalization, and the presence of different amino acids with diverse physicochemical properties such as polarity, hydrophobicity, and charge. To create peptides with cell-penetrating properties, the sequence and physicochemical properties can be optimized.

Proteins and peptides are naturally occurring in the human body and are made up of short chains of amino acid monomers joined together by peptide bonds (–CONH–) [14]. For nearly a century, scientists have described the stepwise assembly of peptides from amino acid precursors. The concept behind peptide synthesis is simple, whereby peptide elongation is accomplished by an amino acid coupling reaction, followed by the elimination of a reversible protecting group [15]. There are two main approaches for peptide synthesis: The solution-phase peptide synthetic approach and the solid phase peptide synthetic approach.

The procedure of solution-phase peptide synthesis involves blocking the carboxyl group of the first amino acid and the amino group of the second amino acid. The peptide bond could then be formed by activating the free carboxyl group, and selective elimination of the two protecting groups would result in the free dipeptide [16].

Bruce Merrifield invented solid-phase synthesis (SPPS) in 1963 as a fast, simple, and efficient method of preparing peptides and small proteins, and he was awarded Nobel Prize for the same [17]. With the introduction of solid-phase methods, peptide synthesis has become a more practical part of modern scientific research [18]. The solid phase method is based on the covalent bonding of the first amino acid of the chain to a solid polymer, following by the insertion of the subsequent amino acids one at a time before the desired sequence is formed, and finally, the

cleavage of the peptide from the solid support [17]. Some crucial advantages of solid-phase peptide synthesis over the solution phase peptide synthesis approach are that the coupling reactions can be carried out more quickly, the excess of the active amino acid derivative can be eliminated at the end of the reaction by easy washing operations, and after each reaction, the product does not need to be purified before the next step [19].

The *t*-butyloxycarbonyl (Boc) group was added to SPPS to provide N^{α} protection. Later, because of the acid-labile Boc group, (Fmoc) group for N^{α} protection was introduced, which requires moderate base for removal of N^{α} protection, and thus offered a chemically mild condition [20]. In the late 1970s, *t*-butyl (tBu)-based side-chain protector and hydroxymethylphenoxy-based linkers were used in Fmoc-based techniques for peptide attachment to the resin. In general, the choice of solid support, properly protected amino acids, linker (between the solid support and the synthesized peptide), coupling methodology, and procedure for cleaving the peptide from the solid support all play important roles in the success of SPPS [15]. In this project, the Fmoc solid-phase peptide method was used for the synthesis of all peptides. Figure 3 shows the general steps of solid-phase peptide synthesis.

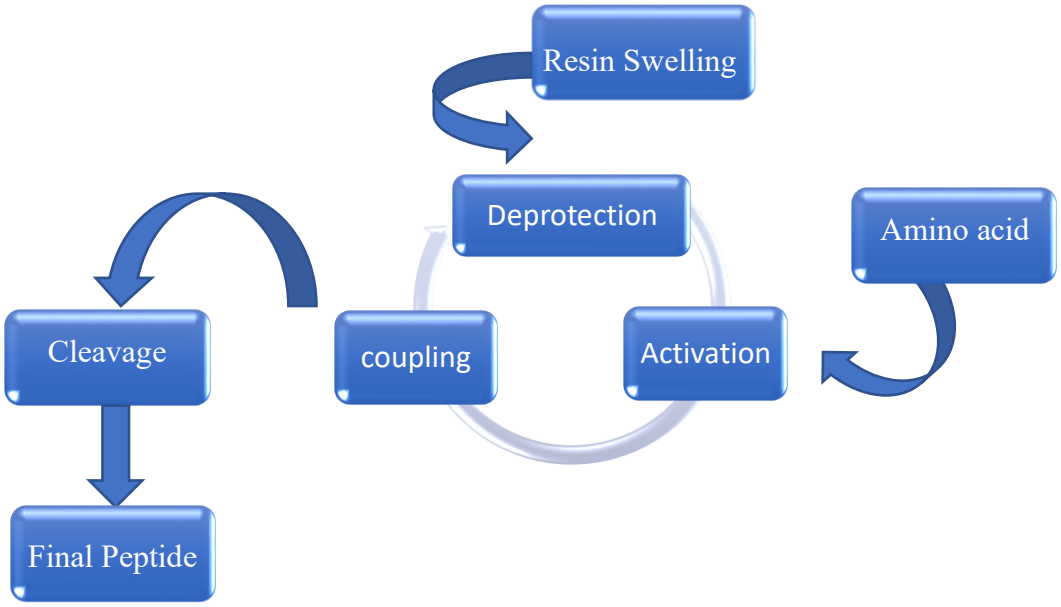

Figure 3. Repeated cycles of (1) Deprotection; (2) Activation of the side-chain protected amino acid; (3) Coupling followed by the cleavage of the assembled peptide.

1.2. Cytotoxicity assay

Cytotoxicity assay is commonly used for *in vitro* biological evaluation studies to determine the concentration of compounds that affects the cell viability and proliferation within a population. It is critical to know that how many viable cells are remaining at the end of the experiment for the data to be accurate. Many biological active agents can cause toxicity by the destruction of cell membranes, prevention of protein synthesis, inhibition of polydeoxynucleotide elongation, irreversible binding to receptors, and enzymatic reactions [21]. There is a need for an inexpensive, effective, and reliable cytotoxicity assay to assess the cell death caused by the physical and chemical agents.

Cell viability assays are based on three main categories: those that exploit the loss of membrane integrity, those that directly measure metabolic markers, and those that assess metabolic activity [22]. The MTS ((5-(3-carboxymethoxyphenyl)-2-(4,5-dimethyl-thiazoly)-3-(4-sulfophenyl) tetrazolium, inner salt assay) assay was utilized in this study for the cytotoxicity study, which is a kind of colorimetric assay, and it can measure the metabolism or enzymatic activity as a marker of live cells. The advantages of the MTS assay over the other cytotoxicity assays are the ease of use, accuracy, acceptable sensitivity, and specificity [23]. The MTS reagent, which is a negatively charged molecule, is typically used in the presence of the intermediate electron acceptor phenazine methosulfate (PMS), which enhances the sensitivity of the reactions and can transfer electrons from the cytoplasm or plasma membrane [24]. The MTS assay is based on the mitochondrial activity of viable cells at 37°C, which can convert and reduce the tetrazolium salt into a colored, water-soluble formazan (Figure 4). Dehydrogenase enzymes produce the formazan, and its amount is directly proportional to the number of viable cells, which can be measured at 492 nm with a spectrophotometer device [23].

Figure 4. Chemical structures of MTS and Formazan product in living cells.

1.3. Flow cytometry

The flow cytometry was used in this study to assess the cellular uptake of cargo molecules and the fluorescence-labeled peptide transporter. Flow cytometry is a powerful technology with applications in immunology, molecular biology, virology, bacteriology, cancer biology, and infectious disease monitoring [25]. Flow cytometry is a sophisticated tool that can detect, count, and sort the cells bypassing them in front of a laser as they flow in a suspension of buffered salt-based solution. The flow cytometry has the ability to analyze each cell or particle, based on visible light scatter and one or multiple fluorescence parameters. Light scattering measures the cells' cell surface area or size through the forward direction (Forward Scatter or FSC). It indicates the complexity and morphological properties of the cell at 90° (Side Scatter or SSC). The amount of fluorescent probe attached to the cell determines the amount of fluorescence produced by the probe [26].

Fluorescence-activated cell sorting (FACS), which is a specialized type of flow cytometry, was used for the cellular uptake analysis of this study. It provides a method for physically sort a heterogeneous mixture of fluorescently-labeled cells into different populations [27]. FACS analysis allows us to simultaneously collect the data of forward-scatter, side-scatter, and fluorescent signal. Each fluorescent compound absorbs light energy at a spectrum of specific wavelengths. The fluorescent-labeled compounds used in this study have a fluorescein isothiocyanate (FITC) label, which has an excitation and emission wavelength of 495 and 520 nm, respectively [28]. In this study, the gating method, a numerical or graphical boundary, was used to gather the cell population and data analysis.

2. Experimental section

2.1. Materials

All amino acids and resins were received from AAPPTEC. 1,1,3,3-Tetramethyluronium hexafluorophosphate (HBTU) was purchased from Oakwood Products, Inc. All other reagents and chemicals were obtained from Sigma-Aldrich Chemical Co. (Milwaukee, WI). The chemical structures and purity of final products were confirmed by high-resolution MALDI-TOF (GT 0264), and UHR-QqTOF (Ultra-High Resolution Qq-Time-Of-Flight) from Bruker Inc. Final compounds were purified by preparative reversed-phase HPLC (Shimadzu LC-20AP Prominence Preparative Liquid Chromatography Shimadzu HPLC) using a gradient system of acetonitrile (CH_3CN) and water containing 0.1% TFA (H_2O) (15−90%, 50 min) and a reversed-phase preparative column (00G-4436-P0-AX, Gemini Prep C18, 10 μm particle size). Fluorescent-labeled phosphopeptide (F′-GpYEEI), fluorescent-labeled anti-human immunodeficiency virus (HIV) drugs [2′,3′-dideoxy-5-fluoro-3′-thiacytidine (emtricitabine, FTC) and 2′,3′-didehydro-2′,3′-dideoxythymidine (stavudine, d4T), and fluorescent-labeled lamivudine (3TC) were prepared according to the previously reported procedures [4-7].

Human leukemia carcinoma cell line (CCRF-CEM, ATCC No. CCL-119), human ovarian adenocarcinoma cells (SKOV-3, ATCC No. HTB-77), human epithelial embryonic kidney healthy (HEK-293, ATCC No. CRL-1573), and human epithelial mammary gland adenocarcinoma cells (MDA-MB-231, ATCC No. HTB-26) were purchased from American Type Culture Collection (ATCC).

2.2. Methods

2.2.1. peptide synthesis

General Linear and cyclic peptide synthesis: Fmoc solid-phase peptide synthesis followed by solution-phase cyclization were utilized to synthesize hybrid cyclic-linear peptides, namely: $[(RW)_5K](RW)$, $[(RW)_5K](RW)_2$, $[(RW)_5K](RW)_3$, $[(RW)_5K](RW)_4$, and $[(RW)_5K](RW)_5$. The linear peptides were assembled on NH_2-Arg(Pbf)-2-chlorotrityl resin as solid support on a 0.30 mmol scale. Fmoc-Arg(Pbf)-OH, Fmoc-Trp(Boc)-OH, and Dde-Lys(Fmoc)-OH were used as the building block amino acids in the synthesis. The resin was swelled in 10 mL of *N*,*N*-dimethylformamide (DMF) for 10 min under dry nitrogen. The excess of the solvent was filtered off. The swelling and filtration steps were repeated two more times. Fmoc-Trp(Boc)-OH (3 equiv.) was coupled to the *N*-terminal of arginine(Pbf)-2-chlorotrityl resin in the presence of 2-(1H-benzotriazole-1-yl)-1,1,3,3-tetramethyluronium hexafluorophosphate (HBTU) (3 equiv.), *N*,*N*-diisopropylethylamine (DIPEA) (6 equiv.) as activating and coupling reagents, respectively, in DMF by mixing for 2 h. After the coupling was completed, the reaction solution was filtered. The resin was washed with 10 mL DMF for 5 min three times, following by *N*-terminal Fmoc deprotection using piperidine in DMF (20% v/v, 10 mL, 2 × 15 min). The reaction solution was drained, and the resin was washed with DMF (15 mL, 3 × 5 min). This process was repeated for the coupling of the next amino acids. The coupling was continued on the side chain of lysine residue with Dde-protected amino group after removing the Fmoc of the side chain protecting group of lysine with piperidine in DMF (20% v/v, 15 mL, 2 × 15 min). After Fmoc deprotection on the last amino acid, the free amino group was capped in the presence of acetic anhydride. The Dde protection group of lysine residue was removed in the presence of hydrazine in DMF (2%

v/v, 15 mL, 3 × 15 min). For the synthesis of linear peptides, trifluoroacetic acid (TFA), anisole, thioanisole, and dithiothreitol (6300 μL:350 μL:210 μL: 257 mg) were used to cleave the peptides from the resin and to remove the protecting groups. The structure of the linear peptides after cleavage was confirmed by MALDI mass spectroscopy.

For the synthesis of cyclic peptides, after washing the resin with DMF, the protected peptides were cleaved from the resin by mixing the resin with cleavage cocktail containing dichloromethane, trifluoroethanol, acetic acid (DCM:TFE:AcOH; 7:2:1 v/v/v, 250 mL) for 3 h. The acetic acid of the mixture was removed by evaporation under low pressure using hexane (2× 20 mL) and DCM (2× 15 mL). The molecular weight of the linear peptides was confirmed by MALDI mass spectroscopy. The cyclization of the protected linear peptide was carried out in the presence of anhydrous DMF (100 mL), anhydrous DCM (25 mL), *N*,*N*′-diisopropylcarbodiimide (DIC) (1.8 mmol,279 μL), and 1-hydroxy-7-azabenzotriazole (HOAt) (0.9 mmol, 122.5mg) overnight under an inert condition with nitrogen. The formation of the cyclization was confirmed by MALDI-TOF. The solvent was removed by using a rotary evaporator under low pressure. The crude peptide was dried overnight. The cleavage cocktail (TFA, anisole, thioanisole, 9:1:2 v/v/v and 50 mg of DTT, 20 ml total volume) was mixed with the crude product for 6 h to remove a protecting group of the side chains. The crude peptide was precipitated by the addition of cold diethyl ether and was centrifuged. The molecular weight of the cyclic peptide was confirmed again with MALDI-TOF. All the peptides were purified using reversed-phase HPLC and lyophilized. As a representative example, the synthesis of linear peptide ($(RW)_5$KRW) and cyclic peptide [$(RW)_5$K](RW) are shown in Schemes 1 and 2.

Synthesis of F'-[(RW)$_5$K](RW): Linear peptide sequence RWRWRWRWRWKRWRWRWRWRW was assembled on the resin using Fmoc solid-phase methodology in the same manner as described above. A short linker Boc-β-alanine-OH (4 equiv.) was coupled with the unprotected amine group of tryptophan in the presence of HBTU/DIPEA (4 and 8 equiv.)) in DMF (8 mL). The resin was washed with DMF (3 × 10 mL). The *N*-terminal Dde protection of lysine was deprotected by treating the resin-bound peptide with hydrazine hydrate in DMF (2% v/v, 60 mL, 3 × 10 min). After washing the resin with DMF, the cleavage of the resin was performed by mixing the resin with cleavage cocktail containing dichloromethane, trifluoroethanol, acetic acid (DCM:TFE: AcOH; 7:2:1 v/v/v, 250 mL) for 3 h. Acetic acid of the mixture was removed by evaporation under low pressure using hexane (2 × 20 mL) and DCM (2 × 15 mL). The structure of the crude linear peptide after cleavage was confirmed by MALDI mass spectroscopy. The cyclization of the protected linear peptide was carried out in the presence of anhydrous DMF (100 mL), anhydrous DCM (25 mL), *N*,*N'*-diisopropylcarbodiimide (DIC), and 1-hydroxy-7-azabenzotriazole (HOAt) overnight under an inert condition with nitrogen. The formation of the cyclization was confirmed by MALDI-TOF. The solvent was removed by using a rotary evaporator under low pressure. The crude peptide was dried overnight. The cleavage cocktail (TFA, anisole, thioanisole, 9:1:2 v/v/v and 50 mg of DTT, 20 ml total volume) was mixed with the crude product for 6 h to remove a protecting group of the side chains. The crude peptide was precipitated by the addition of cold diethyl ether and was centrifuged. The molecular weight of the cyclic peptide was confirmed again with MALDI-TOF. The peptide was purified using reversed-phase HPLC and lyophilized. Fluorescein isothiocyanate isomer I (FITC, 6 equiv.) was used for labeling the peptide. This was achieved by coupling the free *N* terminal of β-alanine of purified cyclic peptide (1 equiv.) in the solution of fluorescein isothiocyanate isomer I (FITC, 6

equiv.), DIPEA (10 equiv.), and DMF (1ml). The mixture was shaken for 4 h at room temperature. The solvent was removed, and the final product was precipitated by the addition of cold diethyl ether and was centrifuged. The structures of fluorescence-labeled peptide (F'-[$(RW)_5$K]$(RW)_5$), where F' is Fluorescein isothiocyanate isomer I, was confirmed by UHR-QqTOF mass spectroscopy. The synthesis of F'-[$(RW)_5$K]$(RW)_5$ is shown in Scheme 3.

Table 1. Molecular weight of synthesized peptides obtained by MALDI-TOF and Q-TOF.

Compound	Chemical Formula	Exact Mass	Found (m/z)
$(RW)_5KRW$	$C_{110}H_{148}N_{38}O_{15}$	2241.1986	2241.3288 $[M]^+$
$(RW)_5K(RW)_2$	$C_{127}H_{170}N_{44}O_{17}$	2583.3791	2583.3675 $[M]^+$
$(RW)_5K(RW)_3$	$C_{144}H_{192}N_{50}O_{19}$	2925.5595	2926.0316 $[M+H]^+$
$(RW)_5K(RW)_4$	$C_{161}H_{214}N_{56}O_{21}$	3267.7399	3267.8411 $[M]^+$
$(RW)_5K(RW)_5$	$C_{178}H_{234}N_{62}O_{22}$	3609.9203	3610.2371 $[M + H]^+$
$[(RW)_5K](RW)$	$C_{110}H_{146}N_{38}O_{14}$	2223.1881	2223.4730$[M]^+$
$[(RW)_5K](RW)_2$	$C_{127}H_{168}N_{44}O_{16}$	2565.3685	2565.3478 $[M]^+$
$[(RW)_5K](RW)_3$	$C_{144}H_{190}N_{50}O_{18}$	2907.5489	2908.0722 $[M + H]^+$
$[(RW)_5K](RW)_4$	$C_{161}H_{212}N_{56}O_{20}$	3249.7293	3250.6246 $[M + H]^+$
$[(RW)_5K](RW)_5$	$C_{178}H_{234}N_{62}O_{22}$	3591.9098	3593.3774 $[M + 2H]^+$
F'-$[(RW)_5K](RW)_5$	$C_{200}H_{246}N_{64}O_{26}S$	3991.9615	805.0307 $[M+5H]^{+5}+Na^+$ 699.6998 $[M+6H]^{+6}+Na^+$ 574.8879 $[M+7H]^{+7}+Na^+$ 502.2778 $[M+8H]^{+8}+Na^+$

2.2.2. In Vitro Cytotoxicity assay

The *in vitro* cytotoxicity of the synthesized peptides was determined by using human leukemia carcinoma cell line (CCRF-CEM, ATCC No. CCL-119), human ovarian adenocarcinoma cells (SKOV-3, ATCC No. HTB-77), human epithelial embryonic kidney healthy (HEK-293, ATCC No. CRL-1573), human epithelial mammary gland adenocarcinoma cells (MDA-MB-231, ATCC No. HTB-26). CCRF-CEM cells were seeded at 50,000 cells in 0.1 mL

per well in 96-well plates. In the case of other cell lines, the cells were seeded at 5,000 cells in 0.1 mL per well of 96-well plates. An appropriate growth medium was used for each cell line (SK-OV-3: McCoy's 5A with L-Glutamine containing fetal bovine serum (FBS) (10%) and penicillin or streptomycin (1%); CCRF-CEM: RPMI-1640 medium with L-glutamine and sodium bicarbonate containing FBS (10%) and penicillin or streptomycin (1%); MDA-MB-231 cells: DMEM/F12 (1:1) (1x) with L-Glutamine and 15 mM HEPES containing FBS (10%) and penicillin or streptomycin (1%), and HEK-293 cells: Minimum Essential Medium Eagle with Earle's salts and sodium bicarbonate, without L-glutamine containing FBS (10%) and penicillin or streptomycin (1%)). All the adherent cells were seeded in the medium 24 h before the experiment [9]. Different concentrations of the compounds (5-75 μM) were added to each well in triplicates and incubated for 3 and 24 h at 37 °C in a humidified atmosphere of 5% CO_2. The cell viability was calculated by measuring the fluorescence intensity at 490 nm using a SpectraMax M2 microplate spectrophotometer after adding 20 μL of the MTS reagent to each well and incubating for 3 additional h. The percentage of cell survival was calculated as [(OD value of cells treated with the test mixture of compounds) − (OD value of culture medium)]/[(OD value of control cells) − (OD value of culture medium)] × 100%.

2.2.3. Cellular uptake study

Cellular uptake studies were performed by FACS (fluorescence activated cell sorting). The cellular uptake of fluorescence-labeled phosphopeptides (F´-GpYEEI), and anti-HIV drugs: (lamivudine (F´-3TC), emtricitabine (F´-FTC), stavudine (F´-d4T)) were measured in the CCRF-CEM and SK-OV-3 cells. The studies were also be conducted in the absence of the synthesized peptide as a control. CCRF-CEM (1×10^6 cells/well) cells were taken in 6-well plates in Opti-

MEM or serum-free RPMI medium. SK-OV-3 (5×10^5 cells/well) were seeded in the medium 24 h prior to experiment in 6 well plates, and after 24 h, the medium was changed with serum-free McCoy's 5A medium or opti-MEM. The cells were then incubated with fluorescence-labeled compounds (2 μM) in the presence and absence of 10 μM of peptides in a 6-well plate for 3 h in an incubator (37 °C in a humidified atmosphere of 5% CO_2). The final volume of each well was 2 mL. The media containing the peptide were removed after 3 h incubation. The cells in the case of SK-OV-3 were digested with 0.05% trypsin/EDTA (0.53 mM) for 5 min to remove any artificial surface binding. Cells were centrifuged at 2500 RPM for 5 min with Fisher Scientific accuSpin Micro 17. The cells were collected as precipitant. Then the cells were washed twice with PBS. The cells were resuspended in flow cytometry buffer and transferred to the Flow cytometry tubes through the 35 μm Strainer Mesh cap. Finally, the cells were analyzed by flow cytometry (FACSCalibur: Becton Dickinson) using the FITC channel and CellQuest software. The data presented were based on the mean fluorescence intensity for 10,000 cells collected. All assays were performed in triplicate. The data from the mean fluorescence signal were shown the ability of the peptides in facilitating cargoes' internalization inside the cell.

3. Results and discussion

3.1. Chemistry

A number of cyclic and linear peptides containing Arg(Pbf)-OH, Fmoc-Trp(Boc)-OH, Dde-Lys(Fmoc)-OH, and Boc-β-alanine-OH amino acids as building blocks were assembled through Fmoc solid-phase peptide synthesis method followed by solution-phase peptide synthesis for cyclization.

Scheme 1 depicts the synthesis of a representative linear peptide. The NH_2-Arg(Pbf)-2-chlorotrityl resin was used as solid support for linear peptide synthesis on a 0.30 mmol scale. The chlorotrityl resin was used since it can be cleaved in mild conditions without deprotection of the side chain, allowing free –COOH and $–NH_2$ to undergo cyclization. Nitrogen gas was used for mixing the solution. The desired linear peptide was assembled on the resin by subsequent coupling of the next Fmoc-protected amino acids (3 equiv.) to the free amino group of the last amino acid on the resin in the presence of HBTU (3 equiv.) as a coupling reagent and DIPEA (6 equiv.) as a base. Fmoc deprotection was conducted in each step by using piperidine in DMF (20% v/v). Lysine residue with a Dde-protected amino group was used to continue the coupling on the side chain of the lysine residue. To make sure the coupling reaction completed, the Kaiser test was performed after each coupling. The reaction was moved forward in the same manner, and the free amino group of the last amino acid was capped with acetic anhydride. The capping was performed to prevent the reaction of the free *N*-terminal of the last amino acid. The Dde protection group of lysine residue was removed in the presence of hydrazine in DMF (2% v/v) to provide the free amino group. Trifluoroacetic acid (TFA), anisole, thioanisole, and dithiothreitol (6300 μL:350 μL:210 μL: 257 mg) were used to cleave the peptides from the resin and to remove the protecting groups (Scheme 1). The structure of the linear peptides after cleavage was confirmed by MALDI mass spectroscopy.

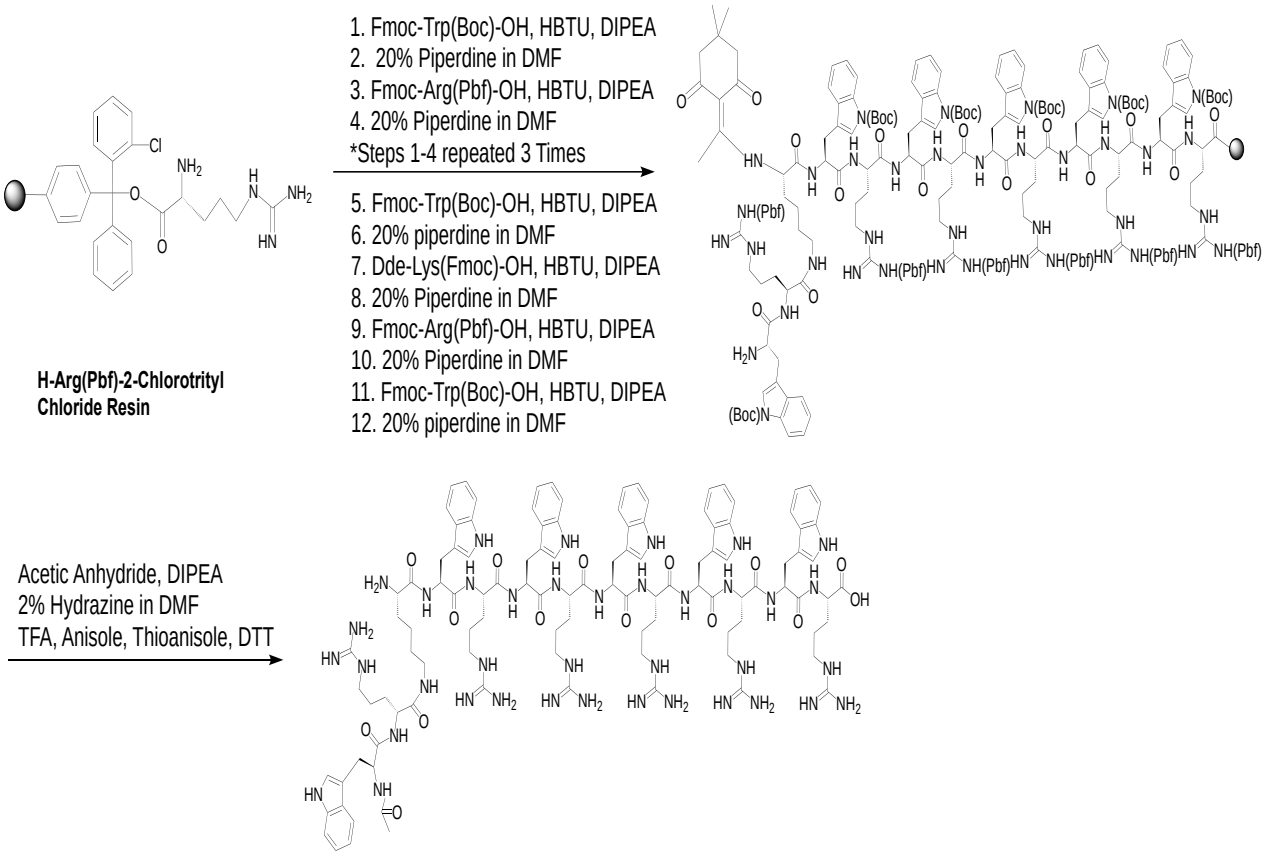

Scheme 1. Synthesis of a $(RW)_5KRW$ peptide.

Scheme 2 shows the synthesis of a representative cyclic peptide. For the synthesis of cyclic peptides, after washing the resin with DMF, the protected peptides were cleaved from the resin by mixing the resin with a cleavage cocktail containing dichloromethane, trifluoroethanol, acetic acid (DCM:TFE:AcOH; 7:2:1 v/v/v, 250 mL) for 3 h. Time was critical in this step, and prolong incubation increased the risk of removing side chain protection groups. The chemical structures of the peptidse were confirmed by MALDI mass spectroscopy. The acetic acid of the mixture was removed by evaporation under low pressure using hexane (2 × 20 mL) and DCM (2× 15 mL). When no more lingering smell of acetic acid is left and, a fluffy white precipitant was formed. Cyclization of a free amino group of lysine with *C*-terminal carboxylic acid of arginine was carried out in the presence of DIC and HOAt in DMF under anhydrous condition. Then the formation of

the cyclic peptide was confirmed by MALDI analysis. Finally, all the protecting groups were removed in the presence of the cleavage cocktail (TFA, anisole, thioanisole, 9:1:2 v/v/v) and 50 mg of DTT (Scheme 2).

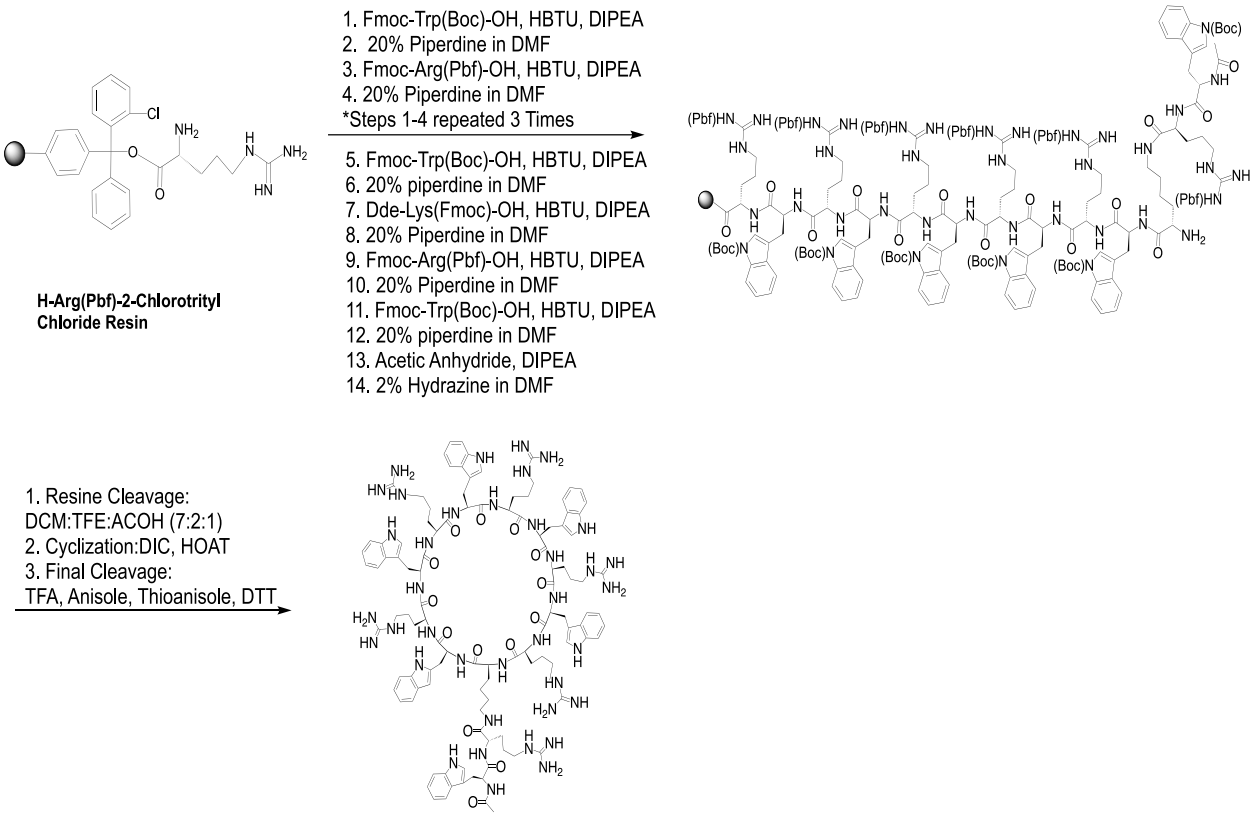

Scheme 2. Synthesis of a $[(RW)_5K](RW)$ peptide.

All the peptides were synthesized in the same manner as described above. The corresponding fluorescence-labeled peptide (F'-$[(RW)_5K](RW)_5$) was synthesized as follows based on the described method above by adding of a β-alanine to the linear chain and conjugation with FITC in the presence of DIPEA in the solution phase (Scheme 3).

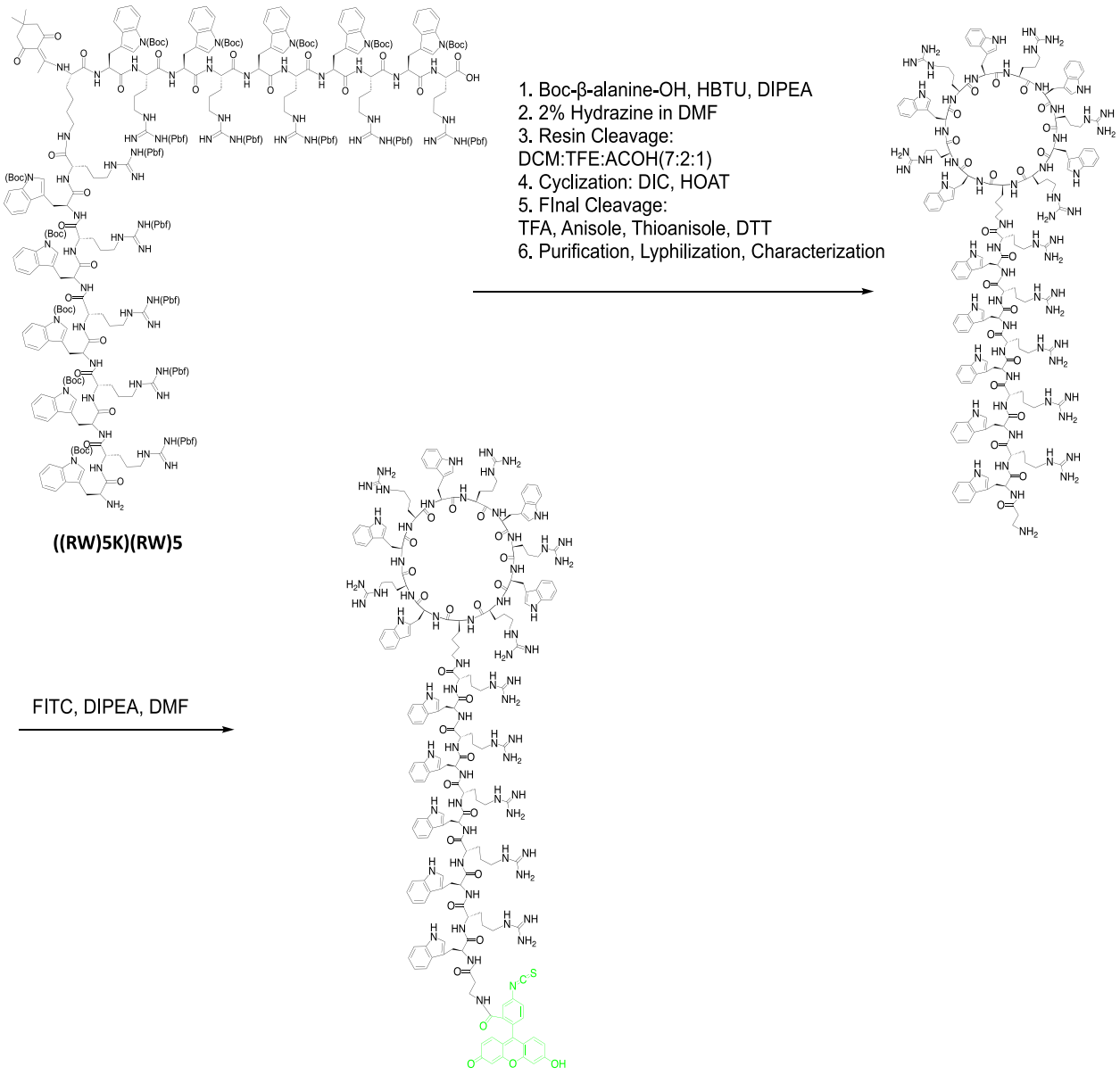

Scheme 3. Synthesis of a F'-[(RW)$_5$K](RW)$_5$.

All the peptides were purified using reversed-phase High-Performance Liquid Chromatography (HPLC) and were lyophilized. A gradient system of acetonitrile (CH_3CN) and water (H_2O) containing 0.1% TFA with a flow rate of 8 ml/min were used for the purification. The retention time was increased by increasing the number of arginine and tryptophan residues in the peptide sequence (15−90%, 50 min). Mass spectra determine the molecular weight using the

positive reflective mode of Matrix-Assisted Laser Desorption/Ionization (MALDI). The molecular weight of fluorescence-labeled peptide (F'-[$(RW)_5$K]$(RW)_5$) could not be detected by MALDI. However, Q-TOF mass spectrometer was used to confirm the mass of F'-[$(RW)_5$K]$(RW)_5$. The structures of the compounds were confirmed by high-resolution MALDI-TOF mass spectroscopy and Q-TOF, as shown in Table 1.

The MALDI spectra results of linear and cyclic peptides are shown in Figures 5-14. The Q-TOF spectra of F'-[$(RW)_5$K]$(RW)_5$ is shown in Figure 15.

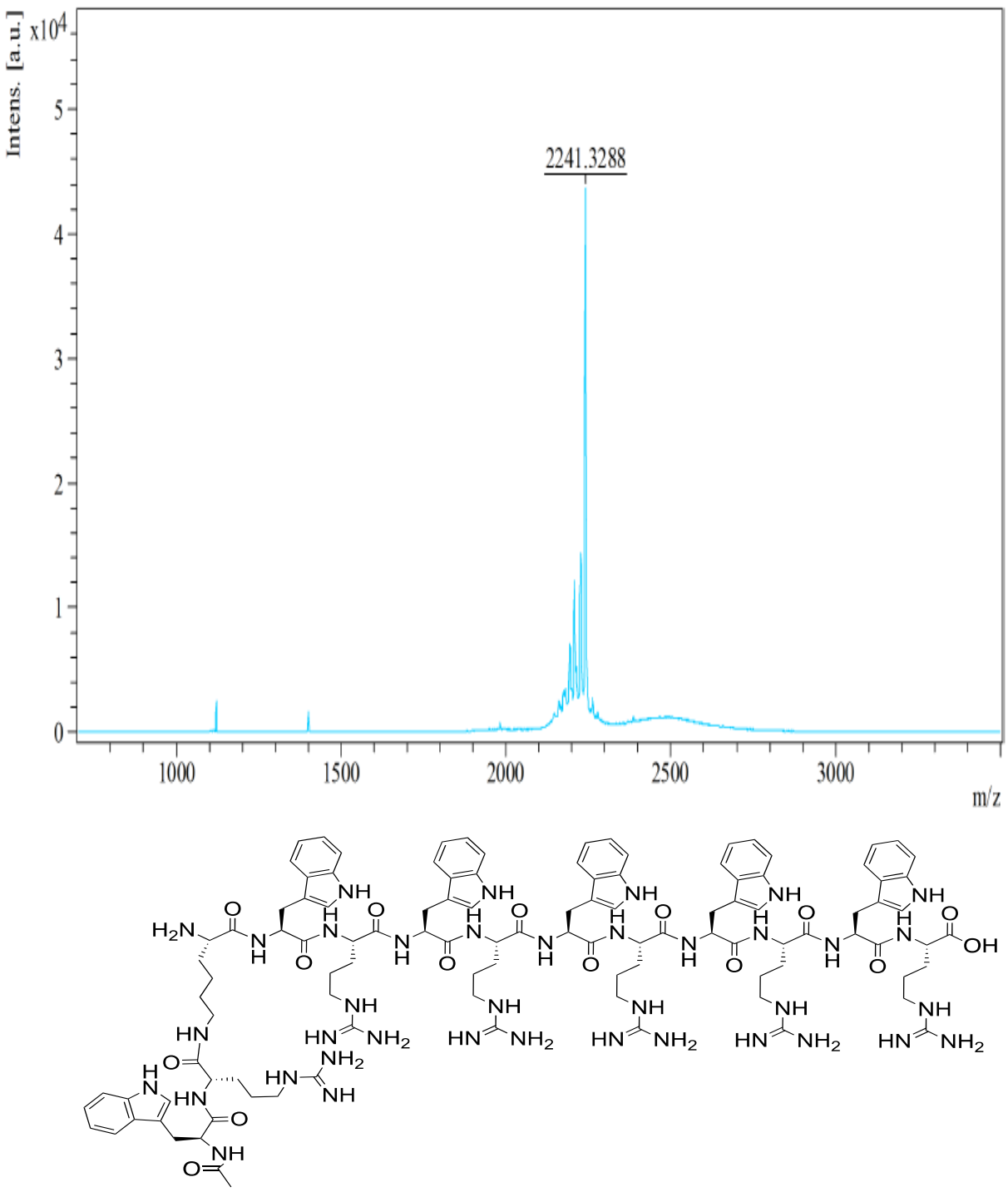

Figure 5. $(RW)_5KRW$, MALDI-TOF (m/z) $C_{110}H_{148}N_{38}O_{15}$, Calculated: 2241.1986, Found: 2241.3288 $[M]^+$.

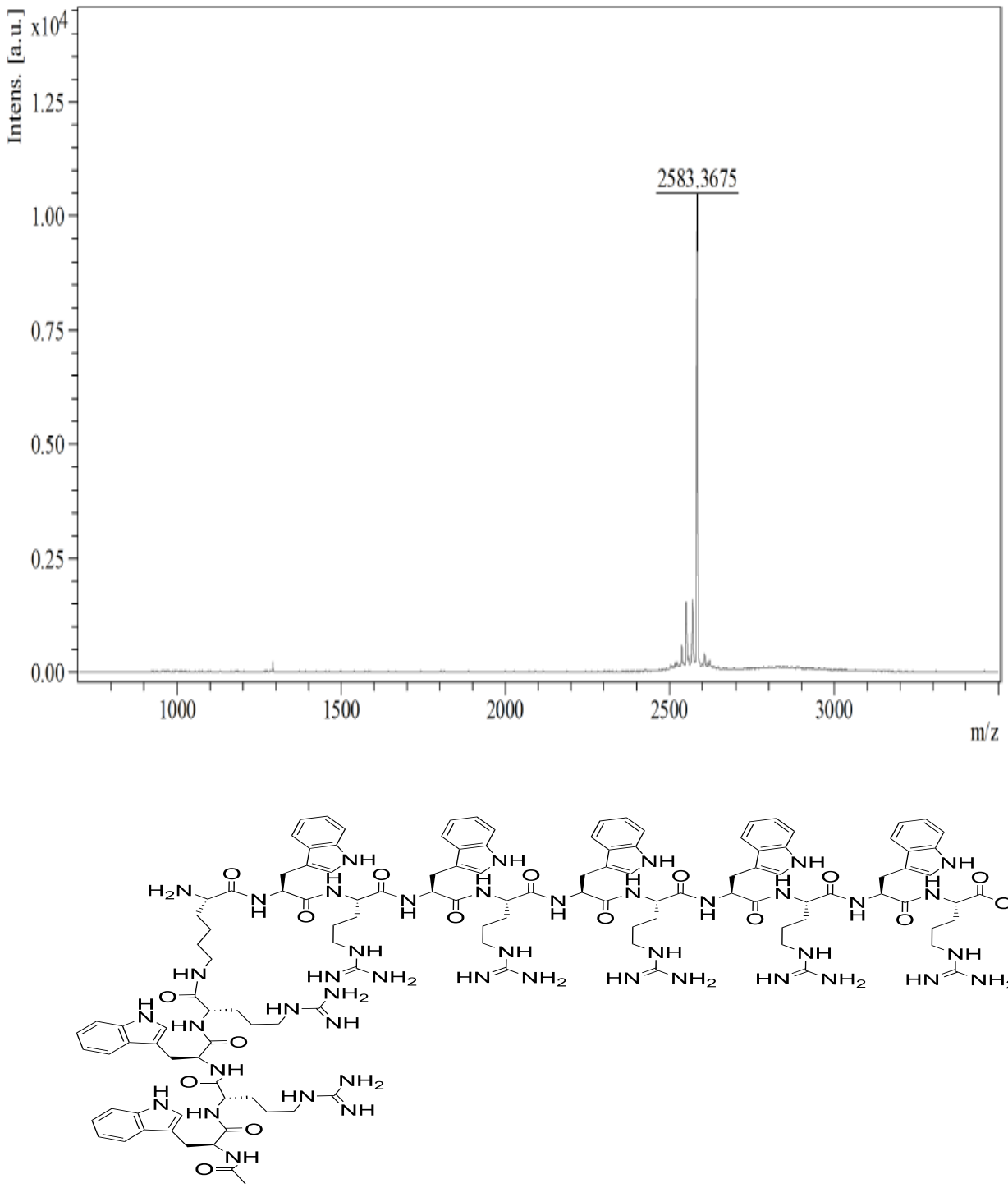

Figure 6. $(RW)_5K(RW)_2$, MALDI-TOF (m/z) $C_{127}H_{170}N_{44}O_{17}$, Calculated: 2583.3791 Found: 2583.3675 $[M]^+$.

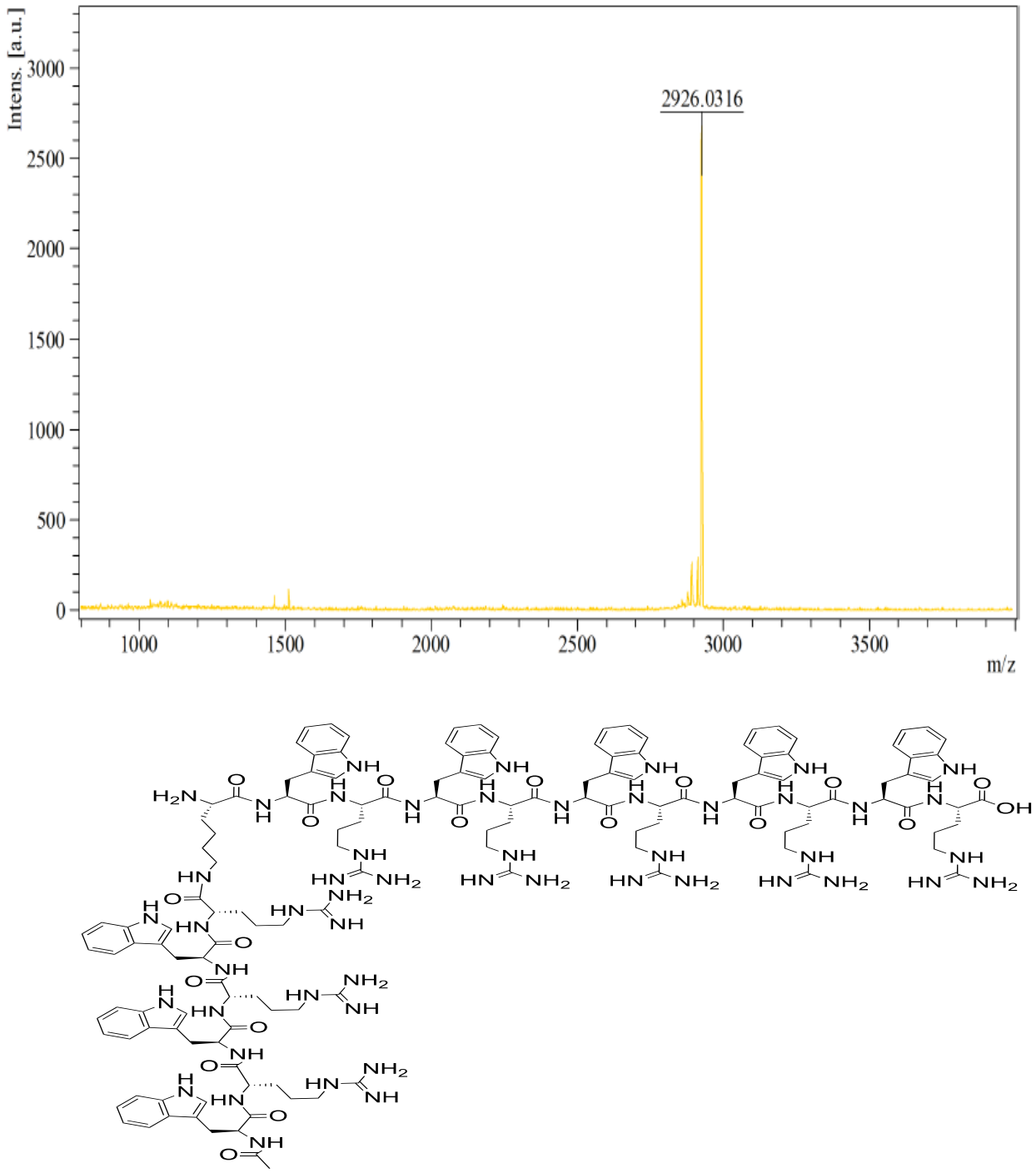

Figure 7. $(RW)_5K(RW)_3$, MALDI-TOF (m/z) $C_{144}H_{192}N_{50}O_{19}$, Calculated: 2925.5595, Found: 2926.0316 $[M+H]^+$.

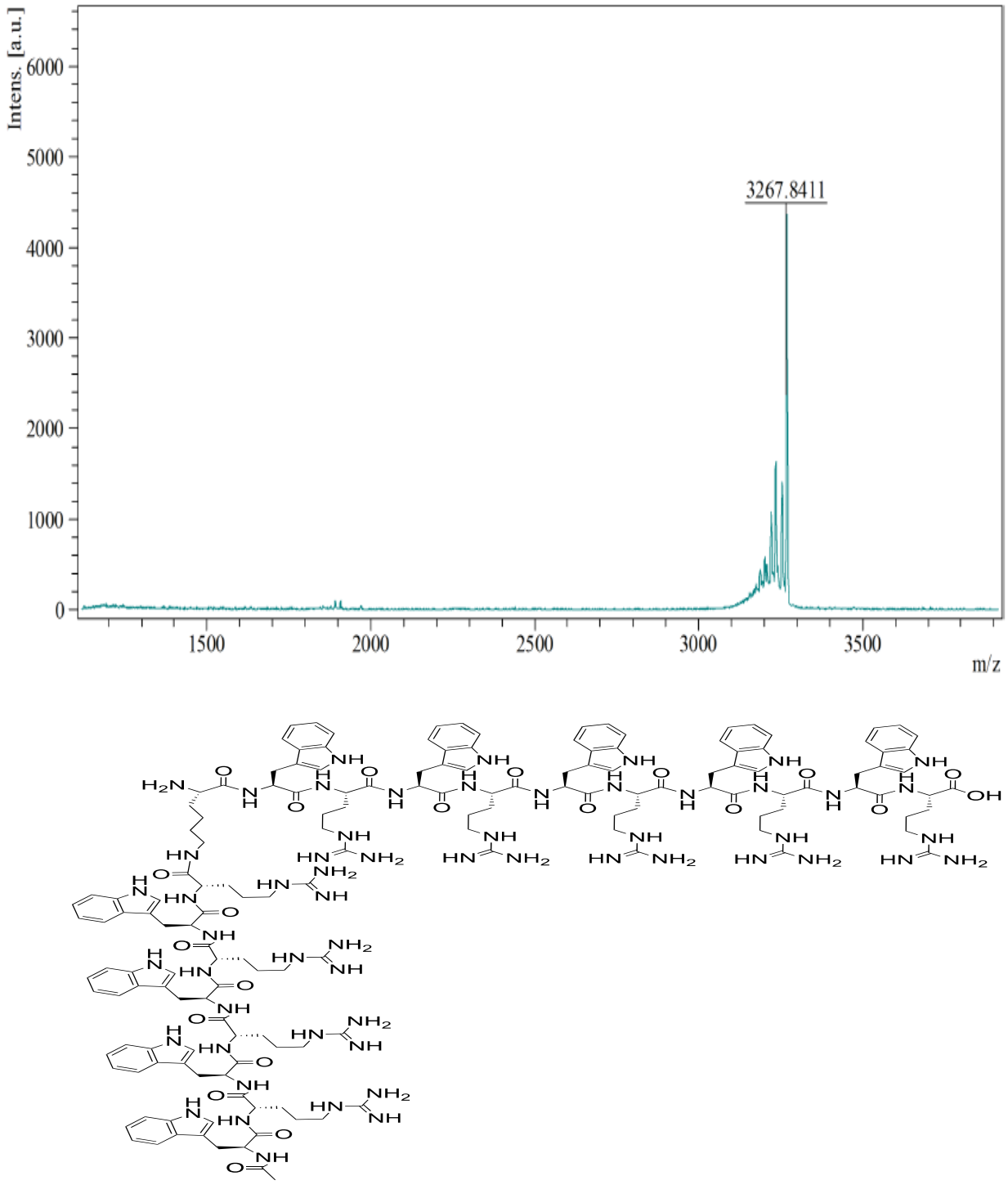

Figure 8. $(RW)_5K(RW)_4$, MALDI-TOF (m/z) $C_{161}H_{214}N_{56}O_{21}$, Calculated: 3267.7399, Found: 3267.8411 $[M]^+$.

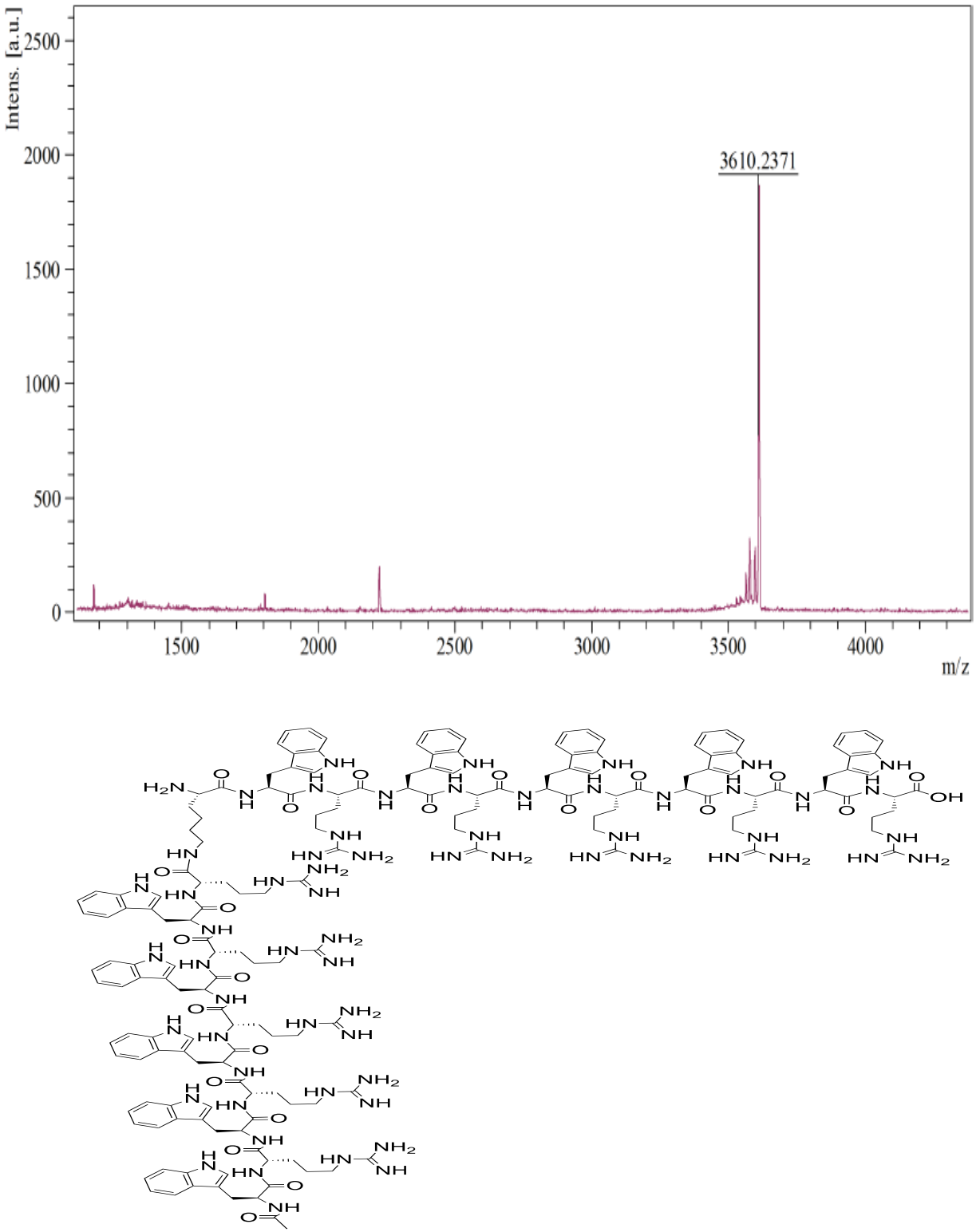

Figure 9. $(RW)_5K(RW)_5$, MALDI-TOF (m/z) $C_{178}H_{234}N_{62}O_{22}$, Calculated: 3609.9203, Found: 3610.2371 $[M+H]^+$.

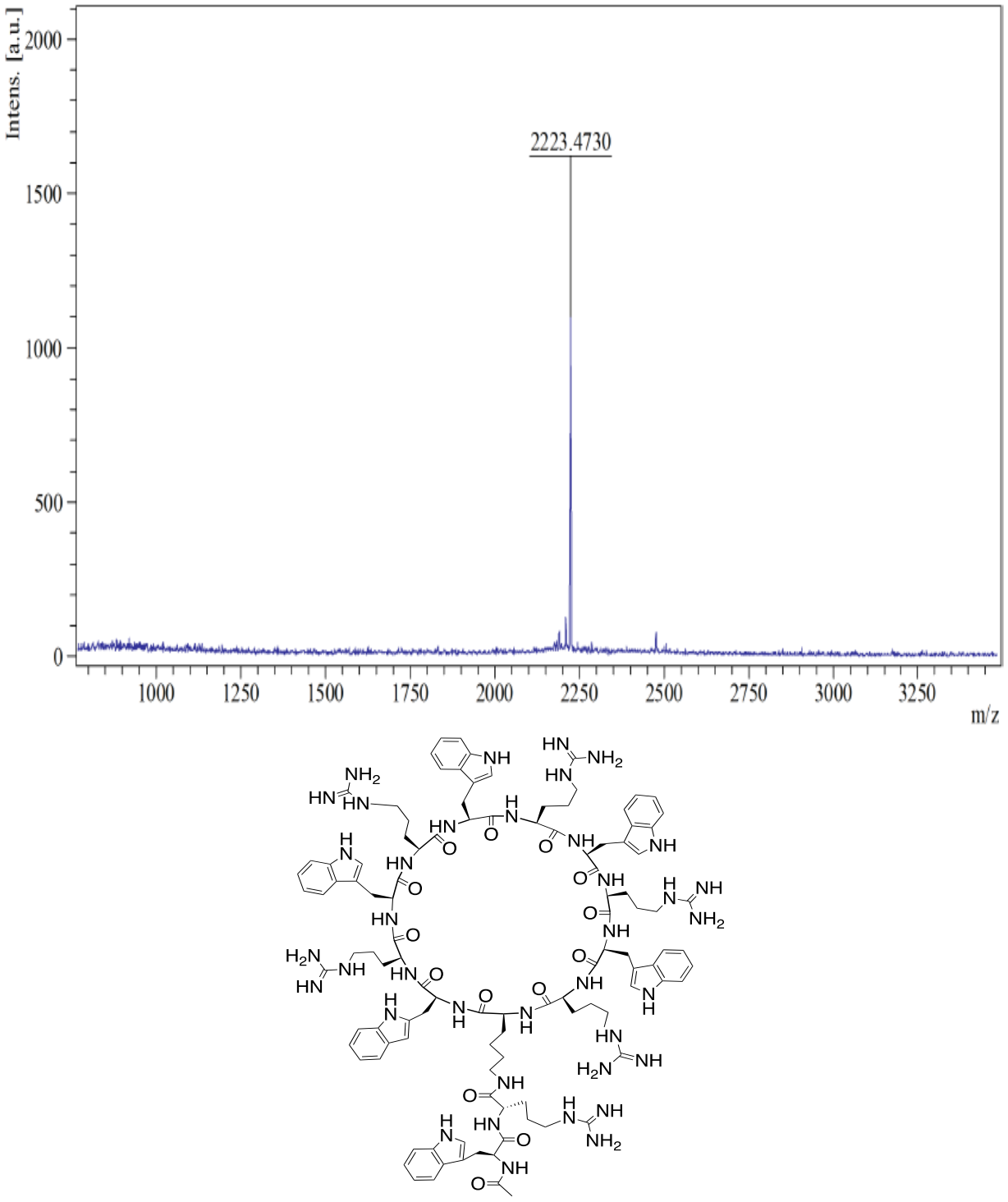

Figure 10. [(RW)$_5$K]RW, MALDI-TOF (m/z) $C_{110}H_{146}N_{38}O_{14}$, Calculated: 2223.1881, Found: 2223.4730 $[M]^+$.

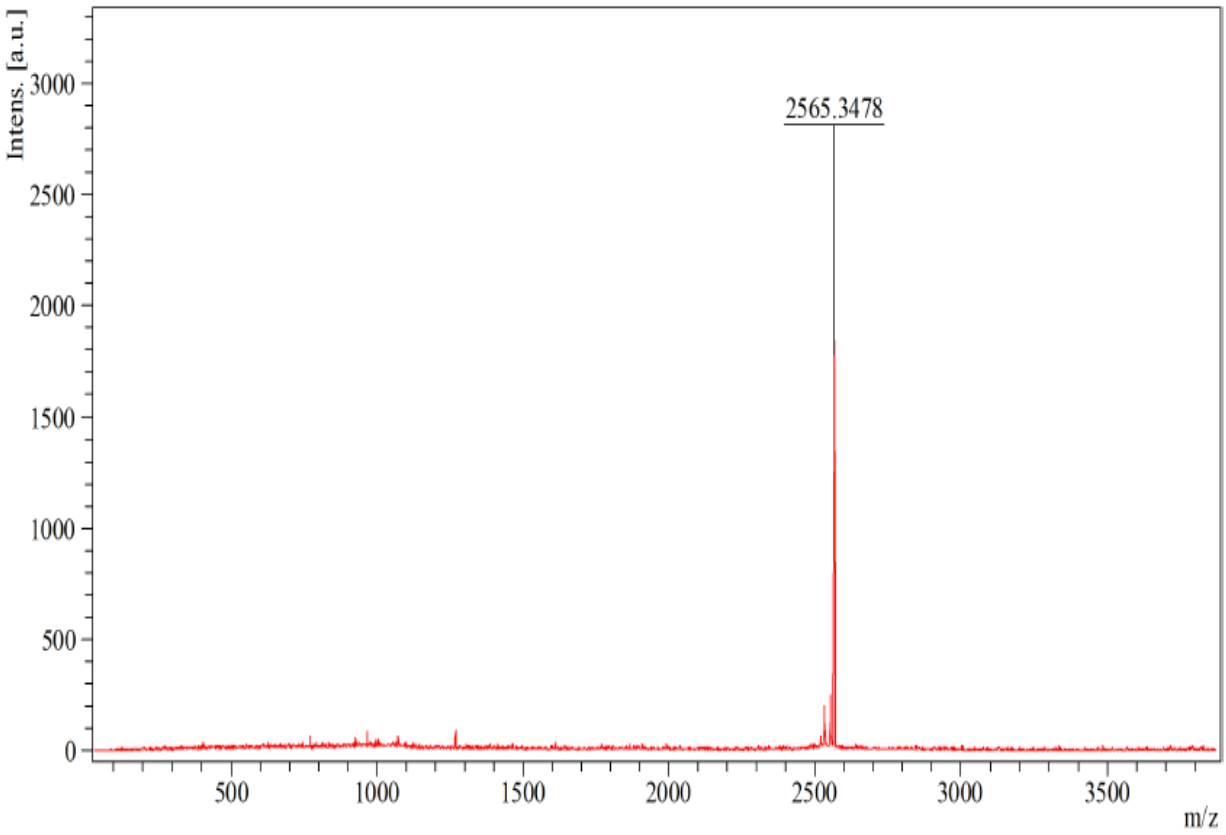

Figure 11. $[(RW)_5K](RW)_2$, MALDI-TOF (m/z) $C_{127}H_{168}N_{44}O_{16}$, Calculated: 2565.3685, Found: 2565.3478 $[M]^+$.

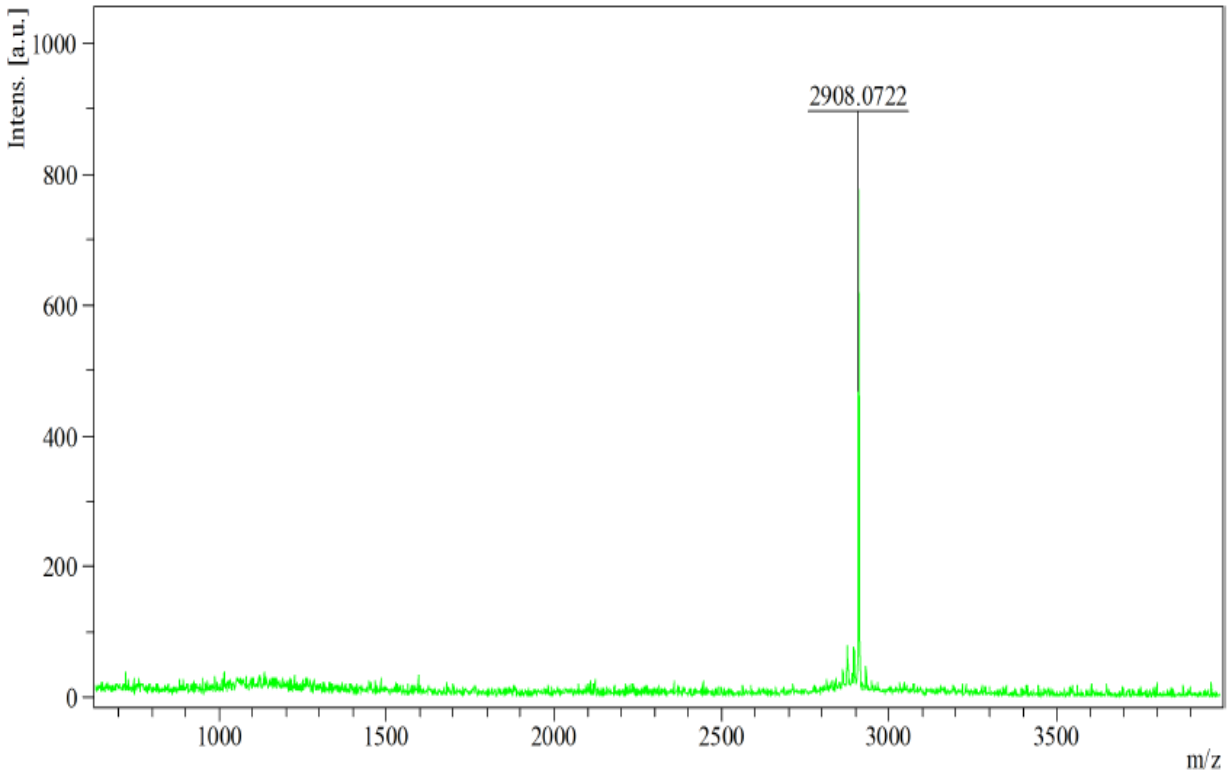

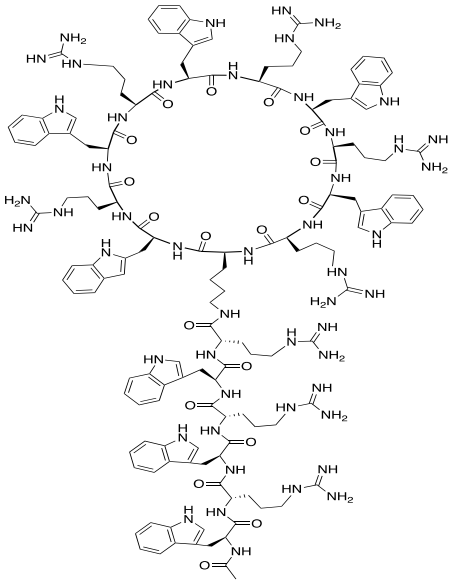

Figure 12. $[(RW)_5K](RW)_3$, MALDI-TOF (m/z) $C_{144}H_{190}N_{50}O_{18}$, Calculated: 2907.5489, Found: 2908.0722 $[M+H]^+$.

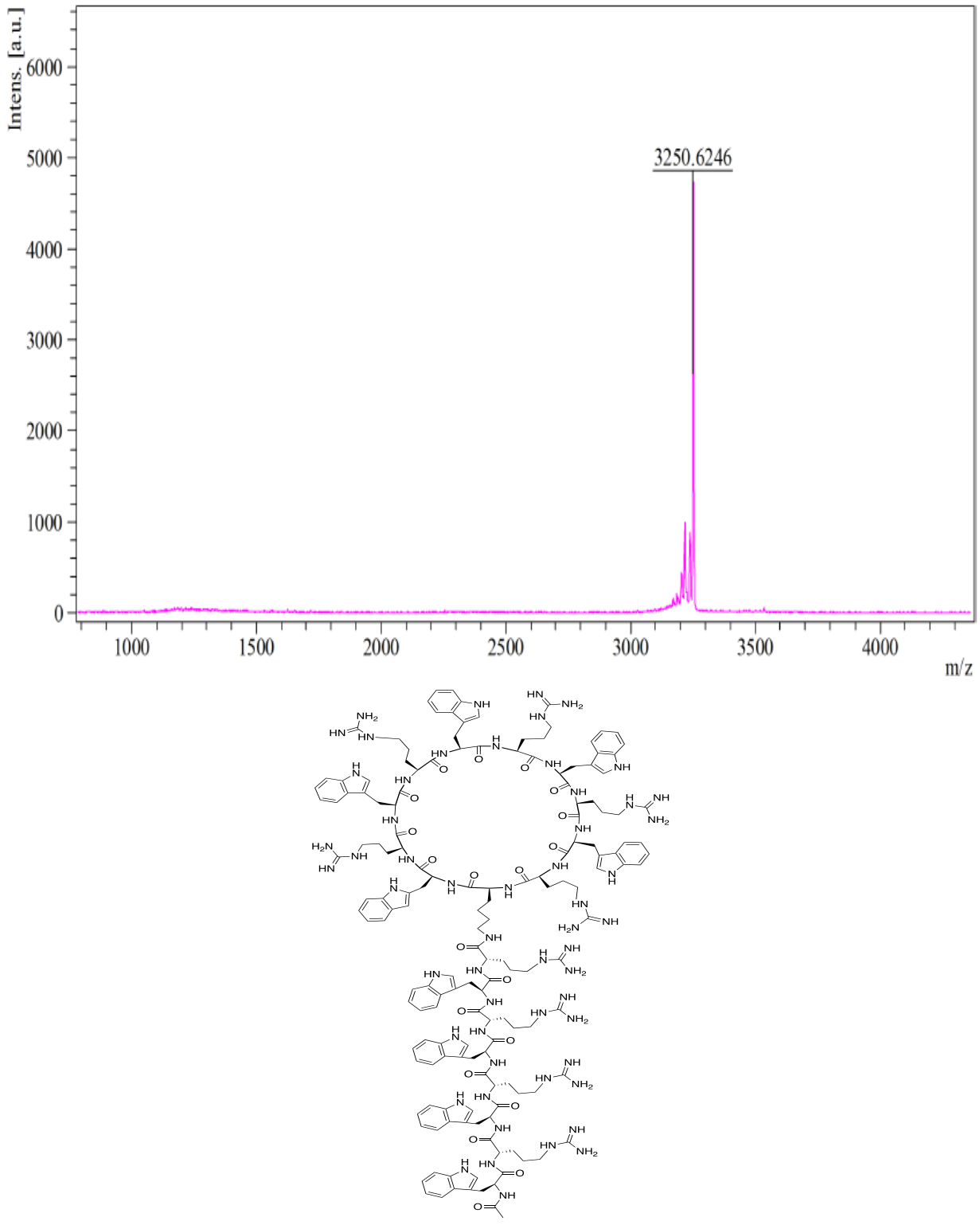

Figure 13. $[(RW)_5K](RW)_4$, MALDI-TOF (m/z) $C_{161}H_{212}N_{56}O_{20}$, Calculated: 3249.7293, Found: 3250.6246 $[M+H]^+$.

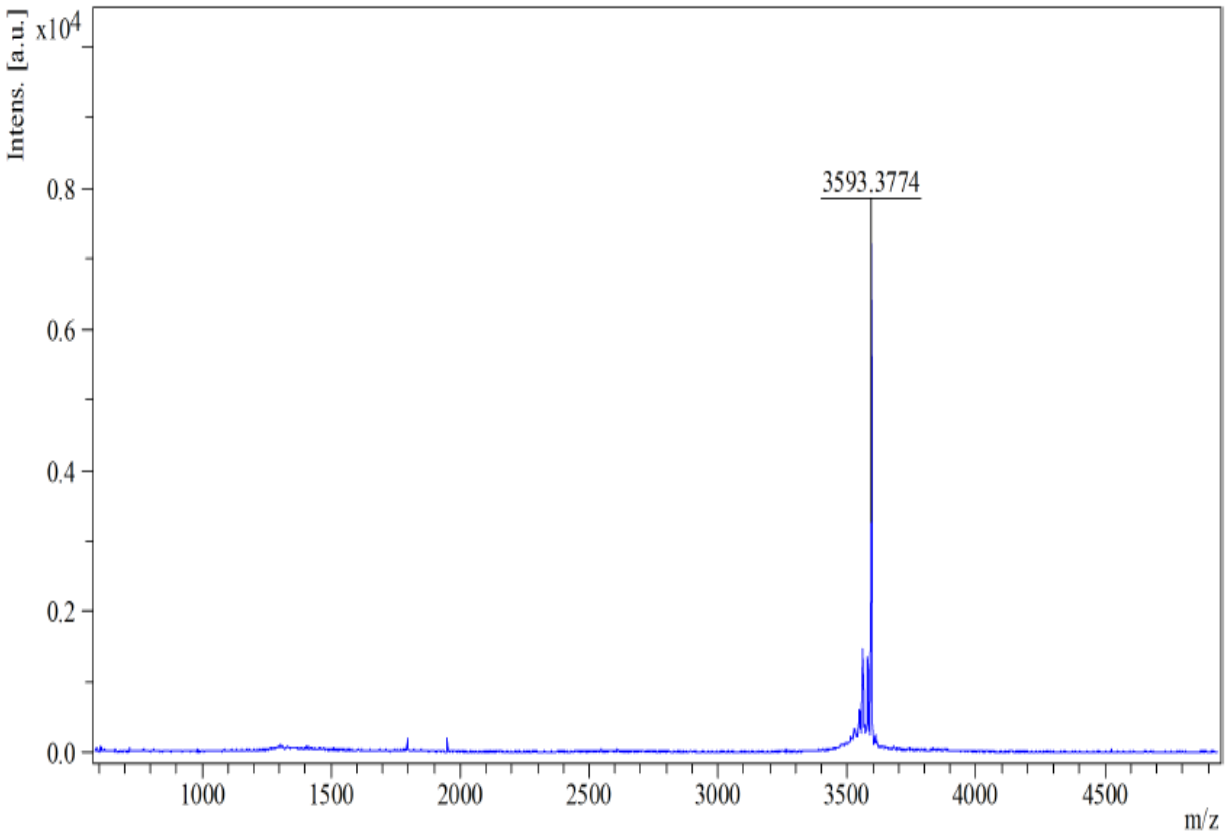

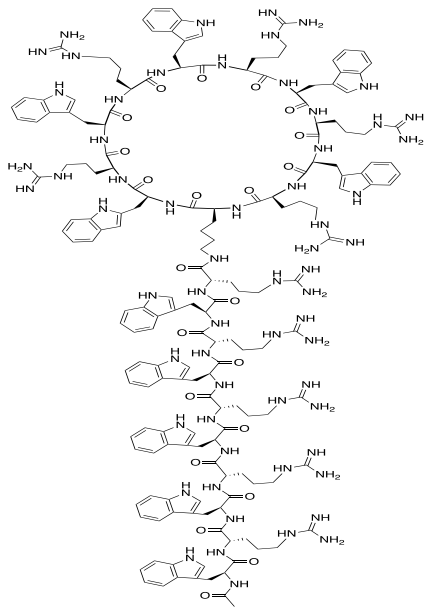

Figure 14. $[(RW)_5K](RW)_5$, MALDI-TOF (m/z) $C_{178}H_{234}N_{62}O_{22}$, Calculated: 3591.9098, Found: 3593.3774 $[M+2H]^+$.

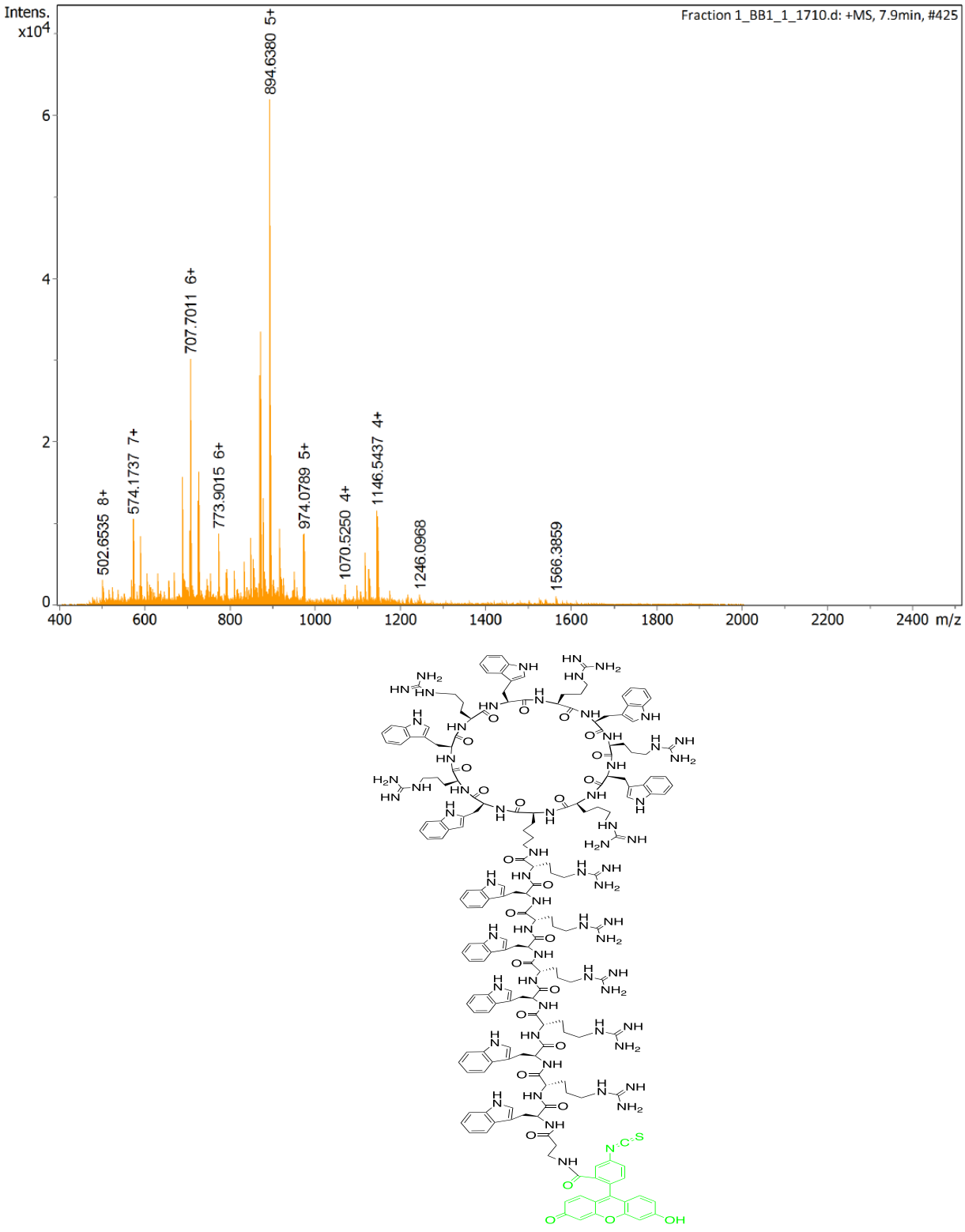

Figure 15. F'-[(RW)$_5$K](RW)5, Q-TOF (m/z) $C_{200}H_{246}N_{64}O_{26}S$, Calculated: 3991.9615, Found: 4013.9241 $[M+Na]^+$.

3.2. In Vitro Cytotoxicity of peptides

To evaluate the cytotoxicity of synthesized linear and hybrid cyclic-linear peptides, a cell viability assay was employed in three different cancer cell lines, CCRF-CEM, SK-OV-3, MDA-MB-231 cells, and one normal cell (HEK-293). To demonstrate that the results are not cell-specific, the experiment was done in various cancer cells and a normal cell. The assay was done in a different range of concentrations (5-75μM) after 3 and 24h incubation. Doxorubicin (Dox 5 μM) was used as a positive control, and pure water was used as a negative control. No treatment is the cells without any treatments. Doxorubicin (5 μM) was not highly cytotoxic after 3 h incubation, while it was cytotoxic after 24 h by reducing the cell viability by 62% at a concentration of 5 μM in CCRF-CEM cells.

Figures 16-23 show the cytotoxicity results of hybrid cyclic-linear and linear $((RW)_5K)(RW)_x$ peptides analogs in CCRF-CEM, SK-OV-3, MDA-MB-231, and HEK-293 cells after 3 and 24 h incubation. The goal of this study was to determine the non-toxic concentration and appropriate time of incubation for all $((RW)_5K)(RW)_x$ peptides analogs at the same time.

Linear $(RW)_5KRW$ and hybrid cyclic-linear $[(RW)_5K](RW)$ did not exhibit any cytotoxicity at the concentration 5 and 10 μM in all the cell lines after 3h incubation (Figures 16-19), however linear $(RW)_5KRW$ and cyclic $[(RW)_5K](RW)$ at 10μM reduced the cell proliferation of SK-OV-3 by 6% and 2%, respectively, after 24 h incubation (Figure 21). Linear $(RW)_5KRW$ and cyclic $[(RW)_5K](RW)$ did not exhibit any cytotoxicity at 10 μM concentration in CCRF-CEM cells after 24 h incubation (Figure 20). Cell proliferation was decreased in the presence of $(RW)_5KRW$ and $[(RW)_5K](RW)$ by 15% and 8% in MDA-MB-231 cells, and 2% and 0% in HEK-293 cells, respectively, after 24 h incubation and 10μM concentration (Figure 22 and 23). The

same pattern was observed for hybrid cyclic-linear and linear $[(RW)_5K](RW)_x$ and $((RW)_5K)(RW)_x$ peptides analogs X=2-5 (Figures 16-23).

The results indicate that linear analogs of $((RW)_5K)(RW)_x$ in most cases are more cytotoxic compared to the hybrid cyclic-linear ones. The reason for that could be the difference between the structure of linear and cyclic peptides, in which the cyclic-linear peptides are more rigid. In contrast, linear peptides have more flexible structures, and they can interact with many proteins and become more cytotoxic.

In general, the higher concentration of the peptides leads to lower cell viability. As an example, $[(RW)_5K](RW)_5$ showed the cell survival of 101-43% at a 5-75 μM concentration in CCRF-CEM cells after 3 h incubation (Figure 16). The compounds exhibited higher toxicity at 24 h (Figures 20-23) when compared with the corresponding concentration at 3 h in most cases, suggesting time-dependent cytotoxicity. For example, $[(RW)_5K](RW)_5$ exhibited 79%, 77%, 71%, 39% cell viability at 25 μM concentration after 24 h incubation compared to 88%, 78%, 105%, 45% cell viability after 3 h incubation in CCRF-CEM, SK-OV-3, MDA-MB-231, and HEK-293, respectively (Figures 16-23).

Also, by increasing the number of arginine and tryptophan residues in the sequence, the cytotoxicity was gradually increased in both hybrid cyclic-linear and linear peptides. For example, cyclic-linear $[(RW)_5K](RW)$ and $[(RW)_5K](RW)_5$ reduced cell proliferation at 25 μM by 2% and 21% in CCRF-CEM cells after 24 h incubation (Figure 20). In most of the cell lines, $[(RW)_5K](RW)_5$ showed the cell viability less than 80% at 25 μM concentration and 3 h incubation.

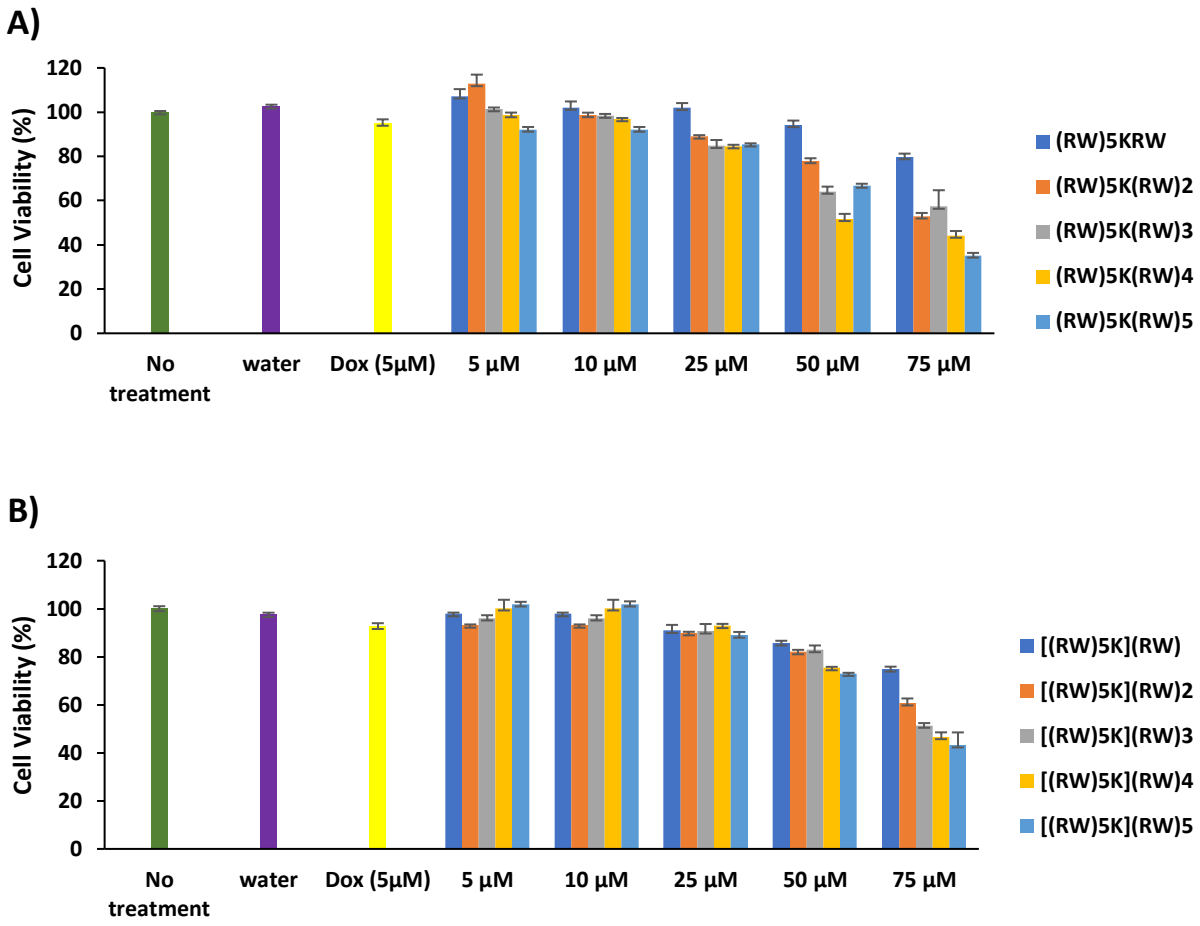

Figure 16. Cytotoxicity study of peptides (A: Linear peptides, B: Hybrid cyclic-linear peptides) in CCRF-CEM cells after 3 h incubation.

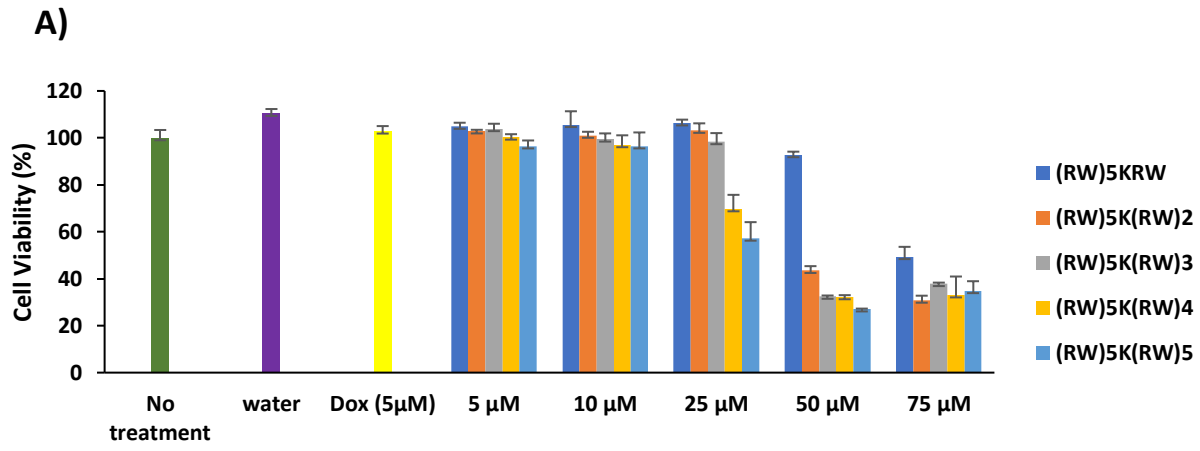

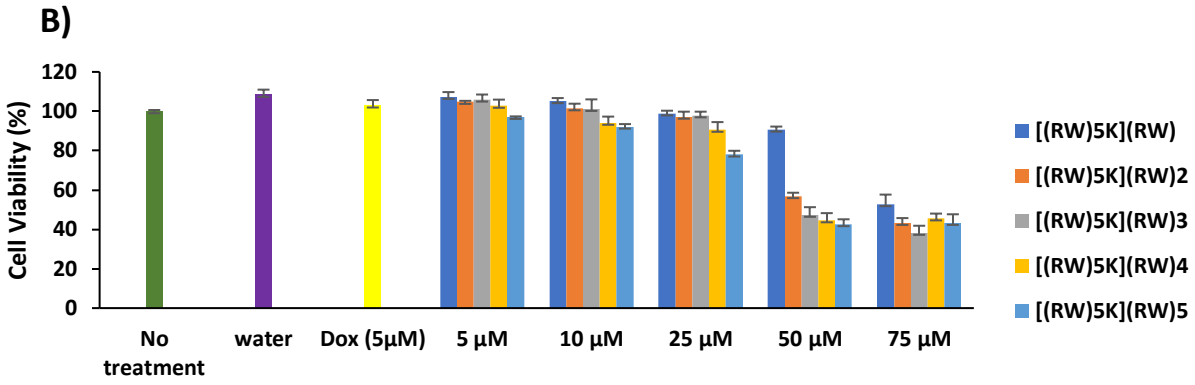

Figure 17. Cytotoxicity study of peptides (A: Linear peptides, B: Hybrid cyclic-linear peptides) in SK-OV-3 cells after 3 h incubation.

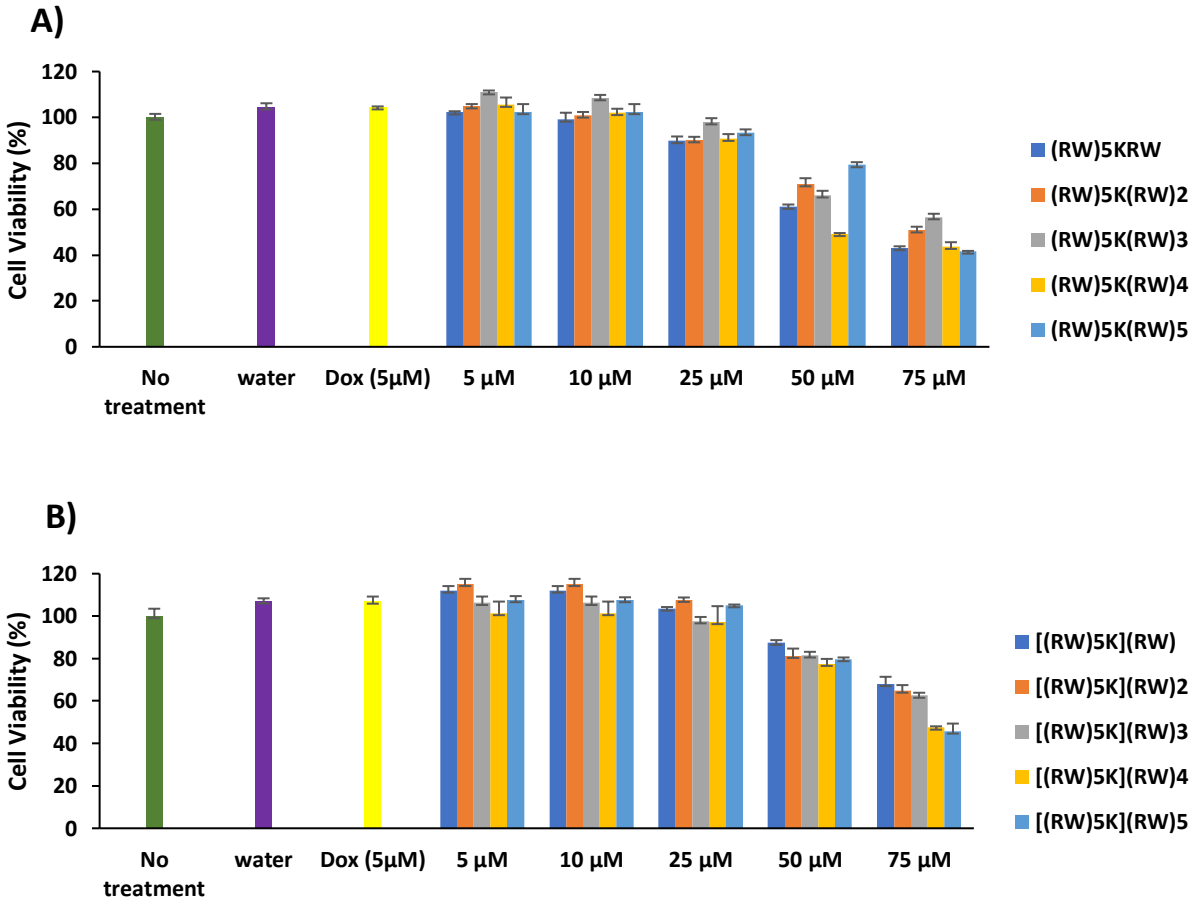

Figure 18. Cytotoxicity study of peptides (A: Linear peptides, B: Hybrid cyclic-linear peptides) in MDA-MB-231 cells after 3 h incubation.

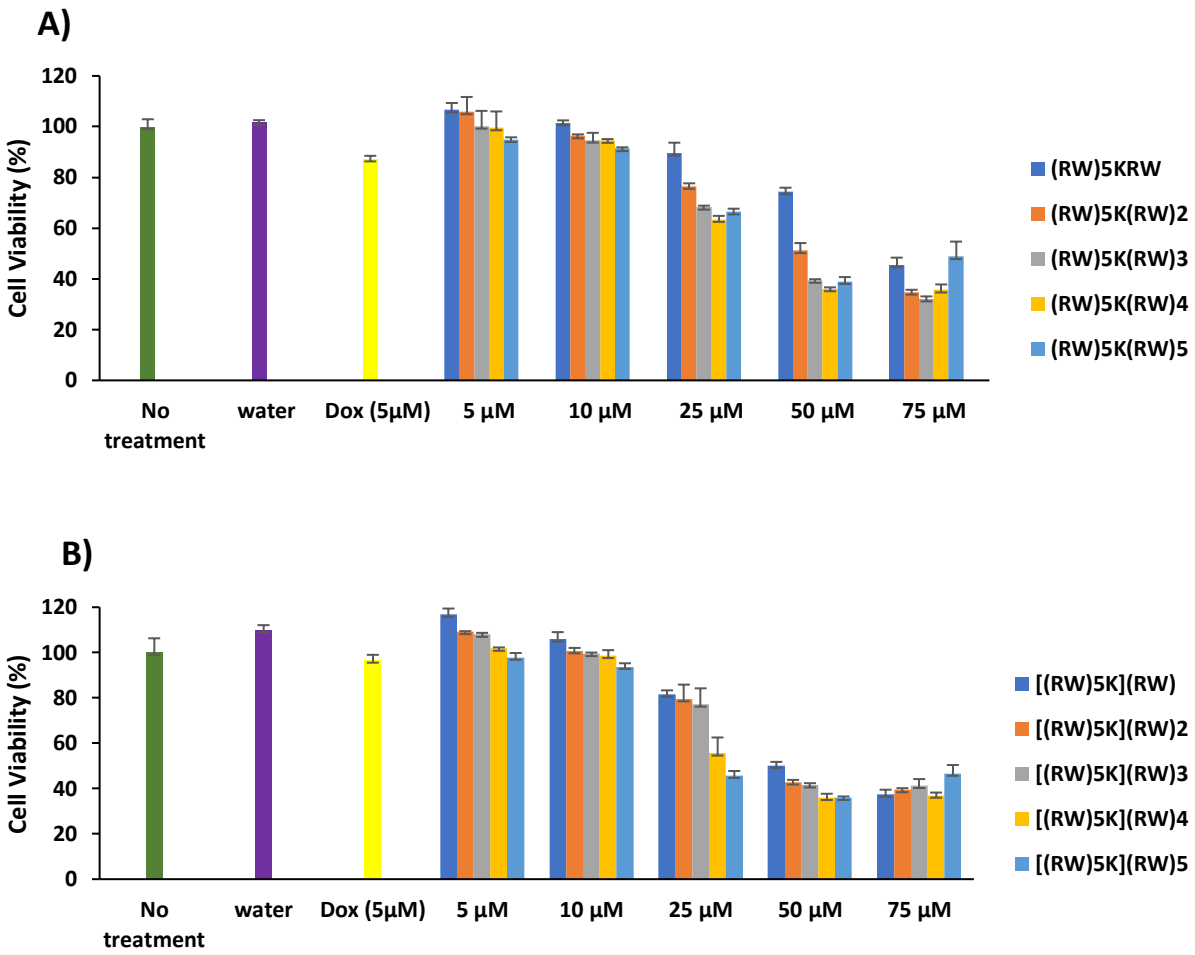

Figure 19. Cytotoxicity study of peptides (A: Linear peptides, B: Hybrid cyclic-linear peptides) in HEK-293 cells after 3 h incubation.

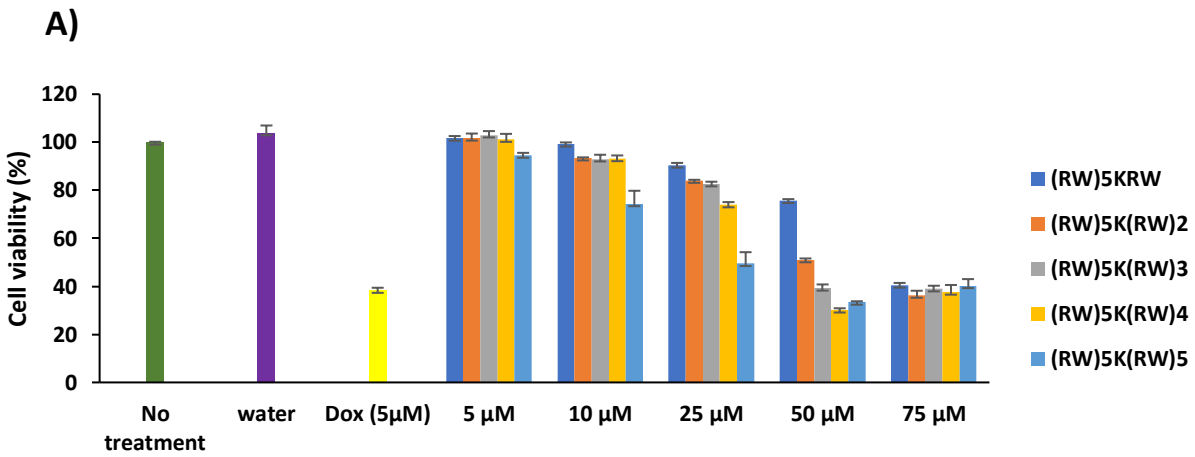

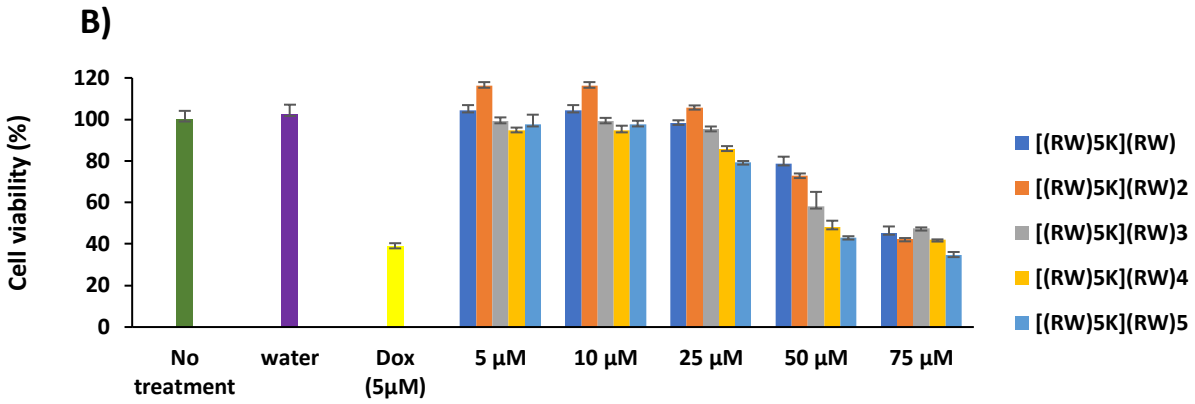

Figure 20. Cytotoxicity study of peptides (A: Linear peptides, B: Hybrid cyclic-linear peptides) in CCRF-CEM cells after 24 h incubation.

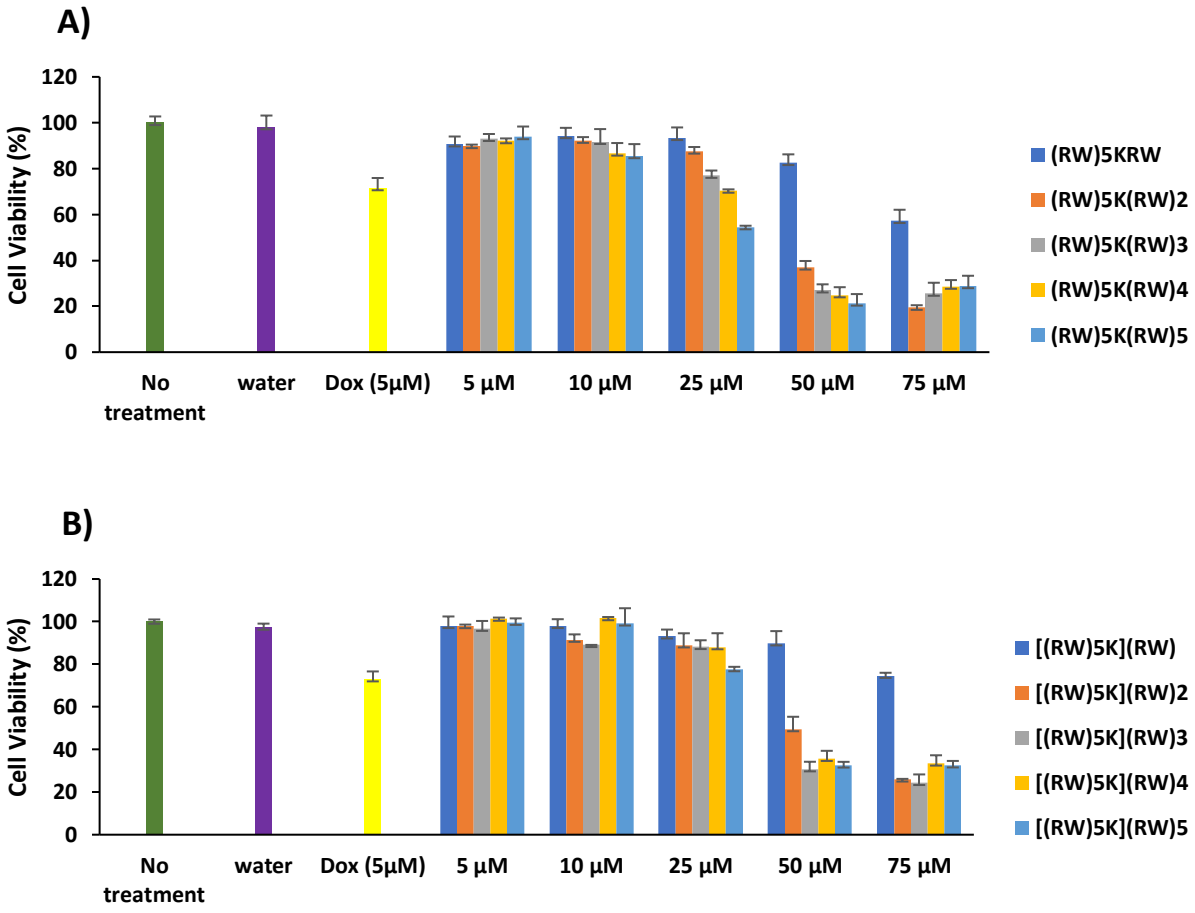

Figure 21. Cytotoxicity study of peptides (A: Linear peptides, B: Hybrid cyclic-linear peptides) in SK-OV-3 cells after 24 h incubation.

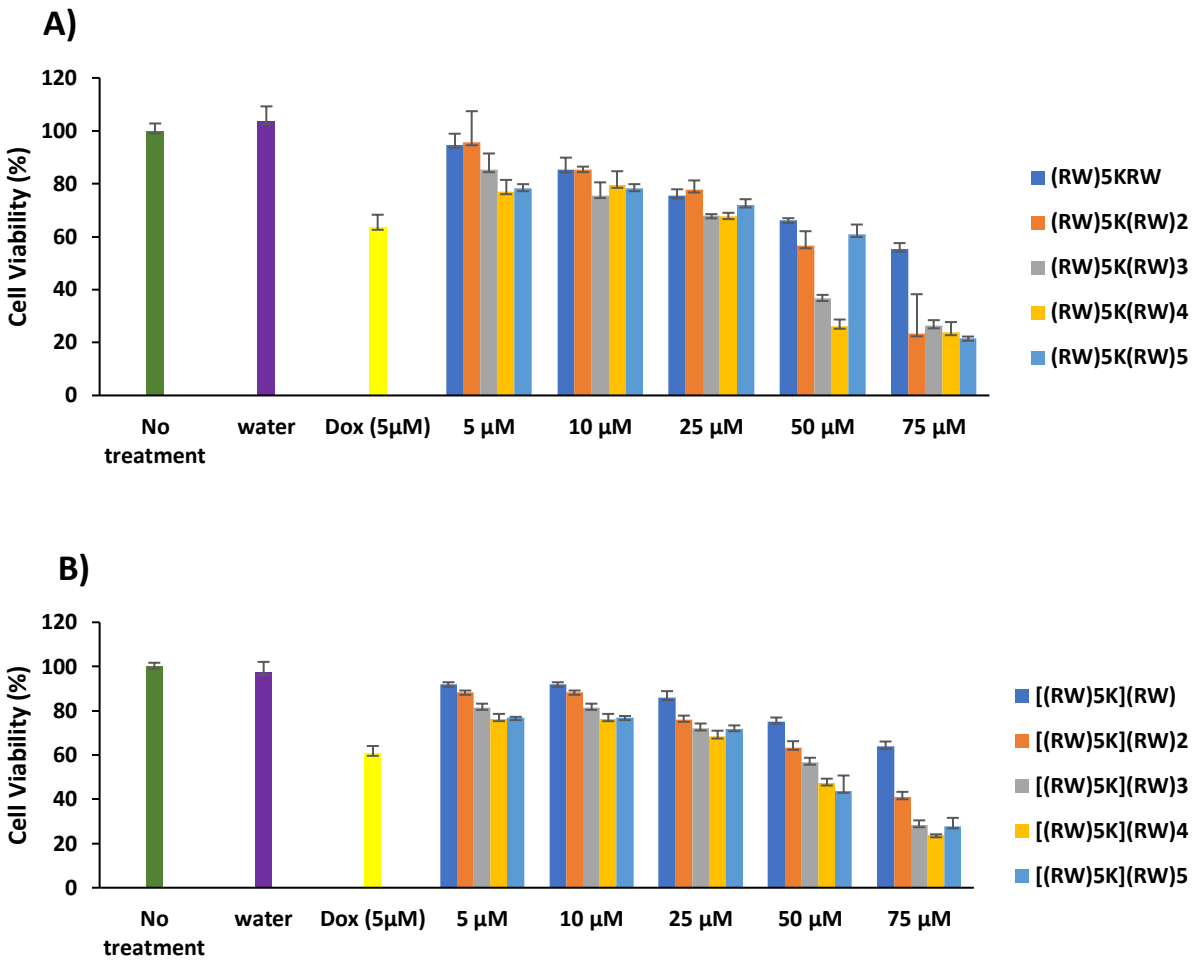

Figure 22. Cytotoxicity study of peptides (A: Linear peptides, B: Hybrid cyclic-linear peptides) in MDA-MB-231 cells after 24 h incubation.

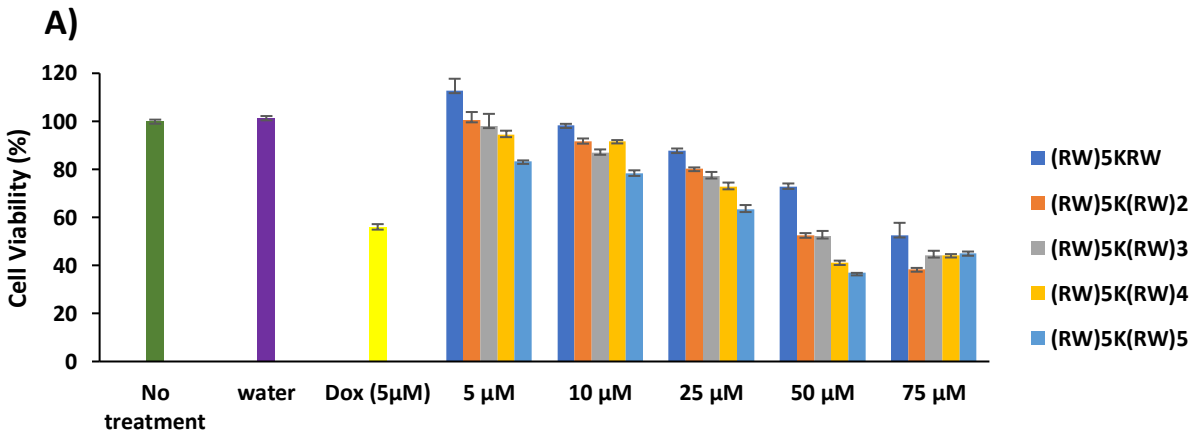

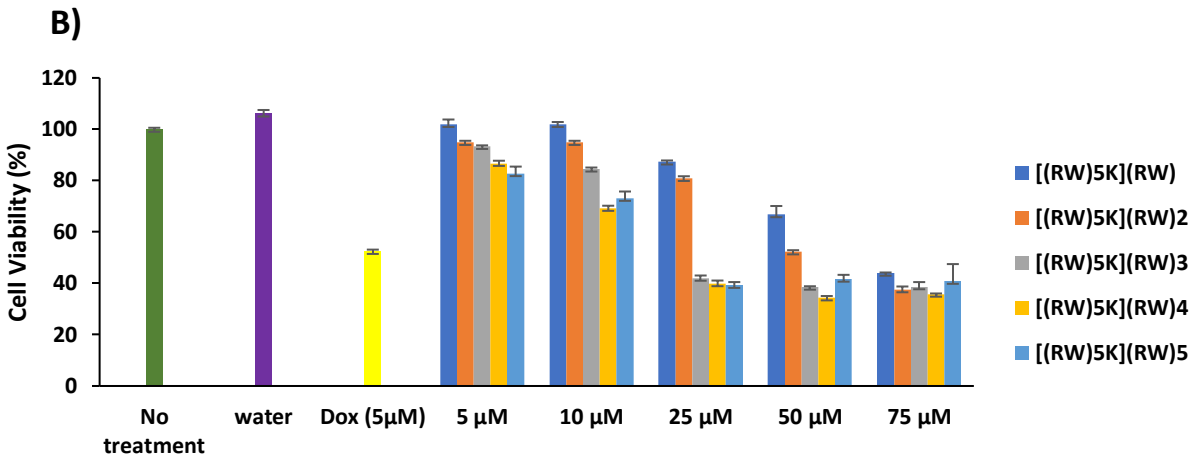

Figure 23. Cytotoxicity study of peptides (A: Linear peptides, B: Hybrid cyclic-linear peptides) in HEK-293 cells after 24 h incubation.

Another study was done to evaluate the cytotoxicity of F'-[$(RW)_5$K]$(RW)_5$ in SK-OV-3 and MDA-MB-231 cell lines after 3 h incubation. F'-[$(RW)_5$K]$(RW)_5$ exhibited the cell viability of 92% and 94% at 10 µM in SK-OV-3 and MDA-MB-231 cell lines after 3 h incubation (Figures 24 and 25).

These data indicated that linear and hybrid cyclic-linear ($(RW)_5$K)$(RW)_x$ X=1-5 and F'-[$(RW)_5$K]$(RW)_5$ did not exhibit any significant cytotoxicity at 10 µM concentration after 3 h incubation. Although the peptides showed the cell viability of more than 80% in most of the cell lines at 25 µM concentration and 3 h incubation. Thus, 10 µM concentration and 3 h incubation were selected for further studies to rule out any cytotoxicity related to compounds.

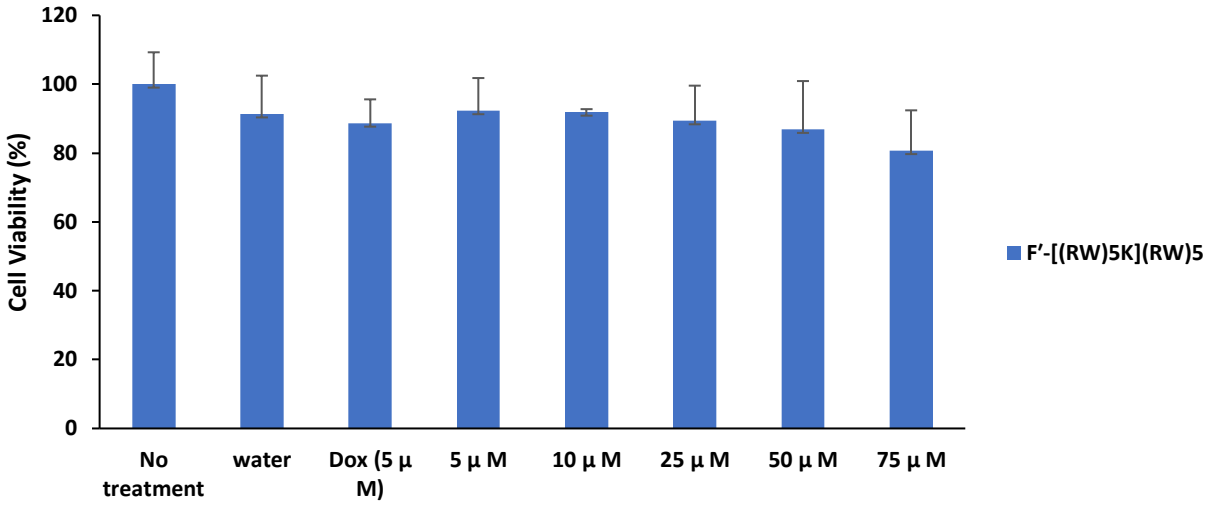

Figure 24. Cytotoxicity study of F'-[(RW)$_5$K](RW)$_5$ in SK-OV-3 cells and 3 h incubation.

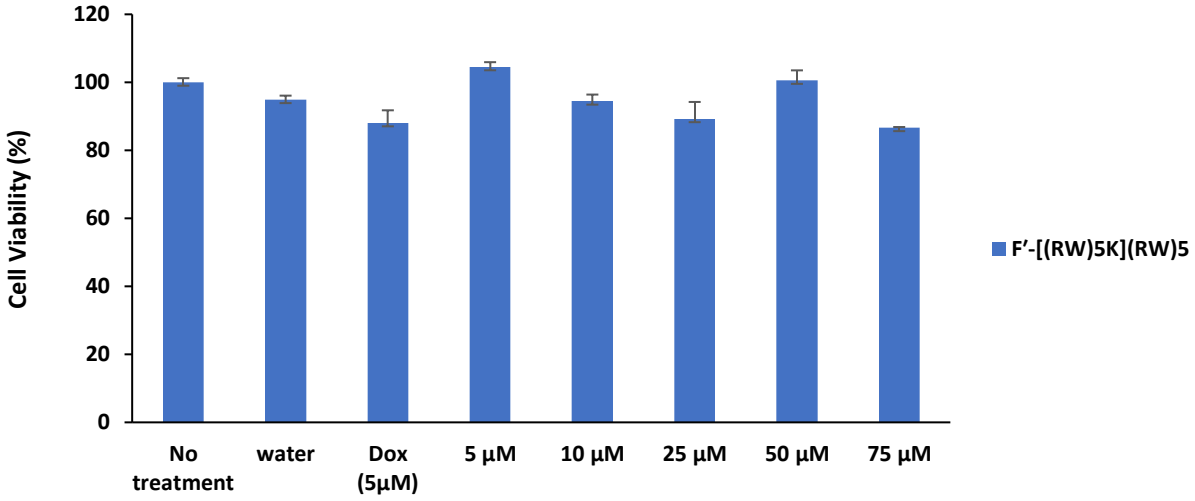

Figure 25. Cytotoxicity study of F'-[(RW)$_5$K](RW)$_5$ in MDA-MB-231 cells after 3 h incubation.

3.2. Cellular uptake study

Cellular uptake studies were performed by FACS (fluorescence activated cell sorting) using CCRF-CEM and SK-OV-3 cells to measure the cellular uptake of fluorescence-labeled phosphopeptides (F´-GpYEEI), and anti-HIV drugs (lamivudine (F´-3TC), emtricitabine (F´-

FTC), stavudine (F´-d4T)) in the presence of hybrid cyclic-linear peptides (10 µM) after 3 h incubation (Figures 26 and 27).

CCRF-CEM cells were used to measure the cellular uptake of linear peptides in the presence of fluorescence-labeled phosphopeptides (F´-GpYEEI) (Figure 28). The concentration of 2 µM was selected for F´-GpYEEI and anti-HIV drugs based on the previous study, which confirmed an appropriate ratio of 5 to 1 between the peptide and phosphopeptide needed for more efficient uptake [29]. $[WR]_5$, which has been previously reported as a molecular transporter [8], was used as a positive control. F´-GpYEEI and anti-HIV drugs alone were used as negative controls. After 3 h incubation, CCRF-CEM and SK-OV-3 cells were analyzed by flow cytometry. All assays were performed in triplicate. The data were based on the mean fluorescence signal for 10,000 cells collected.

In general, by increasing the number of arginine and tryptophan residues in the sequence, the cellular uptake was enhanced in both cyclic-linear and linear peptides. For example, $[(RW)_5K](RW)$ (10 µM) increased the cellular uptake of F′-GpYEEI (2 µM) by 3.8 fold whereas the $[(RW)_5K](RW)_5$ (10 µM) enhanced the cellular uptake of F′-GpYEEI (2 µM) by 18 fold in CCRF-CEM cells (Figure 26).

The physical mixture of F′-GpYEEI (2 µM) with $[(RW)_5K](RW)_5$ (10 µM) significantly enhanced the cellular uptake by 18- and 11-fold when compared to F′-GpYEEI (2 µM) alone, while the physical mixture of F′-GpYEEI (2 µM) with $[WR]_5$ enhanced the uptake by 3.6- and 2-fold in CCRF-CEM and SK-OV-3 cells, respectively (Figure 26).

$[(RW)_5K](RW)_5$ was found to be more effective when compared with other cyclic-linear peptides and $[WR]_5$ in improving the cellular uptake of the phosphopeptide, presumably because of a higher number of positive charges provide adequate interaction between negatively charged

phosphopeptide in comparison to other cyclic-linear peptides and $[WR]_5$. As number of tryptophan and arginine residues increased, the uptake of the phosphopeptide cargo was enhanced. Thus, cyclic-linear $[(RW)_5K](RW)_5$ was found to be the most effective peptide as the molecular transporter of fluorescence-labeled phosphopeptide among the synthesized hybrid cyclic-linear peptides.

To evaluate the cellular uptake efficiency of the synthesized peptide for small molecules, FACS analysis was performed in the presence of cyclic-linear peptides and fluorescence-labeled anti-HIV drugs: (lamivudine (F´-3TC), emtricitabine (F´-FTC), stavudine (F´-d4T)) in CCRF-CEM and SK-OV-3 cells (Figure 27). The same trend was observed for the fluorescence-labeled anti-HIV drugs in CCRF-CEM and SK-OV-3 cells, when $[(RW)_5K](RW)_5$ (10 μM) significantly increased the cell uptake of F´-3TC, F´-FTC F´-d4T (2 μM) in CCRF-CEM by 4.3, 7, and 7.6 as shown by mean fluorescence intensity, respectively.

For the comparison, cellular uptake studies were performed by using CCRF-CEM to measure the cellular uptake of fluorescence-labeled phosphopeptides (F´-GpYEEI) in the presence of linear peptides (10 μM) after 3 h incubation (Figure 28). The cellular uptake of linear $((RW)_5K)(RW)$ in the presence of F´-GpYEEI (2 μM) was much less than cyclic-linear $[(RW)_5K](RW)_5$. For example, the physical mixture of F′-GpYEEI (2 μM) with linear $((RW)_5KRW)$ enhanced the uptake by 9-fold in CCRF-CEM while cyclic $[(RW)_5K](RW)_5$ increased the cell uptake F´-GpYEEI by 18-fold in CCRF-CEM (Figure 26 and 28). Thus, the cellular uptake in the presence of linear peptides was much less than cyclic-linear peptides, possibly due to enhanced cellular permeability of cyclic-linear peptides versus the corresponding linear one.

The difference in the rate of increased cellular uptake in CCFR-CEM and SK-OV-3 cells could be because of the difference in uptake mechanism, receptors, and lipid structure between two cell lines.

The cellular uptake of various fluorescence-labeled compounds differed significantly. In the case of F′-GpYEEI, cyclic-linear $[(RW)_5K](RW)_5$ showed a higher cellular uptake F´-GpYEEI (18-fold) compared to F´-3TC (4.3-fold) in CCRF-CEM cells (Figure 26 and 27), presumably due to the more efficient interactions of the positively charged $[(RW)_5K](RW)_5$ with the negatively charged phosphopeptide versus small-molecule antiviral agents. $[(RW)_5K](RW)_5$ was found to be a significantly more efficient transporter among peptides in the delivery of a larger linear phosphopeptide in comparison to small molecules. Furthermore, the differential cellular uptake of anti-HIV compounds can be attributed to the fact that different cargos show different behaviors.

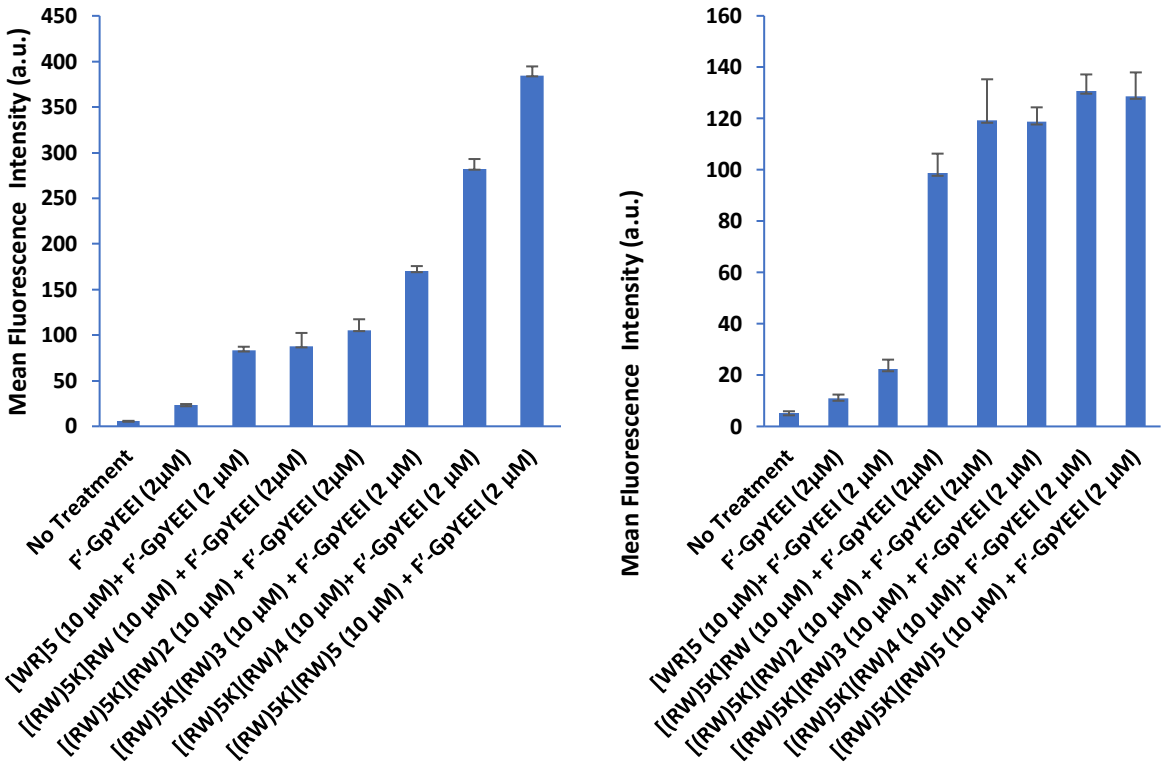

Figure 26. Cellular uptake of F´-GpYEEI (2 μM) in the presence of cyclic-linear peptides (10 μM) in CCRF-CEM (left) and SK-OV-3 cells (right) after 3 h incubation.

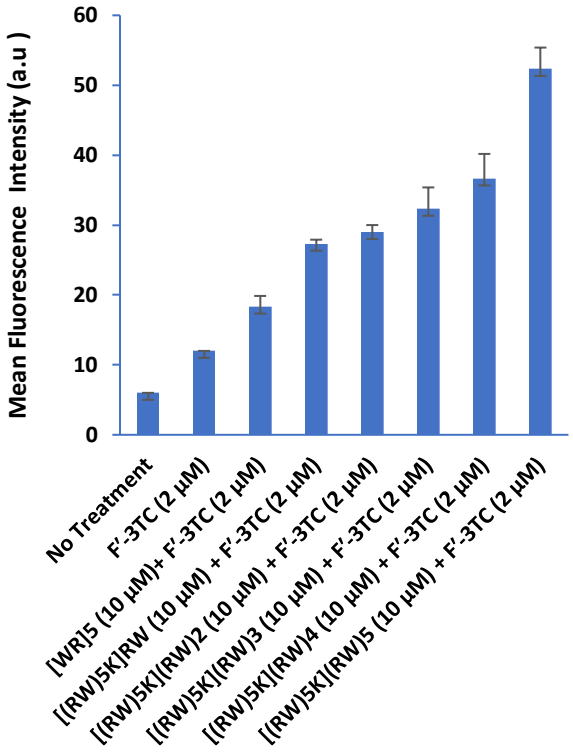
Mean Fluorescence Intensity (a.u)
60
50
40
30
20
10
0
No Treatment
F′-3TC (2 μM)
[WR]5 (10 μM)+ F′-3TC (2 μM)
[(RW)5K]RW (10 μM) + F′-3TC (2 μM)
[(RW)5K](RW)2 (10 μM) + F′-3TC (2 μM)
[(RW)5K](RW)3 (10 μM) + F′-3TC (2 μM)
[(RW)5K](RW)4 (10 μM) + F′-3TC (2 μM)
[(RW)5K](RW)5 (10 μM) + F′-3TC (2 μM)

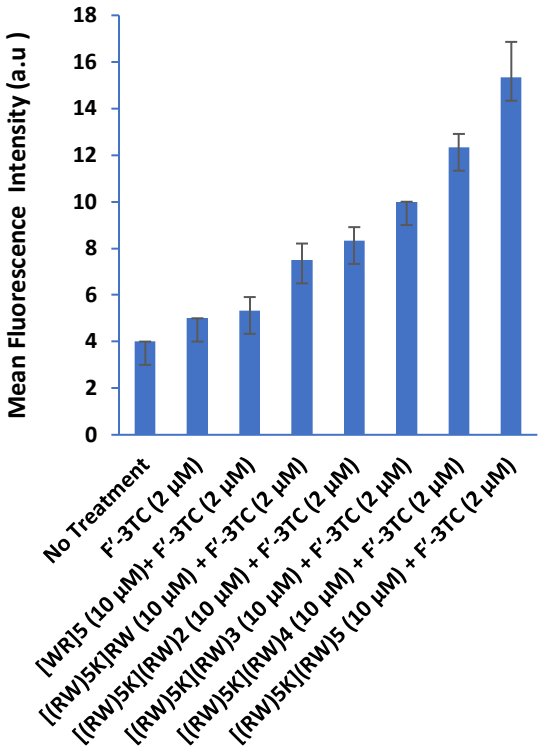
Mean Fluorescence Intensity (a.u)
18
16
14
12
10
8
6
4
2
0
No Treatment
F′-3TC (2 μM)
[WR]5 (10 μM)+ F′-3TC (2 μM)
[(RW)5K]RW (10 μM) + F′-3TC (2 μM)
[(RW)5K](RW)2 (10 μM) + F′-3TC (2 μM)
[(RW)5K](RW)3 (10 μM) + F′-3TC (2 μM)
[(RW)5K](RW)4 (10 μM) + F′-3TC (2 μM)
[(RW)5K](RW)5 (10 μM) + F′-3TC (2 μM)

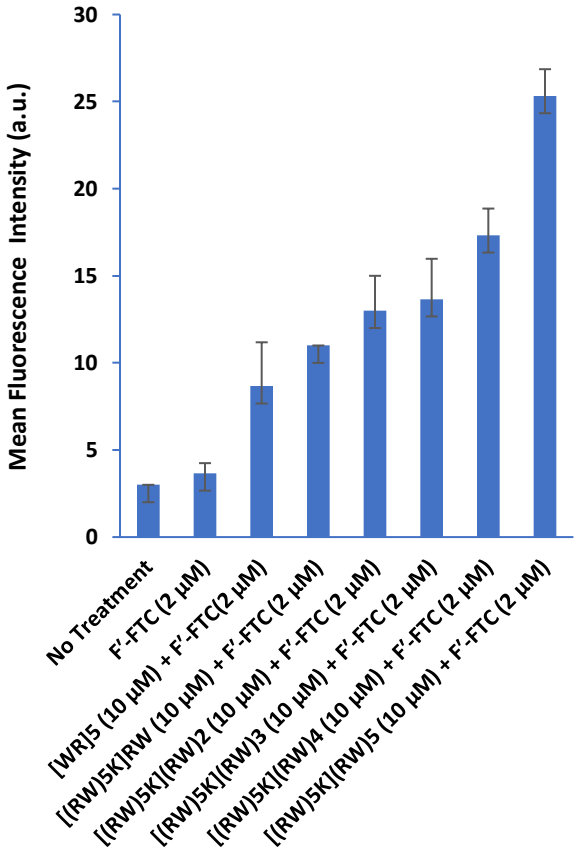
Mean Fluorescence Intensity (a.u.)
30
25
20
15
10
5
0
No Treatment
F′-FTC (2 μM)
[WR]5 (10 μM) + F′-FTC(2 μM)
[(RW)5K]RW (10 μM) + F′-FTC (2 μM)
[(RW)5K](RW)2 (10 μM) + F′-FTC (2 μM)
[(RW)5K](RW)3 (10 μM) + F′-FTC (2 μM)
[(RW)5K](RW)4 (10 μM) + F′-FTC (2 μM)
[(RW)5K](RW)5 (10 μM) + F′-FTC (2 μM)

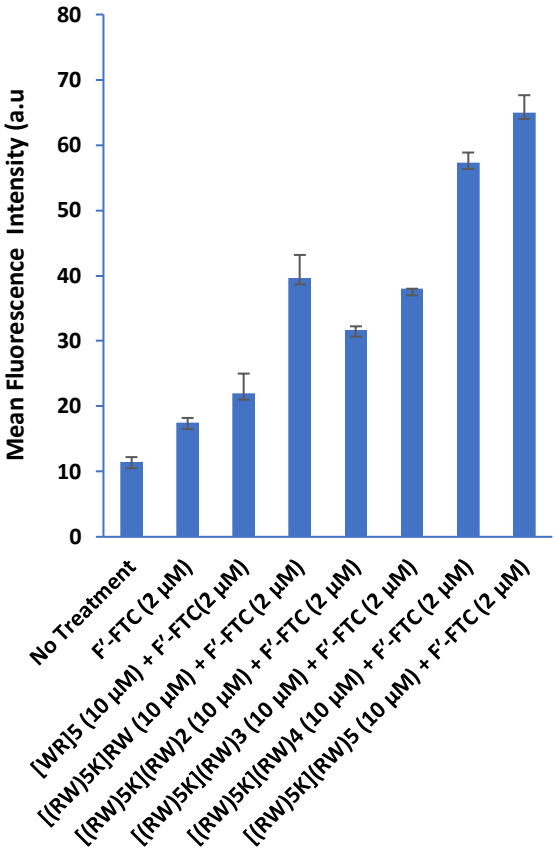
Mean Fluorescence Intensity (a.u
80
70
60
50
40
30
20
10
0
No Treatment
F′-FTC (2 μM)
[WR]5 (10 μM) + F′-FTC(2 μM)
[(RW)5K]RW (10 μM) + F′-FTC (2 μM)
[(RW)5K](RW)2 (10 μM) + F′-FTC (2 μM)
[(RW)5K](RW)3 (10 μM) + F′-FTC (2 μM)
[(RW)5K](RW)4 (10 μM) + F′-FTC (2 μM)
[(RW)5K](RW)5 (10 μM) + F′-FTC (2 μM)

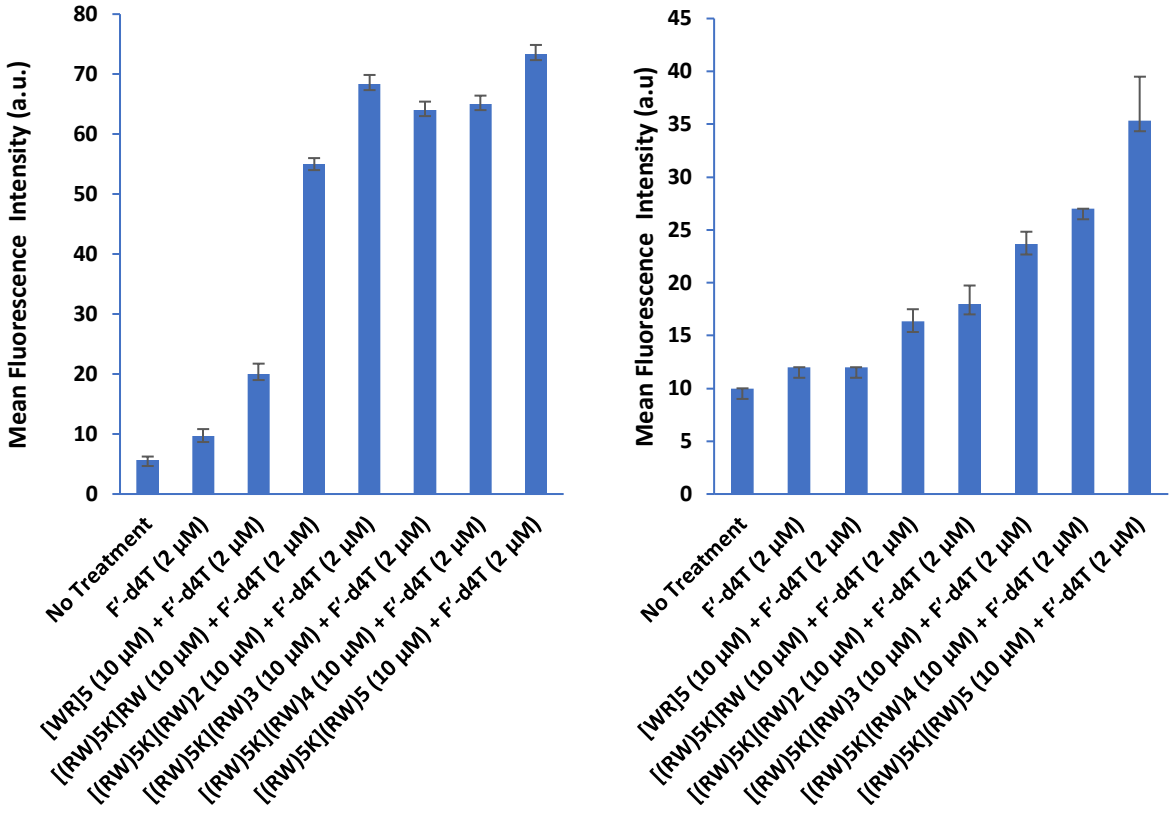

Figure 27. Cellular uptake of F´-d4T, F´-3TC, and F´-FTC (2 µM) in the presence of cyclic-linear peptides (10 µM) in CCRF-CEM (left) and SK-OV-3 cells (right) after 3 h incubation.

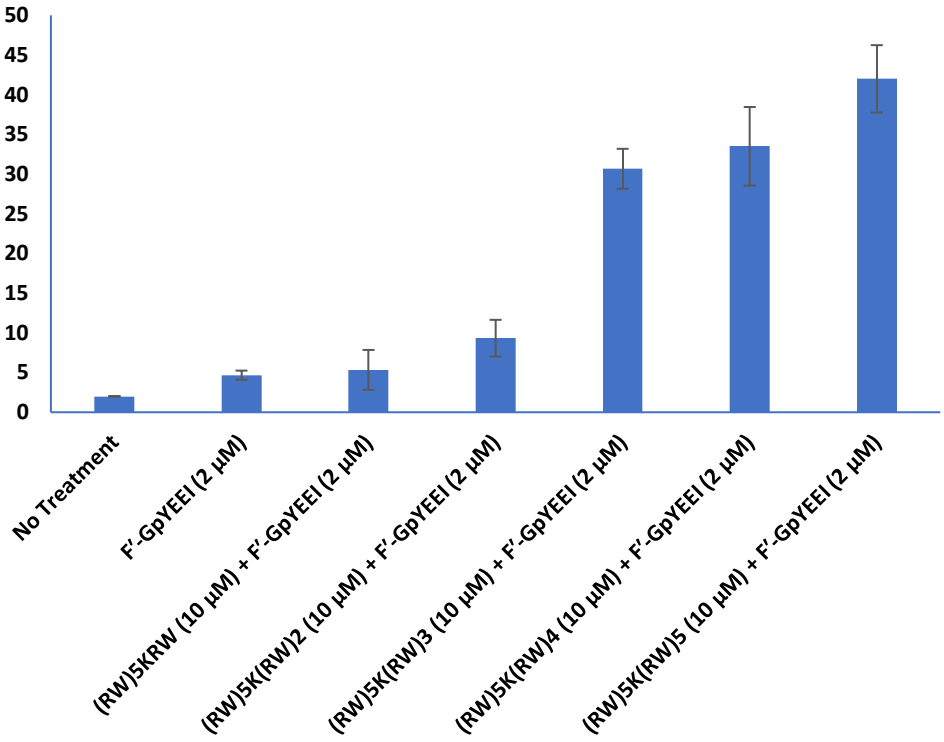

Figure 28. Cellular uptake of F´-GpYEEI (2μM) in the presence of linear peptides (10 μM) in CCRF-CEM cells after 3 h incubation.

Conclusions

The structure-cellular uptake relationship of $[(RW)_5K](RW)_x$ analogs was performed to determine the optimal number of arginine and tryptophan residues on the linear tail for efficient molecular transporter properties. For this purpose, a number of linear and cyclic-linear peptides composed of alternative arginine and tryptophan residues were synthesized and characterized. The newly synthesized peptides did not exhibit any significant cytotoxicity at a concentration of 10 μM after 3 h incubation in CCRF-CEM, SK-OV-3, MDA-MB-231, and HEK-293 cells. Among all peptides, $[(RW)_5K](RW)_5$ (10 μM) showed to be a significantly efficient transporter in the delivery of F´-GpYEEI in comparison to small molecules and could improve the cellular uptake

by 18 fold in CCRF-CEM cells after 3 h incubation. These findings indicate that hybrid cyclic-linear peptide containing a higher number of alternating arginine residues and tryptophan residues on the linear tail can act as efficient molecular transporter of cargo molecules.

References

1. Habault, J., & Poyet, J. (2019). Recent advances in cell penetrating peptide-based anticancer therapies. *Molecules, 24*(5), 927. doi:10.3390/molecules24050927
2. Böhmová, E., Machová, D., Pechar, M., Pola, R., Venclíková, K., Janoušková, O., & Etrych, t. (2018). Cell-penetrating peptides: A useful tool for the delivery of Various Cargoes into cells. *Physiological Research*. doi:10.33549/physiolres.933975
3. Kardani, K., Milani, A., H. Shabani, S., & Bolhassani, A. (2019). Cell penetrating peptides: the potent multi-cargo intracellular carriers. *Expert Opinion on Drug Delivery*, *16*(11), 1227-1258. doi:10.1080/17425247.2019.1676720
4. Shirazi, A.N., Tiwari, R. K., Oh, D., Banerjee, A., Yadav, A., & Parang, K. (2013). Efficient delivery of cell impermeable phosphopeptides by a cyclic peptide amphiphile containing tryptophan and arginine. *Molecular Pharmaceutics*, *10*(5), 2008-2020. doi:10.1021/mp400046u
5. Agarwal, H. K., Chhikara, B. S., Bhavaraju, S., Mandal, D., Doncel, G. F., & Parang, K. (2012). Emtricitabine prodrugs with improved anti-HIV activity and cellular uptake. *Molecular Pharmaceutics, 10*(2), 467-476. doi:10.1021/mp300361a
6. Agarwal, H. K., Chhikara, B. S., Hanley, M. J., Ye, G., Doncel, G. F., & Parang, K. (2012). Synthesis and biological evaluation of fatty acyl ester derivatives of (−)-2′,3′-dideoxy-3′-thiacytidine. *Journal of Medicinal Chemistry*,*55*(10), 4861-4871. doi:10.1021/jm300492q
7. Agarwal, H. K., Loethan, K., Mandal, D., Doncel, G. F., & Parang, K. (2011). Synthesis and biological evaluation of fatty acyl ester derivatives of 2′,3′-didehydro-2′,3′-dideoxythymidine. *Bioorganic & Medicinal Chemistry Letters*, *21*(7), 1917-1921. doi:10.1016/j.bmcl.2011.02.070

8. Mandal, D., Shirazi, A.N., & Parang, K. (2011). Cell-penetrating homochiral cyclic peptides as nuclear-targeting molecular transporters. *Angewandte Chemie, 123*(41), 9807-9811. doi:10.1002/ange.201102572
9. Shirazi, A.N., Tiwari, R., Chhikara, B. S., Mandal, D., & Parang, K. (2013). Design and biological evaluation of cell-penetrating peptide–doxorubicin conjugates as prodrugs. *Molecular Pharmaceutics, 10*(2), 488-499. doi:10.1021/mp3004034
10. El-Sayed, N. S., Shirazi, A. N., Sajid, M. I., Park, S. E., Parang, K., & Tiwari, R. K. (2019). Synthesis and antiproliferative activities of conjugates of paclitaxel and camptothecin with a cyclic cell-penetrating peptide. *Molecules, 24*(7), 1427. doi:10.3390/molecules24071427
11. Shirazi, A.N., Salem El-Sayed, N., Kumar Tiwari, R., Tavakoli, K., & Parang, K. (2016). Cyclic peptide containing hydrophobic and positively charged residues as a drug delivery system for curcumin. *Current Drug Delivery, 13*(3), 409-417. doi:10.2174/1567201812666151029101102
12. Shirazi, A.N., Tiwari, R. K., Oh, D., Sullivan, B., Kumar, A., Beni, Y. A., & Parang, K. (2014). Cyclic peptide–selenium nanoparticles as drug transporters. *Molecular Pharmaceutics, 11*(10), 3631-3641. doi:10.1021/mp500364a
13. Shirazi, A.N., Mandal, D., Tiwari, R. K., Guo, L., Lu, W., & Parang, K. (2012). Cyclic peptide-capped gold nanoparticles as drug delivery systems. *Molecular Pharmaceutics, 10*(2), 500-511. doi:10.1021/mp300448k
14. Yin, N. (2014). Enhancing the oral bioavailability of peptide drugs by using chemical modification and other approaches. *Medicinal Chemistry*. doi:10.4172/2161-0444.1000227

15. Fields, G. B. (2001). Introduction to peptide synthesis. *Current Protocols in Protein Science, 26*(1). doi:10.1002/0471140864.ps1801s26
16. Nobel lecture, 8 December, 1984 by bruce merrifield solid-phase synthesis, The Rockefeller University, 1230 York Avenue, New York, N.Y. 10021-6399
17. Sachdeva, S. (2016). Peptides as 'drugs': The journey so far. *International Journal of Peptide Research and Therapeutics*,*23*(1), 49-60. doi:10.1007/s10989-016-9534-8
18. Palomo, J. M. (2014). Solid-phase peptide synthesis: An overview focused on the preparation of biologically relevant peptides. *RSC Adv., 4*(62), 32658-32672. doi:10.1039/c4ra02458c
19. Coin, I., Beyermann, M., & Bienert, M. (2007). Solid-phase peptide synthesis: From standard procedures to the synthesis of difficult sequences. *Nature Protocols, 2*(12), 3247-3256. doi:10.1038/nprot.2007.454
20. Carpino, L. A., & Han, G. Y. (1970). 9-Fluorenylmethoxycarbonyl function, a new base-sensitive amino-protecting group. *Journal of the American Chemical Society, 92*(19), 5748-5749. doi:10.1021/ja00722a043
21. Ishiyama, M., Tominaga, H., Shiga, M., Sasamoto, K., Ohkura, Y., & Ueno, K. (1996). A combined assay of cell viability and in vitro cytotoxicity with a highly water-soluble tetrazolium salt, neutral red and crystal violet. *Biological and Pharmaceutical Bulletin, 19*(11), 1518-1520. doi:10.1248/bpb.19.1518
22. Cobb, L. (2019). Cell proliferation assays and cell viability assays. *Materials and Methods, 9*. doi:10.13070/mm.en.9.2799

23. Malich, G., Markovic, B., & Winder, C. (1997). The sensitivity and specificity of the MTS tetrazolium assay for detecting the in vitro cytotoxicity of 20 chemicals using human cell lines. *Toxicology, 124*(3), 179-192. doi:10.1016/s0300-483x(97)00151-0

24. Riss TL, Moravec RA, Niles AL, Duellman S, Benink HA, Worzella TJ, Minor L. (2013). Cell viability assays. Assay Guidance Manual. PMID: 23805433.

25. McKinnon, K. M. (2018). Flow cytometry: An overview. *current protocols in immunology*, *120*(1). doi:10.1002/cpim.40

26. Macey, M. G. (n.d.). Principles of flow cytometry. *Flow Cytometry*, 1-15. doi:10.1007/978-1-59745-451-3_1

27. Zhao, P., & Sun, M. (2015). The maternal-to-zygotic transition in higher plants. *Current Topics in Developmental Biology*,373-398. doi:10.1016/bs.ctdb.2015.06.006

28. Adan, A., Alizada, G., Kiraz, Y., Baran, Y., & Nalbant, A. (2016). Flow cytometry: Basic principles and applications. *Critical Reviews in Biotechnology*, *37*(2), 163-176. doi:10.3109/07388551.2015.1128876

29. Hanna, S. E., Mozaffari, S., Tiwari, R. K., & Parang, K. (2018). Comparative molecular transporter efficiency of cyclic Peptides containing tryptophan and arginine residues. *ACS Omega, 3*(11), 16281-16291. doi:10.1021/acsomega.8b02589

Chapter 3

Determination of Cellular Uptake Mechanism of Hybrid Cyclic-Linear Peptide $[(RW)_5K](RW)_5$ and Fluorescence Microscopy

Abstract

The cellular uptake of the F'-[$(RW)_5$K]$(RW)_5$ was investigated in different concentrations and timelines by flow cytometry in MDA-MB-231 cells. The cellular uptake of F'-[$(RW)_5$K]$(RW)_5$ was enhanced in a time- and concentration-dependent manner. The flow cytometry results showed that the cellular uptake of F'-[$(RW)_5$K]$(RW)_5$ was slightly reduced in MDA-MB-231 cells in the presence of endocytic inhibitors, such as chlorpromazine, chloroquine, and methyl β-cyclodextrin. However, the uptake was not completely prevented by the presence of endocytosis inhibitors, suggesting the combination of energy-dependent and energy-independent pathways involved in the uptake. Moreover, the major partial inhibition was in the presence of chlorpromazine, suggesting the partial uptake through the clathrin-mediated endocytosis pathway. The confocal microscopy data were consistent with the flow cytometry results. Confocal microscopy images demonstrated the potential of [$(RW)_5$K]$(RW)_5$ peptide as a molecular transporter of the negatively charged F′-GpYEEI compared to $[WR]_5$. The physical mixture of F′-GpYEEI and [$(RW)_5$K]$(RW)_5$ or F'-[$(RW)_5$K]$(RW)_5$ showed fluorescein localization mainly in the cytosol after 3 h incubation in MDA-MB-231 cells.

1. Background

CPPs have different uptake mechanisms depending on the physicochemical properties of the CPPs, concentration, incubation time, temperature, membrane structure, type of cell, the primary and secondary structure of CPP, and cargo type [1]. Direct membrane translocation via energy-independent pathways and endocytosis with energy consumption have been suggested as two major mechanisms of permeation through cell membranes [2]. It was proposed that a CPP translocases plasma membrane directly at high concentration while the penetration occurs via endocytosis pathways at the low concentration [3]. However, there are some deviations from this rule, which a major mechanism of the uptake for the peptide at high concentration could switch to the direct penetration via the energy-independent pathway, while endocytosis is probable at low concentration of the peptide [4].

Electrostatic interactions between the positively charged CPP and negatively charged cell membrane components, such as heparan sulfate (HS) and phospholipid bilayer, are responsible for the direct internalization [5,6]. The inverted micelle model [7], pore formation [8], the carpet model [9] are the most popular mechanism proposed for the direct translocation of CPPs. The contribution of endocytosis to the different CPP internalization mechanisms and their cargo molecules was found after revealing the experimental artifacts using the fixed cells in experiments [10].

Thus, Reevaluation studies that were conducted on the live cells showed that endocytosis played an important role in peptide internalization. Endocytosis is an energy-dependent and active mechanism, which is composed of various pathway, including phagocytosis for uptake of large molecules and pinocytosis for solute uptake. Pinocytosis classifies as macropinocytosis, clathrin-

dependent endocytosis, caveolin-dependent endocytosis, clathrin- and/or caveolin-independent endocytosis [11,12].

In order to investigate the uptake mechanism of the newly synthesized hybrid peptide with the fluorescent-labeled hybrid cyclic-linear peptide, the cellular uptake was examined in the presence of endocytosis inhibitors, such as nystatin, chloroquine, chlorpromazine, and methyl-β-cyclodextrin.

Chlorpromazine is a drug that inhibits clathrin-mediated endocytosis [13]. Chlorpromazine is a cationic amphiphilic agent that blocks AP2, one of the main adaptor proteins in clathrin-mediated endocytosis, from operating. Chlorpromazine has also been shown to trap receptors within endosomes, preventing them from being recycled. As a result, this compound inhibits clathrin-mediated endocytosis on several levels [14].

Methyl-β-cyclodextrin is a powerful agent used for cholesterol depletion. Since cholesterol is required for proper membrane permeability and fluidity, cholesterol depletion may be a quite destructive treatment for cells. Furthermore, methyl-β-cyclodextrin exposure affects not only caveolae-mediated endocytosis but also any endocytic mechanism, greatly depending on the concentration used and the cells [14,15]. Methyl-β-cyclodextrin extracts cholesterol from the cell membrane and thus inhibits macropinocytosis and both clathrin-mediated endocytosis and clathrin-independent endocytosis [15].

Chloroquine inhibits clathrin-dependent endocytosis by affecting the function of clathrin and clathrin-coated vesicles, which inhibit acidification of endosomes [16]. Chloroquine reduces the expression of phosphatidylinositol binding clathrin assembly protein (PICALM), one of the three most abundant proteins in clathrin-coated pits, according to mechanistic studies [17].

Entry by caveolae is dependent on cholesterol, and the inhibitor nystatin is a highly selective inhibitor that is a steroid-binding agent and decomposes cholesterol and other lipids from cell membranes [18]. Thus, it inhibits caveolae/lipid-mediated endocytosis [19].

2. Experimental Section

2.1. Methods

2.1.1. Dose- and time-dependent study and mechanistic studies

Flow cytometry studies were performed in MDA-MB-231 cells to measure the cellular uptake of the F'-[$(RW)_5$K]$(RW)_5$ in different concentrations and timelines. MDA-MB-231 (5×10^5 cells/well) were seeded in the medium 24 h prior to experiment in 6 well plates, and after 24h the medium was changed with opti-MEM. The cells were then incubated with 5(6)-carboxyfluorescein (FAM) (2, 5, and 10 μM) and F'-[$(RW)_5$K]$(RW)_5$ (2, 5, and 10 μM) for 5-, 30 -, and 60 min (37 °C in a humidified atmosphere of 5% CO_2). The final volume of each well was 2 ml. The media containing the peptide were removed after 5-, 30-, and 60-min incubation. The cells were digested with 0.05% trypsin/EDTA (0.53 mM) for 5 min to remove any artificial surface binding. Cells were centrifuged at 2500 RPM for 5 min with Fisher Scientific accuSpin Micro 17. The cells were collected as precipitant. Then the cells were washed twice with PBS. The cells were resuspended in flow cytometry buffer and transferred to the Flow cytometry tubes through the 35 μm Strainer Mesh cap. Finally, the cells were analyzed by flow cytometry (FACSCalibur: Becton Dickinson) using the FITC channel and CellQuest software. The data presented were based on the mean fluorescence intensity for 10,000 cells collected. All assays were performed in triplicate. The data from the mean fluorescence signal were shown the internalization ability of F'-[$(RW)_5$K]$(RW)_5$ inside the cell in a time- and concentration-dependent manner.

Another study was performed in MDA-MB-231 to determine the mechanism of cellular uptake of F'-[$(RW)_5$K]$(RW)_5$. MDA-MB-231 cells were seeded in 6-well plates (5×10^5 cells/well) in opti-MEM. The cells were preincubated by various endocytosis inhibitors including nystatin (50 μg/mL), chloroquine (100 μM), chlorpromazine (30 μM), and methyl-β-cyclodextrin (2.5 mM) for 30 min. The cells were then incubated with F'-[$(RW)_5$K]$(RW)_5$ (10μM) in the presence of inhibitors for 3 h. The flow cytometry study was performed as described above.

2.1.2. Confocal microscopy

MDA-MB-231 and SK-OV-3 (1×10^5 cells/well) were seeded with a medium on a coverslip 24 h prior to the experiment in 6 well plates. After 24 h, the medium was changed with opti-MEM. The cells were then treated with F'-[$(RW)_5$K]$(RW)_5$ (10 μM) or $(RW)_5$K]$(RW)_5$ (10μM) + F′-GpYEEI (2 μM) in Opti-MEM and incubated for 3 h at 37 °C. After 3 h incubation, the media was removed, and cells were washed three times with PBS in each well. Then, the cells were fixed with 3.7% formaldehyde for 10 min, followed by washing 3 times with PBS for 5min (pH 7.6). The Texas red solution for staining the cell membrane (40 μL of Texas Red in 10 mL of PBS and 100 mg BSA) was added to each well for 1 h at room temperature. Cells were washed at least 3 times with PBS for 5 min. The DAPI (40μL) for staining the nuclei was placed on a microscope slide, and it was covered with the coverslip with the cell-attached side facing down. The slides were standing horizontally in a dark place that has airflow to dry faster. The cells were photographed by using Nikon Instruments A1 Confocal Laser Microscope Series. The scan mode was selected as Galvano. The magnification and resolution were set on 40× and 1024, respectively.

Another confocal microscopy experiment was performed for cellular uptake mechanism identification. MDA-MB-231 cells (1×10^5 cells/well) were seeded with a medium on a coverslip

24h prior to the experiment in 6 well plates. After 24h, the medium was changed with opti-MEM. The cells were preincubated by various endocytosis inhibitors, including nystatin (50 µg/mL), chloroquine (100 µM), chlorpromazine (30 µM), and methyl-β-cyclodextrin (2.5 mM) for 30 min. The cells were then incubated with F'-[(RW)5K](RW)$_5$ in the presence of inhibitors for 3 h. Then, the confocal microscopy study was carried out as described above.

3. Result and discussion

3.1. Dose- and time-dependent study

Flow cytometry studies were performed in MDA-MB-231 cells to measure the cellular uptake of the F'-[(RW)$_5$K](RW)$_5$ in different concentrations and timelines. 5(6)-carboxyfluorescein (FAM) was used as a negative control. The cells were then incubated with FAM and F'-[(RW)$_5$K](RW)$_5$ (2, 5, and 10 µM) for 5-, 30-, and 60 min. All assays were performed in triplicate. The FAM did not show any concentration- and time-dependent cellular uptake; however, the cellular uptake of F'-[(RW)$_5$K](RW)$_5$ was significantly enhanced by increasing the concentration and time (Figure 29). The highest cellular uptake for F'-[(RW)$_5$K](RW)$_5$ was observed at 10 µM and after 60 min incubation. Thus, the cellular uptake of the F'-[(RW)$_5$K](RW)$_5$ was found to increase in a concentration- and time-dependent manner. As the fluorescence-labeled peptide did not show significant cytotoxicity at concentration 10 µM and 3 h incubation, this concentration and timeline were used for mechanistic studies.

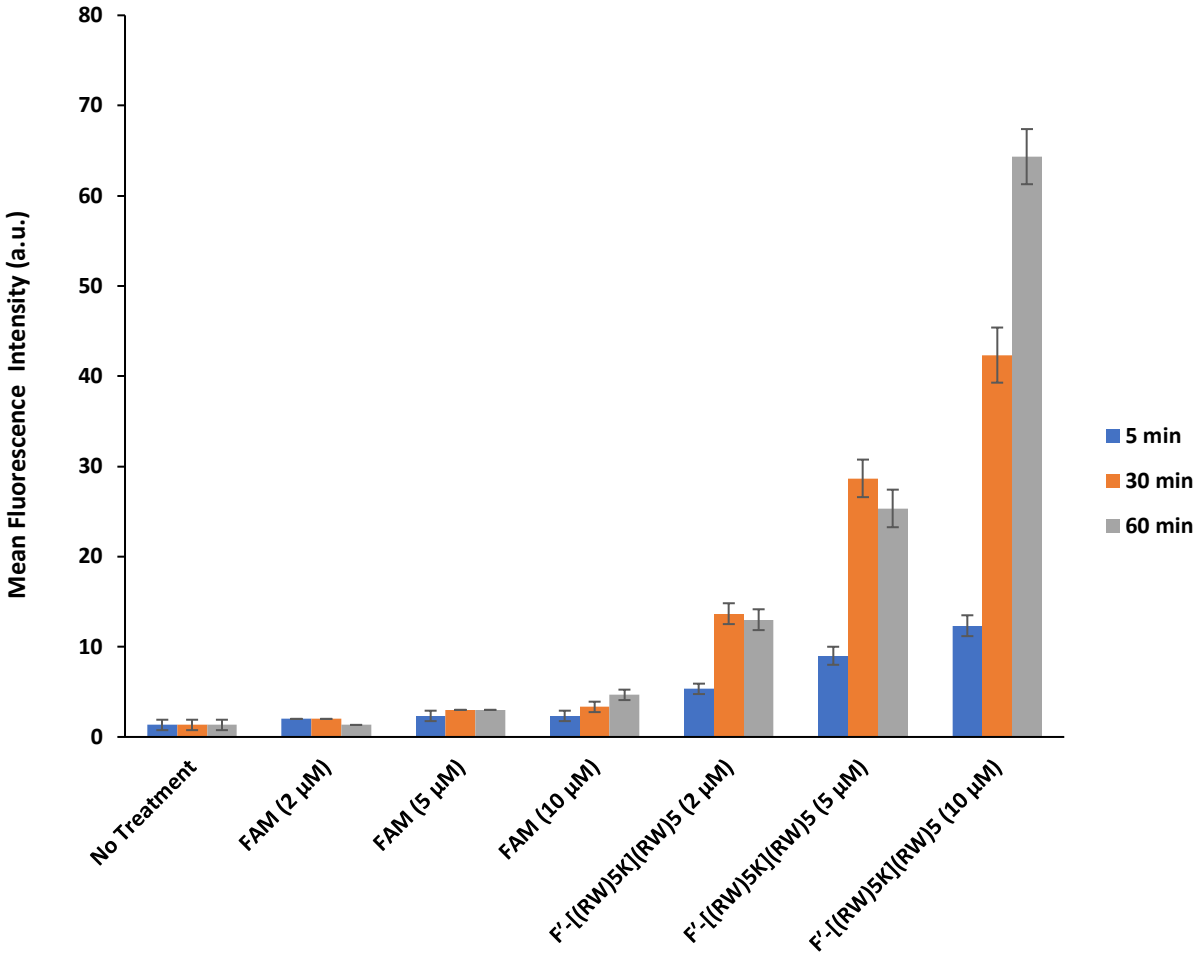

Figure 29. Dose- and time-dependent cellular uptake of FAM (2, 5, 10 μM) and F'-[(RW)$_5$K](RW)$_5$ (2, 5, 10 μM) in MDA-MB-231, after 5 min, 30 min, and 60 min incubation.

3.2. Mechanistic studies

Mechanistic studies were performed to show that whether the cellular uptake of the fluorescence-labeled peptide is endocytosis-dependent. These studies were conducted by flow cytometry in MDA-MB-231 cells to measure the uptake of F'-[(RW)$_5$K](RW)$_5$ in the presence of various endocytosis inhibitors, including nystatin (50 μg/mL), chloroquine (100 μM), chlorpromazine (30 μM), and methyl-β-cyclodextrin (2.5 mM). MDA-MB-231 cells were preincubated by various endocytosis inhibitors for 30 min. Then, the cells were incubated with F'-

$[(RW)_5K](RW)_5$ (10µM) for 3 h in the presence of endocytosis inhibitors. All assays were performed in triplicate, and FAM was used as a negative control (Figure 30). The cellular uptake of F'-$[(RW)_5K](RW)_5$ (10µM) was not reduced by nystatin, ruling out caveolae-mediated endocytosis as the major mechanism of uptake. Chloroquine (100 µM), chlorpromazine (30 µM), and methyl-β-cyclodextrin (2.5 mM) decreased the cellular uptake F'-$[(RW)_5K](RW)_5$ (10µM) by 12%, 64%, 25%, respectively. None of the endocytosis inhibitors could completely stop the cellular uptake; however, the major inhibition was for chlorpromazine. The uptake of F'-$[(RW)_5K](RW)_5$ was partially inhibited by chlorpromazine endocytosis inhibitor after 3 h incubation in MDA-MB-231 cells, suggesting the partial uptake through the clathrin-mediated endocytosis pathway. As a result, the combination of direct penetration and clathrin-mediated endocytosis were involved in the uptake of the fluorescence-labeled peptide across the cell membrane.

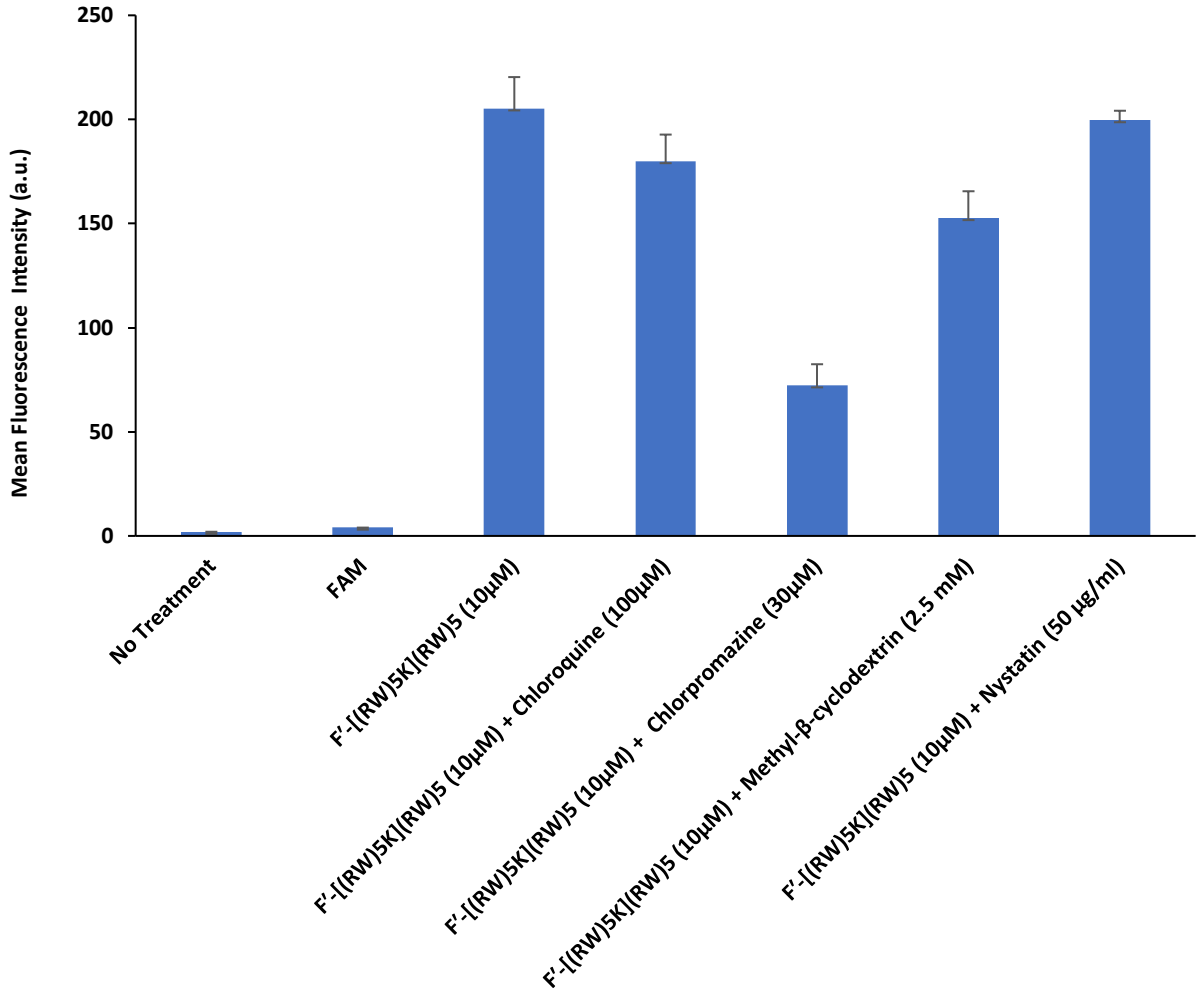

Figure 30. Cellular uptake study of F'-[$(RW)_5$K]$(RW)_5$ (10 μM) in the presence of endocytosis inhibitors in MDA-MB-231 cells after 3 h incubation.

3.2. Confocal microscopy study

A confocal microscopy study was performed using MDA-MB-231 and SK-OV-3 cells to monitor the cellular uptake and intracellular localization of F′-GpYEEI in the presence and absence of [$(RW)_5$K]$(RW)_5$ after 3 h incubation. DAPI and Texas red were used for staining the nuclei and cell membrane, respectively. F′-GpYEEI alone and physical mixture of F′-GpYEEI and $[WR]_5$ did not show any significant uptake in MDA-MB-231 and SK-OV-3 cells (Figures 31 and 32).

However, a higher cellular uptake and higher intensity of the fluorescence-labeled phosphopeptide (F′-GpYEEI) was observed in the presence of $[(RW)_5K](RW)_5$ compared to F′-GpYEEI alone and the physical mixture of F′-GpYEEI and $[WR]_5$. These data confirmed the potential of $[(RW)_5K](RW)_5$ as a molecular transporter of the negatively charged F′-GpYEEI compared to $[WR]_5$. Also, F′-GpYEEI in the presence of $[(RW)_5K](RW)_5$ was localized mainly in the cytosol in MDA-MB-231 and SK-OV-3 cells after 3 h incubation (Figures 31 and 32).

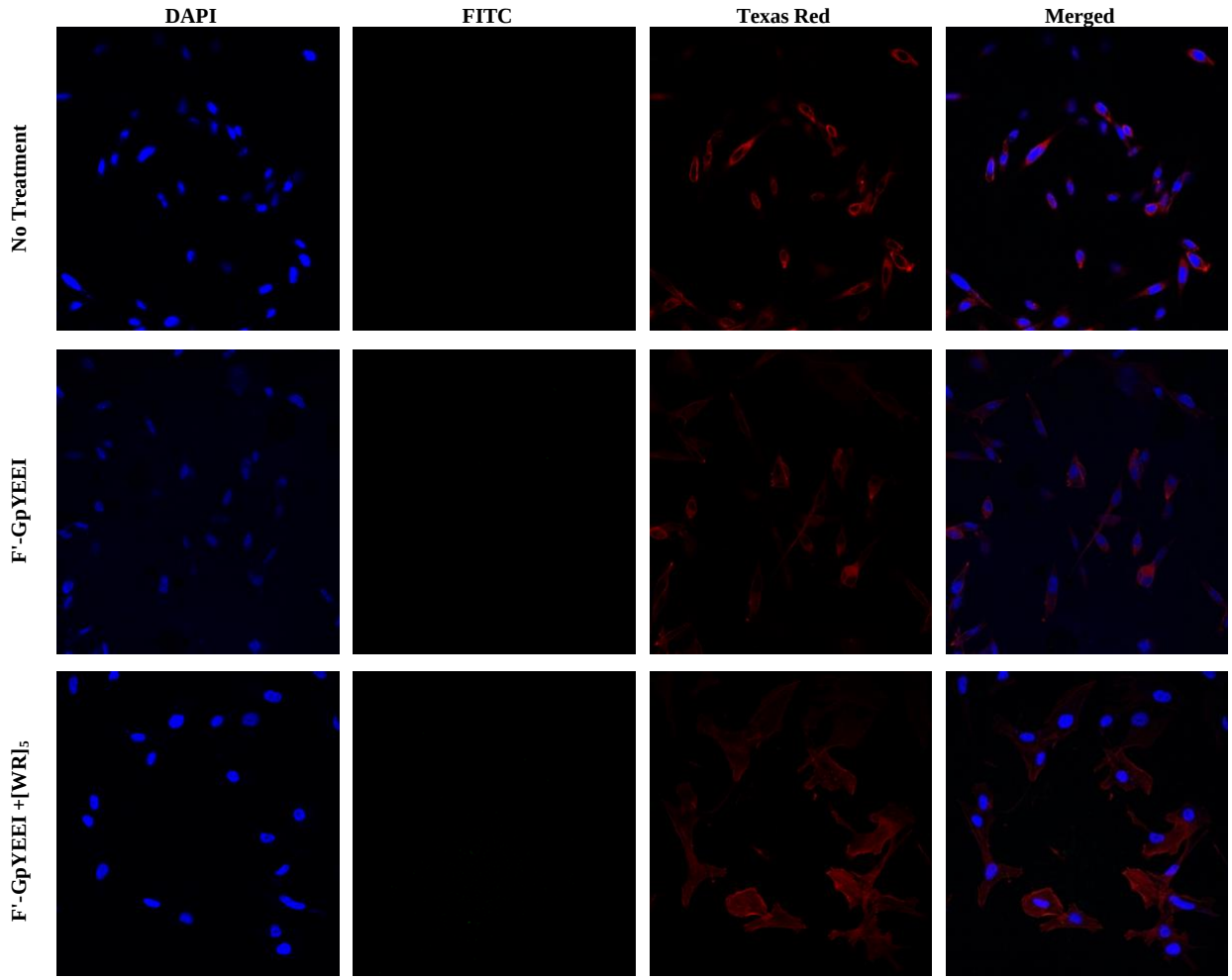

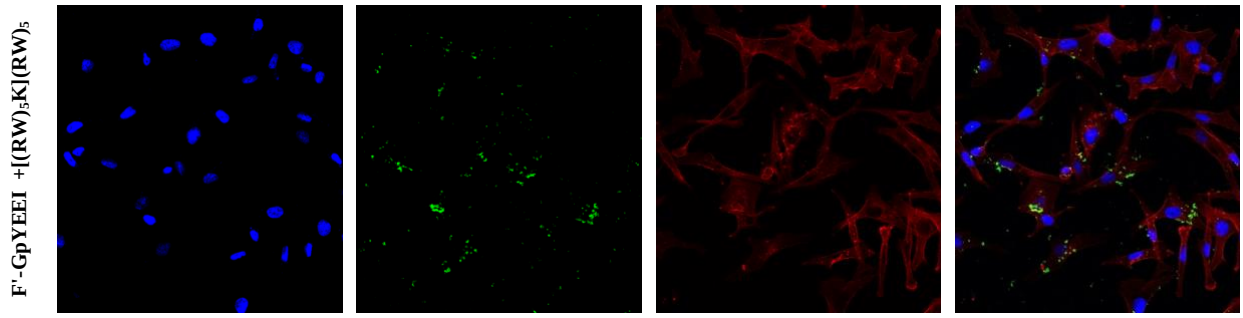

Figure 31. Confocal microscopy images of F´-GpYEEI in the presence of $[(RW)_5K](RW)_5$ (10 μM) or $[WR]_5$ (10μM) in the presence of F´-GpYEEI (2 μM) in MDA-MB-231 cells after 3 h incubation.

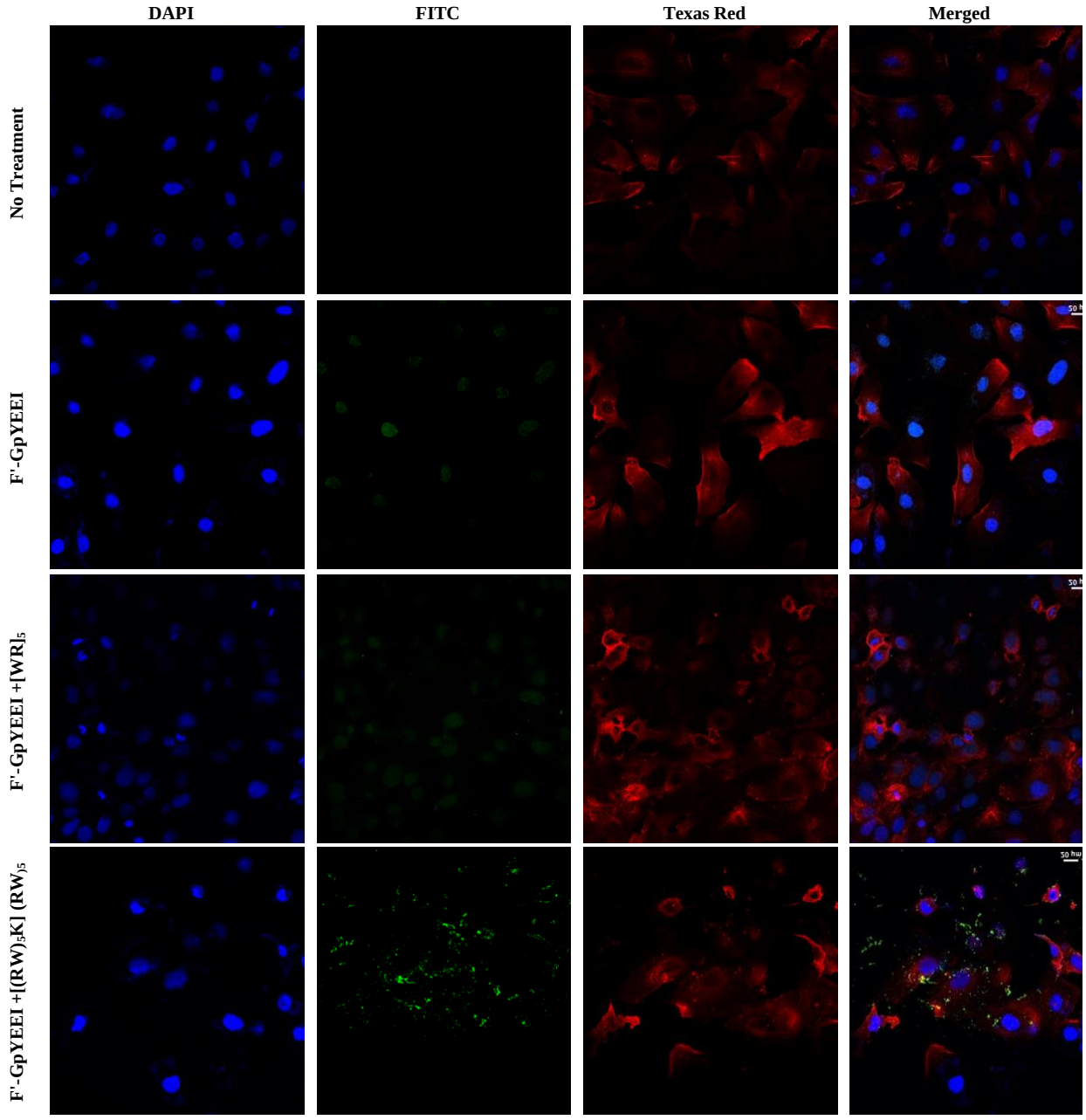

Figure 32. Confocal microscopy images of F´-GpYEEI (2 μM) alone and in the presence of $[(RW)_5K](RW)_5$ (10 μM) or $[WR]_5$ (10 μM) in SK-OV-3 cells after 3 h incubation.

Another Confocal microscopy study was carried out in MDA-MB-231 cells to monitor the intracellular localization of F'-$[(RW)_5K](RW)_5$ and the cellular uptake of F'-$[(RW)_5K](RW)_5$ in the presence of various endocytosis inhibitors, including nystatin (50 μg/mL), chloroquine (100

μM), chlorpromazine (30 μM), and methyl-β-cyclodextrin (2.5 mM) (Figure 33). The data indicate that the F'-[$(RW)_5$K]$(RW)_5$ was localized mainly in the cytosol, and the high fluorescent signal of F'-[$(RW)_5$K]$(RW)_5$ shows the high cell permeability properties of the peptide (Figure 33).

In order to confirm the result of mechanistic studies from FACS analysis, the experiment was performed by confocal microscopy. MDA-MB-231 cells were preincubated by various endocytosis inhibitors including nystatin (50 μg/mL), chloroquine (100 μM), chlorpromazine (30 μM), or methyl-β-cyclodextrin (2.5 mM) for 30 min. The cells were then incubated with F'-[$(RW)_5$K]$(RW)_5$ in the presence of inhibitors for 3 h. The confocal microscopy images confirmed the results from the FACS analysis, which were shown above (Figure 30). The major inhibition and the lowest fluorescence intensity were observed for chlorpromazine (Figure 33). The data indicate the partial uptake through the clathrin-mediated endocytosis pathway.

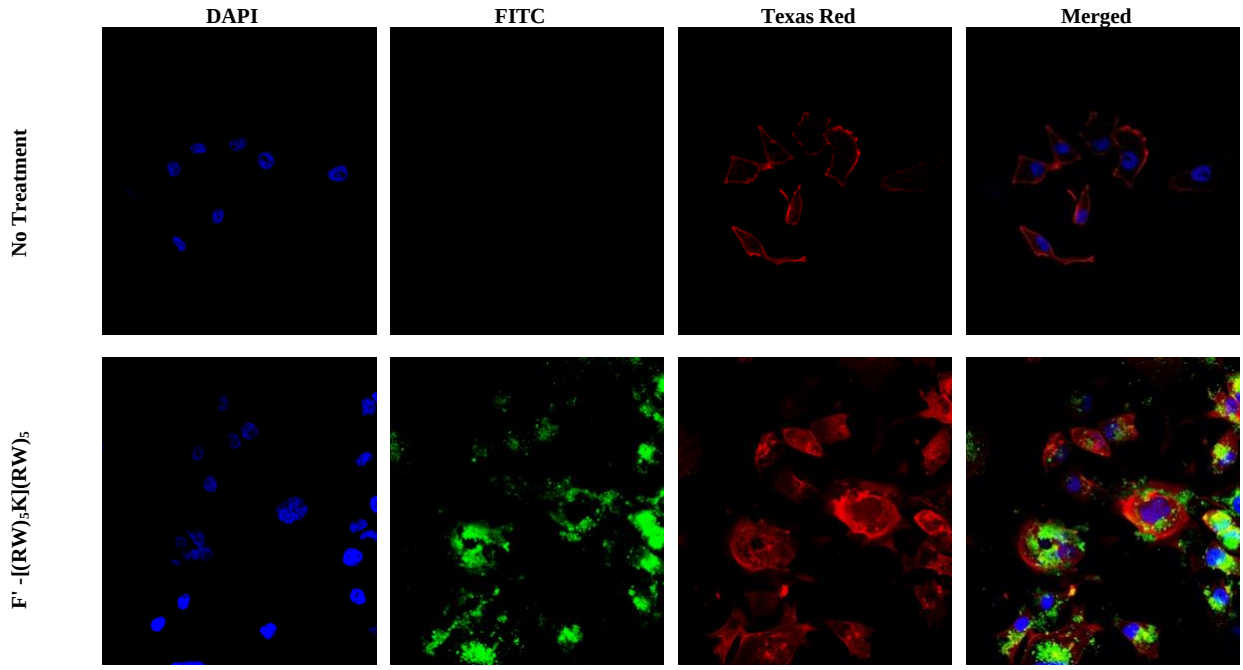

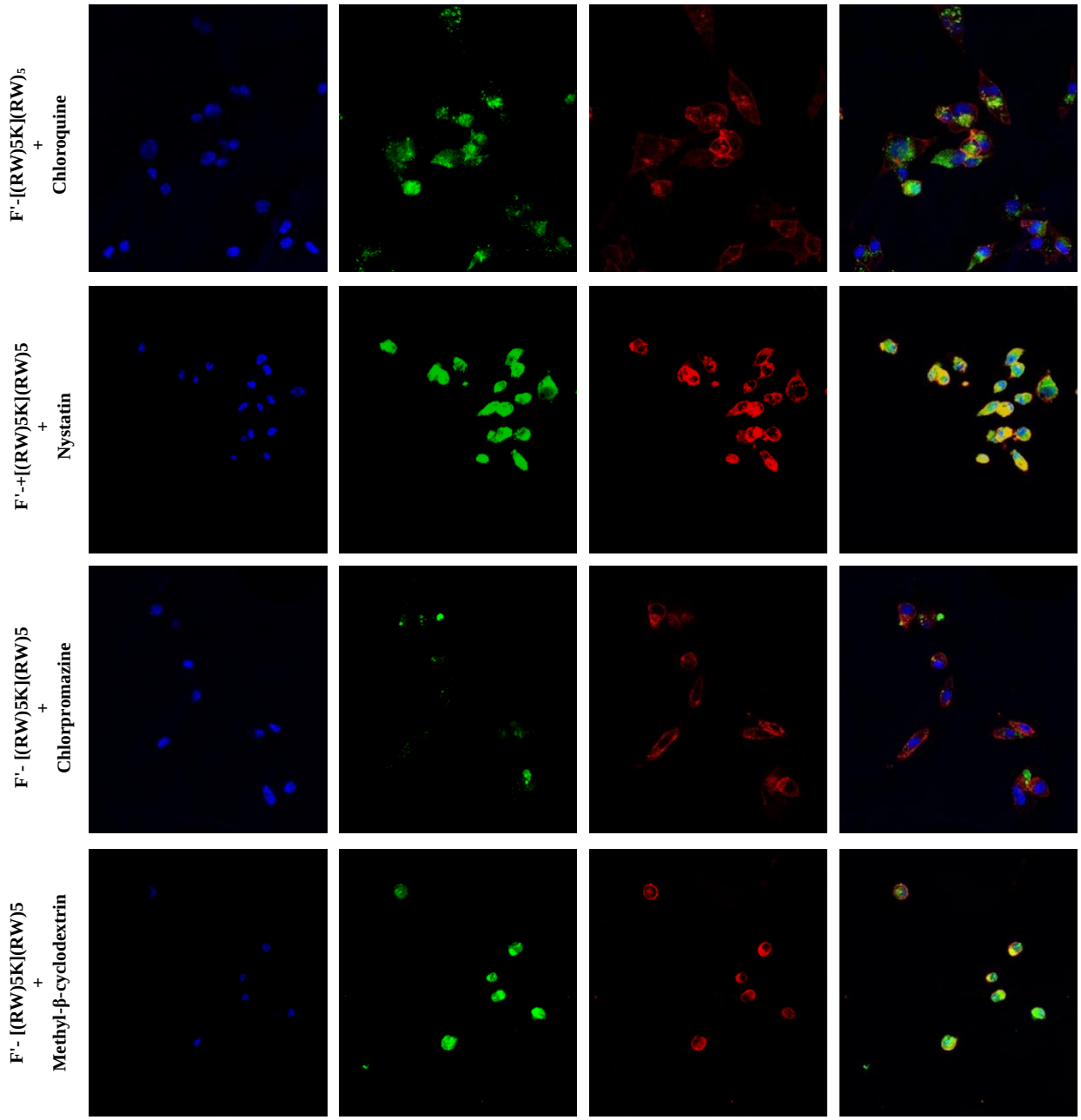

Figure 33. Confocal microscopy images of F'-[(RW)$_5$K](RW)$_5$ (10 μM) alone and in the presence of various endocytosis inhibitors including nystatin (50 μg/mL), chloroquine (100 μM), chlorpromazine (30 μM), or methyl-β-cyclodextrin (2.5 mM) in MDA-MB-231 cells after 3 h incubation.

Conclusions

The cellular uptake of fluorescently labeled conjugate F'-[$(RW)_5$K]$(RW)_5$ was found to be time- and concentration-dependent. The mechanistic studies indicate the partial uptake of the peptide through the clathrin-mediated endocytosis pathway. Intracellular localization of F'-[$(RW)_5$K]$(RW)_5$ was confirmed to be mostly in the cytosol in MDA-MB-231 cells, as shown by confocal microscopy.

References

1. Böhmová, E., Machová, D., Pechar, M., Pola, R., Venclíková, K., Janoušková, O., & Eetrych, T. (2018). Cell-penetrating peptides: a useful tool for the delivery of various cargoes into cells. *Physiological Research*, 67(suppl2), S267-S279. doi:10.33549/physiolres.933975).
2. Reissmann, S. (2014). Cell penetration: Scope and limitations by the application of cell-penetrating peptides. *Journal of Peptide Science, 20*(10), 760-784. doi:10.1002/psc.2672
3. Guidotti, G., Brambilla, L., & Rossi, D. (2017). Cell-penetrating peptides: from basic research to clinics. *Trends in Pharmacological Sciences, 38*(4), 406-424. doi:10.1016/j.tips.2017.01.003
4. Pae, J., Säälik, P., Liivamägi, L., Lubenets, D., Arukuusk, P., Langel, Ü, & Pooga, M. (2014). Translocation of cell-penetrating peptides across the plasma membrane is controlled by cholesterol and microenvironment created by membranous proteins. *Journal of Controlled Release, 192*, 103-113. doi:10.1016/j.jconrel.2014.07.002
5. Herbig, M. E., Weller, K., Krauss, U., Beck-Sickinger, A. G., Merkle, H. P., & Zerbe, O. (2005). Membrane surface-associated helices promote lipid interactions and cellular uptake of human calcitonin-derived cell penetrating peptides. *Biophysical Journal, 89*(6), 4056-4066. doi:10.1529/biophysj.105.068692
6. Mai, J. C., Shen, H., Watkins, S. C., Cheng, T., & Robbins, P. D. (2002). Efficiency of protein transduction is cell type-dependent and is enhanced by dextran sulfate. *Journal of Biological Chemistry, 277*(33), 30208-30218. doi:10.1074/jbc.m204202200
7. Derossi, D., Calvet, S., Trembleau, A., Brunissen, A., Chassaing, G., & Prochiantz, A. (1996). Cell internalization of the third helix of the antennapedia homeodomain is receptor-

independent. *Journal of Biological Chemistry, 271*(30), 18188-18193. doi:10.1074/jbc.271.30.18188

8. Matsuzaki, K., Yoneyama, S., Murase, O., & Miyajima, K. (1996). transbilayer transport of ions and lipids coupled with mastoparan x translocation. *Biochemistry, 35*(25), 8450-8456. doi:10.1021/bi960342a
9. Pouny, Y., Rapaport, D., Mor, A., Nicolas, P., & Shai, Y. (1992). Interaction of antimicrobial dermaseptin and its fluorescently labeled analogs with phospholipid membranes. *Biochemistry, 31*(49), 12416-12423. doi:10.1021/bi00164a017
10. Richard, J. P., Melikov, K., Vives, E., Ramos, C., Verbeure, B., Gait, M. J., Chernomordik, L. V., & Lebleu, B. (2003). Cell-penetrating Peptides. *Journal of Biological Chemistry*, *278*(1), 585–590. https://doi.org/10.1074/jbc.m209548200
11. Jones, A. T. (2007). Macropinocytosis: Searching for an endocytic identity and role in the uptake of cell penetrating peptides. *Journal of Cellular and Molecular Medicine, 11*(4), 670-684. doi:10.1111/j.1582-4934.2007.00062.x
12. Mayor, S., & Pagano, R. E. (2007). Pathways of clathrin-independent endocytosis. *Nature Reviews Molecular Cell Biology, 8*(8), 603-612. doi:10.1038/nrm2216
13. Vercauteren, D., Vandenbroucke, R. E., Jones, A. T., Rejman, J., Demeester, J., De Smedt, S. C., Sanders, N. N., & Braeckmans, K. (2010). The Use of Inhibitors to Study Endocytic Pathways of Gene Carriers: Optimization and Pitfalls. *Molecular Therapy*, *18*(3), 561–569. https://doi.org/10.1038/mt.2009.281
14. Francia, V., Reker-Smit, C., Boel, G., & Salvati, A. (2019). Limits and challenges in using transport inhibitors to characterize how nano-sized drug carriers enter cells. *Nanomedicine, 14*(12), 1533-1549. doi:10.2217/nnm-2018-0446

15. Iversen, T., Skotland, T., & Sandvig, K. (2011). Endocytosis and intracellular transport of nanoparticles: Present knowledge and need for future studies. *Nano Today, 6*(2), 176-185. doi:10.1016/j.nantod.2011.02.003

16. Chen, C., Hou, W., Liu, I., Hsiao, G., Huang, S. S., & Huang, J. S. (2009). Inhibitors of clathrin-dependent endocytosis enhance tgfβ signaling and responses. *Journal of Cell Science, 122*(11), 1863-1871. doi:10.1242/jcs.038729

17. Hu, T. Y., Frieman, M., & Wolfram, J. (2020). Insights from nanomedicine into chloroquine efficacy against COVID-19. *Nature Nanotechnology, 15*(4), 247-249. doi:10.1038/s41565-020-0674-9

18. Plummer, E. M., & Manchester, M. (2012). Endocytic uptake Pathways utilized by cpmv Nanoparticles. *Molecular Pharmaceutics, 10*(1), 26-32. doi:10.1021/mp300238w

19. Yang, Z., Wu, F., Yang, H., & Zhou, P. (2017). Endocytosis mechanism of a novel proteoglycan, extracted from ganoderma lucidum, in hepg2 cells. *RSC Advances, 7*(66), 41779-41786. doi:10.1039/c7ra07520k

Bibliography

Adan, A., Alizada, G., Kiraz, Y., Baran, Y., & Nalbant, A. (2016). Flow cytometry: Basic principles and applications. *Critical Reviews in Biotechnology, 37*(2), 163-176. doi:10.3109/07388551.2015.1128876

Agarwal, H. K., Chhikara, B. S., Bhavaraju, S., Mandal, D., Doncel, G. F., & Parang, K. (2012). Emtricitabine prodrugs with improved anti-HIV activity and cellular uptake. *Molecular Pharmaceutics, 10*(2), 467-476. doi:10.1021/mp300361a

Agarwal, H. K., Chhikara, B. S., Hanley, M. J., Ye, G., Doncel, G. F., & Parang, K. (2012). Synthesis and biological evaluation of fatty acyl ester derivatives of (−)-2′,3′-dideoxy-3′-thiacytidine. *Journal of Medicinal Chemistry,55*(10), 4861-4871. doi:10.1021/jm300492q

Agarwal, H. K., Loethan, K., Mandal, D., Doncel, G. F., & Parang, K. (2011). Synthesis and biological evaluation of fatty acyl ester derivatives of 2′,3′-didehydro-2′,3′-dideoxythymidine. *Bioorganic & Medicinal Chemistry Letters, 21*(7), 1917-1921. doi:10.1016/j.bmcl.2011.02.070

Akbarzadeh, A., Rezaei-Sadabady, R., Davaran, S., Joo, S. W., Zarghami, N., Hanifehpour, Y., Nejati-Koshki, K. (2013). Liposome: classification, preparation, and applications. *Nanoscale Research Letters, 8*(1). doi:10.1186/1556-276x-8-102Böhmová, E., Machová, D., Pechar, M., Pola, R., Venclíková, K., Janoušková, O., & Eetrych, T. (2018). Cell-penetrating peptides: a useful tool for the delivery of various cargoes into cells. *Physiological Research*, 67(suppl2), S267-S279. doi:10.33549/physiolres.933975).

Carpino, L. A., & Han, G. Y. (1970). 9-Fluorenylmethoxycarbonyl function, a new base-sensitive amino-protecting group. *Journal of the American Chemical Society, 92*(19), 5748-5749. doi:10.1021/ja00722a043

Chen, C., Hou, W., Liu, I., Hsiao, G., Huang, S. S., & Huang, J. S. (2009). Inhibitors of clathrin-dependent endocytosis enhance tgfβ signaling and responses. *Journal of Cell Science, 122*(11), 1863-1871. doi:10.1242/jcs.038729

Cobb, L. (2019). Cell proliferation assays and cell viability assays. *Materials and Methods, 9*. doi:10.13070/mm.en.9.2799

Coin, I., Beyermann, M., & Bienert, M. (2007). Solid-phase peptide synthesis: From standard procedures to the synthesis of difficult sequences. *Nature Protocols, 2*(12), 3247-3256. doi:10.1038/nprot.2007.454

Danhier, F., Ansorena, E., Silva, J. M., Coco, R., Le Breton, A., & Préat, V. (2012). PLGA-based nanoparticles: An overview of biomedical applications. *Journal of Controlled Release, 161*(2), 505-522. doi:10.1016/j.jconrel.2012.01.043

Danhier, F., Ansorena, E., Silva, J. M., Coco, R., Le Breton, A., & Préat, V. (2012). PLGA-based nanoparticles: An overview of biomedical applications. *Journal of Controlled Release, 161*(2), 505-522. doi:10.1016/j.jconrel.2012.01.043

Derakhshankhah, H., & Jafari, S. (2018). Cell penetrating peptides: A concise review with emphasis on biomedical applications. *Biomedicine & Pharmacotherapy, 108,* 1090-1096. doi:10.1016/j.biopha.2018.09.097

Derossi, D., Calvet, S., Trembleau, A., Brunissen, A., Chassaing, G., & Prochiantz, A. (1996). Cell internalization of the third helix of the antennapedia homeodomain is receptor-independent. *Journal of Biological Chemistry, 271*(30), 18188-18193. doi:10.1074/jbc.271.30.18188

Derossi, D., Chassaing, G., & Prochiantz, A. (1998). Trojan peptides: The penetratin system for intracellular delivery. *Trends in Cell Biology, 8*(2), 84-87. doi:10.1016/s0962-8924(98)80017-2

Do, H., Sharma, M., El-Sayed, N. S., Mahdipoor, P., Bousoik, E., Parang, K., & Montazeri Aliabadi, H. (2017). Difatty acyl-conjugated linear and cyclic peptides for Sirna delivery. *ACS Omega, 2*(10), 6939-6957. doi:10.1021/acsomega.7b00741

El-Sayed, N. S., Shirazi, A. N., Sajid, M. I., Park, S. E., Parang, K., & Tiwari, R. K. (2019). Synthesis and antiproliferative activities of conjugates of paclitaxel and camptothecin with a cyclic cell-penetrating peptide. *Molecules, 24*(7), 1427. doi:10.3390/molecules24071427

Fields, G. B. (2001). Introduction to peptide synthesis. *Current Protocols in Protein Science, 26*(1). doi:10.1002/0471140864.ps1801s26

Francia, V., Reker-Smit, C., Boel, G., & Salvati, A. (2019). Limits and challenges in using transport inhibitors to characterize how nano-sized drug carriers enter cells. *Nanomedicine, 14*(12), 1533-1549. doi:10.2217/nnm-2018-0446

Guidotti, G., Brambilla, L., & Rossi, D. (2017). Cell-penetrating peptides: from basic research to clinics. *Trends in Pharmacological Sciences, 38*(4), 406-424. doi:10.1016/j.tips.2017.01.003

Habault, J., & Poyet, J. (2019). Recent advances in cell penetrating peptide-based anticancer therapies. *Molecules*, *24*(5), 927. doi:10.3390/molecules24050927

Hall, R., Alasmari, A., Mozaffari, S., Mahdipoor, P., Parang, K., & Montazeri Aliabadi, H. (2021). Peptide/Lipid-Associated nucleic Acids (PLANAS) as a multicomponent Sirna delivery system. *Molecular Pharmaceutics,18*(3), 986-1002. doi:10.1021/acs.molpharmaceut.0c00969

Hanna, S. E., Mozaffari, S., Tiwari, R. K., & Parang, K. (2018). Comparative molecular transporter efficiency of cyclic Peptides containing tryptophan and arginine residues. *ACS Omega*, *3*(11), 16281-16291. doi:10.1021/acsomega.8b02589

Herbig, M. E., Weller, K., Krauss, U., Beck-Sickinger, A. G., Merkle, H. P., & Zerbe, O. (2005). Membrane surface-associated helices promote lipid interactions and cellular uptake of human calcitonin-derived cell penetrating peptides. *Biophysical Journal, 89*(6), 4056-4066. doi:10.1529/biophysj.105.068692

Hu, T. Y., Frieman, M., & Wolfram, J. (2020). Insights from nanomedicine into chloroquine efficacy against COVID-19. *Nature Nanotechnology*, *15*(4), 247-249. doi:10.1038/s41565-020-0674-9Ichimizu, S., Watanabe, H., Maeda, H., Hamasaki, K., Nakamura, Y., Chuang, V. T., Kinoshita, R., Nishida, K., Tanaka, R., Enoki, Y., Ishima, Y., Kuniyasu, A., Kobashigawa, Y., Morioka, H., Futaki, S., Otagiri, M., & Maruyama, T. (2018). Design and tuning of a cell-

penetrating albumin derivative as a versatile nanovehicle for intracellular drug delivery. *Journal of Controlled Release, 277*, 23–34. https://doi.org/10.1016/j.jconrel.2018.02.037

Ishiyama, M., Tominaga, H., Shiga, M., Sasamoto, K., Ohkura, Y., & Ueno, K. (1996). A combined assay of cell viability and in vitro cytotoxicity with a highly water-soluble tetrazolium salt, neutral red and crystal violet. *Biological and Pharmaceutical Bulletin, 19*(11), 1518-1520. doi:10.1248/bpb.19.1518

Iversen, T., Skotland, T., & Sandvig, K. (2011). Endocytosis and intracellular transport of nanoparticles: Present knowledge and need for future studies. *Nano Today, 6*(2), 176-185. doi:10.1016/j.nantod.2011.02.003

Jafari, S., Maleki Dizaj, S., & Adibkia, K. (2017). Cell-penetrating peptides and their analogues as novel nanocarriers for drug delivery. *BioImpacts, 5*(2), 103-111. doi:10.15171/bi.2015.10Javadzadeh, Y., & Azharshekoufeh Bahari, L. (2017). Therapeutic nanostructures for dermal and Transdermal drug delivery. *Nano- and Microscale Drug Delivery Systems*, 131-146. doi:10.1016/b978-0-323-52727-9.00008-x

Jobin, M.-L., Blanchet, M., Henry, S., Chaignepain, S., Manigand, C., Castano, S., Lecomte, S., Burlina, F., Sagan, S., & Alves, I. D. (2015). The role of tryptophans on the cellular uptake and membrane interaction of arginine-rich cell penetrating peptides. *Biochimica Et Biophysica Acta (BBA) - Biomembranes*, *1848*(2), 593–602. https://doi.org/10.1016/j.bbamem.2014.11.013

Jones, A. T. (2007). Macropinocytosis: Searching for an endocytic identity and role in the uptake of cell penetrating peptides. *Journal of Cellular and Molecular Medicine, 11*(4), 670-684. doi:10.1111/j.1582-4934.2007.00062.x

Kardani, K., Milani, A., H. Shabani, S., & Bolhassani, A. (2019). Cell penetrating peptides: the potent multi-cargo intracellular carriers. *Expert Opinion on Drug Delivery, 16*(11), 1227-1258. doi:10.1080/17425247.2019.1676720Koren, E., & Torchilin, V. P. (2012). Cell-penetrating peptides: breaking through to the other side. *Trends in Molecular Medicine, 18*(7), 385-393. doi:10.1016/j.molmed.2012.04.012

Macey, M. G. (n.d.). Principles of flow cytometry. *Flow Cytometry,* 1-15. doi:10.1007/978-1-59745-451-3_1

Mai, J. C., Shen, H., Watkins, S. C., Cheng, T., & Robbins, P. D. (2002). Efficiency of protein transduction is cell type-dependent and is enhanced by dextran sulfate. *Journal of Biological Chemistry, 277*(33), 30208-30218. doi:10.1074/jbc.m204202200

Makadia, H. K., & Siegel, S. J. (2011). Poly lactic-co-glycolic Acid (PLGA) as biodegradable controlled drug delivery carrier. *Polymers, 3*(3), 1377-1397. doi:10.3390/polym3031377

Malich, G., Markovic, B., & Winder, C. (1997). The sensitivity and specificity of the MTS tetrazolium assay for detecting the in vitro cytotoxicity of 20 chemicals using human cell lines. *Toxicology, 124*(3), 179-192. doi:10.1016/s0300-483x(97)00151-0

Mandal, D., Shirazi, A.N., & Parang, K. (2011). Cell-penetrating homochiral cyclic peptides as nuclear-targeting molecular transporters. *Angewandte Chemie, 123*(41), 9807-9811. doi:10.1002/ange.201102572

Matsuzaki, K., Yoneyama, S., Murase, O., & Miyajima, K. (1996). transbilayer transport of ions and lipids coupled with mastoparan x translocation. *Biochemistry, 35*(25), 8450-8456. doi:10.1021/bi960342a

Mayor, S., & Pagano, R. E. (2007). Pathways of clathrin-independent endocytosis. *Nature Reviews Molecular Cell Biology, 8*(8), 603-612. doi:10.1038/nrm2216

McDonough, J., Dixon, H., & Ladika, M. (2010). Nasal delivery of micro- and nano-encapsulated drugs. *Handbook of Non-Invasive Drug Delivery Systems,* 193-208. doi:10.1016/b978-0-8155-2025-2.10008-3

McKinnon, K. M. (2018). Flow cytometry: An overview. *current protocols in immunology, 120*(1). doi:10.1002/cpim.40Mozaffari, S., Bousoik, E., Amirrad, F., Lamboy, R., Coyle, M., Hall, R., Alasmari, A., Mahdipoor, P., Parang, K., & Montazeri Aliabadi, H. (2019). Amphiphilic Peptides for Efficient siRNA Delivery. *Polymers, 11*(4), 703. https://doi.org/10.3390/polym11040703

Nobel lecture, 8 December, 1984 by bruce merrifield solid-phase synthesis, The Rockefeller University, 1230 York Avenue, New York, N.Y. 10021-6399

Nosova, A. S., Koloskova, O. O., Nikonova, A. A., Simonova, V. A., Smirnov, V. V., Kudlay, D., & Khaitov, M. R. (2019). Diversity of PEGylation methods of liposomes and their influence on RNA delivery. *MedChemComm,10*(3), 369-377. doi:10.1039/c8md00515j

Oh, D., Shirazi, A.N., Northup, K., Sullivan, B., Tiwari, R. K., Bisoffi, M., & Parang, K. (2014). Enhanced cellular uptake of short polyarginine peptides through fatty acylation and cyclization. *Molecular Pharmaceutics,11*(8), 2845-2854. doi:10.1021/mp500203e

Olusanya, T., Haj Ahmad, R., Ibegbu, D., Smith, J., & Elkordy, A. (2018). Liposomal drug delivery systems and anticancer drugs. *Molecules, 23*(4), 907. doi:10.3390/molecules23040907

Pae, J., Säälik, P., Liivamägi, L., Lubenets, D., Arukuusk, P., Langel, Ü, & Pooga, M. (2014). Translocation of cell-penetrating peptides across the plasma membrane is controlled by cholesterol and microenvironment created by membranous proteins. *Journal of Controlled Release, 192*, 103-113. doi:10.1016/j.jconrel.2014.07.002

Palomo, J. M. (2014). Solid-phase peptide synthesis: An overview focused on the preparation of biologically relevant peptides. *RSC Adv., 4*(62), 32658-32672. doi:10.1039/c4ra02458c

Park, S. E., Sajid, M. I., Parang, K., & Tiwari, R. K. (2019). Cyclic cell-penetrating peptides as efficient intracellular drug delivery tools. *Molecular Pharmaceutics, 16*(9), 3727-3743. doi:10.1021/acs.molpharmaceut.9b00633

Plummer, E. M., & Manchester, M. (2012). Endocytic uptake Pathways utilized by cpmv Nanoparticles. *Molecular Pharmaceutics, 10*(1), 26-32. doi:10.1021/mp300238w

Pouny, Y., Rapaport, D., Mor, A., Nicolas, P., & Shai, Y. (1992). Interaction of antimicrobial dermaseptin and its fluorescently labeled analogs with phospholipid membranes. *Biochemistry, 31*(49), 12416-12423. doi:10.1021/bi00164a017

Reissmann, S. (2014). Cell penetration: Scope and limitations by the application of cell-penetrating peptides. *Journal of Peptide Science, 20*(10), 760-784. doi:10.1002/psc.2672

Richard, J. P., Melikov, K., Vives, E., Ramos, C., Verbeure, B., Gait, M. J., . . . Lebleu, B. (2003). Cell-penetrating peptides. *Journal of Biological Chemistry, 278*(1), 585-590. doi:10.1074/jbc.m209548200

Riss TL, Moravec RA, Niles AL, Duellman S, Benink HA, Worzella TJ, Minor L. (2013). Cell viability assays. Assay Guidance Manual. PMID: 23805433.

Romberg, B., Hennink, W. E., & Storm, G. (2007). Sheddable coatings for long-circulating Nanoparticles. *Pharmaceutical Research, 25*(1), 55-71. doi:10.1007/s11095-007-9348-7

Sachdeva, S. (2016). Peptides as 'drugs': The journey so far. *International Journal of Peptide Research and Therapeutics,23*(1), 49-60. doi:10.1007/s10989-016-9534-8

Shirazi, A.N., Mandal, D., Tiwari, R. K., Guo, L., Lu, W., & Parang, K. (2012). Cyclic peptide-capped gold nanoparticles as drug delivery systems. *Molecular Pharmaceutics, 10*(2), 500-511. doi:10.1021/mp300448k

Shirazi, A.N., Salem El-Sayed, N., Kumar Tiwari, R., Tavakoli, K., & Parang, K. (2016). Cyclic peptide containing hydrophobic and positively charged residues as a drug delivery

system for curcumin. *Current Drug Delivery, 13*(3), 409-417. doi:10.2174/15672018126661510291011 02

Shirazi, A.N., Tiwari, R. K., Oh, D., Banerjee, A., Yadav, A., & Parang, K. (2013). Efficient delivery of cell impermeable phosphopeptides by a cyclic peptide amphiphile containing tryptophan and arginine. *Molecular Pharmaceutics, 10*(5), 2008-2020. doi:10.1021/mp400046u

Shirazi, A.N., Tiwari, R. K., Oh, D., Sullivan, B., Kumar, A., Beni, Y. A., & Parang, K. (2014). Cyclic peptide–selenium nanoparticles as drug transporters. *Molecular Pharmaceutics, 11*(10), 3631-3641. doi:10.1021/mp500364a

Shirazi, A.N., Tiwari, R., Chhikara, B. S., Mandal, D., & Parang, K. (2013). Design and biological evaluation of cell-penetrating peptide–doxorubicin conjugates as prodrugs. *Molecular Pharmaceutics, 10*(2), 488-499. doi:10.1021/mp3004034

Sokalingam, S., Raghunathan, G., Soundrarajan, N., & Lee, S. (2012). A study on the effect of surface lysine to arginine mutagenesis on protein stability and structure using green fluorescent protein. *PLoS ONE, 7*(7). doi:10.1371/journal.pone.0040410

Suk, J. S., Xu, Q., Kim, N., Hanes, J., & Ensign, L. M. (2016). PEGylation as a strategy for improving Nanoparticle-based drug and gene delivery. *Advanced Drug Delivery Reviews, 99*, 28-51. doi:10.1016/j.addr.2015.09.012

Traboulsi, H., Larkin, H., Bonin, M., Volkov, L., Lavoie, C. L., & Marsault, É. (2015). Macrocyclic cell penetrating Peptides: A study of structure-penetration properties. *Bioconjugate Chemistry, 26*(3), 405-411. doi:10.1021/acs.bioconjchem.5b00023

Vercauteren, D., Vandenbroucke, R. E., Jones, A. T., Rejman, J., Demeester, J., De Smedt, S. C., Braeckmans, K. (2010). The use of inhibitors to study endocytic pathways of gene carriers: Optimization and pitfalls. *Molecular Therapy, 18*(3), 561-569. doi:10.1038/mt.2009.281

Watson, H. (2015). Biological membranes. *Essays in Biochemistry, 59*, 43-69. doi:10.1042/bse0590043

Yang, Z., Wu, F., Yang, H., & Zhou, P. (2017). Endocytosis mechanism of a novel proteoglycan, extracted from ganoderma lucidum, in hepg2 cells. *RSC Advances, 7*(66), 41779-41786. doi:10.1039/c7ra07520k

Yin, N. (2014). Enhancing the oral bioavailability of peptide drugs by using chemical modification and other approaches. *Medicinal Chemistry*. doi:10.4172/2161-0444.1000227

Zhang, R., Qin, X., Kong, F., Chen, P., & Pan, G. (2019). Improving cellular uptake of therapeutic entities through interaction with components of cell membrane. *Drug Delivery, 26*(1), 328-342. doi:10.1080/10717544.2019.1582730

Zhao, P., & Sun, M. (2015). The maternal-to-zygotic transition in higher plants. *Current Topics in Developmental Biology*,373-398. doi:10.1016/bs.ctdb.2015.06.006